

Judit Adam

Catalytic conversion of biomass to produce higher quality liquid bio-fuels

Trondheim, September, 2005

PhD thesis

Norwegian University of Science and Technology

Faculty of Engineering Science and Technology

Department of Energy and Process Engineering





The Norwegian University of Science and Technology
Norges Teknisk-Naturvitenskapelige Universitet

Report no:
2005:187

Classification:
Open

| | | |
|--------------------------|---------------------------------|---------------------------------|
| ADDRESS: | TELEPHONE | TELEFAX |
| NTNU | Switchboard NTNU: 73 59 40 00 | Department office: 73 59 83 90 |
| DEPARTMENT OF ENERGY AND | Department office: 73 59 27 00 | Hydropower section: 73 59 38 54 |
| PROCESS Engineering | Hydropower section: 73 59 38 57 | |
| Kolbjørn Hejes vei 1A | | |
| N-7491 Trondheim - NTNU | | |

| | |
|---|------------------------------------|
| Title of report Catalytic conversion of biomass to produce higher quality liquid bio-fuels | Date September, 2005 |
| | No. Of pages/appendixes 142/62 |
| Author Judith Adam | Project manager Johan E. Hustad |
| Division Faculty of Engineering Science and technology Department of Energy and Process Engineering | Project no. |
| ISBN no. 82-471-7267-4 | Price group |

Abstract

The aim of this work was to improve the characteristics of a liquid bio-fuel, the bio-oil, with the help of mesoporous materials. Seven different mesoporous materials have been tested; four Al-MCM-41 catalysts (K1-K4), a commercial FCC catalyst (K5) and two SBA-15 catalysts (K6-K7). The Al-MCM-41 catalyst group had a Si/Al ratio of 20 and consisted of an unmodified Al-MCM-41 (K1), two catalysts with enlarged pores (K2 and K3) and a transition metal (Cu) modified catalyst (K4). The pore enlargement in sample K2 was carried out with a spacer (mesitylene, C₉H₁₂), and in sample K3 by altering the template chain length from C₁₄ to C₁₈. The SBA-15 catalyst group consisted of a pure siliceous SBA-15 (K6) and an SBA-15 catalyst with aluminium incorporation (K7). The tests were carried out in three different pyrolysis systems, which were: analytical fast pyrolysis-GC/MS, TG/MS, and a fixed bed system. The used biomass was spruce, and in order to study the effect of the biomass type, some experiments in the fixed bed reactor were carried out with miscanthus.

As a result of the catalytic cracking of the vapours, the amount of water increased compared to the non-catalytic experiments with all the catalysts in each of the reactors. When spruce was pyrolysed in the presence of unmodified Al-MCM-41 catalyst, the yields of furan ring containing compounds increased considerably. The yields of phenols, light phenol substitutes, hydrocarbons and PAHs increased, but the yields of alcohols, aldehydes, heavy phenol substitutes and heavy compounds decreased. With increasing pore diameter the changes show the same trends, but in a smaller degree. Metal incorporation into the parent Al-MCM-41 without any pore modifications shows similar yields as the catalyst with the largest pores, however, there can be small differences in the yields of a few compounds.

Spruce pyrolysis in the presence of SBA-15 catalyst shows similar yields as the uncatalysed experiments in most cases, however, the yields of furan-ring containing compounds increased and some other compounds varied slightly. Aluminium incorporation into the SBA-15 framework changed the product yields considerably. Both the desirable and the undesirable product yields increased. The SBA-15 catalysts compared to the MCM-41 catalysts, has lower surface areas, especially the aluminium incorporated SBA-15, and considerably larger mesopores. During spruce pyrolysis in the presence of SBA-15 catalysts, compared to the Al-MCM-41 catalysts, increased the desirable product yield, mostly with Al-SBA-15, however, in this case, the undesirable product yield increased considerably as well. According to the published results, among the studied catalysts, the FCC catalyst produces the best-quality bio-oil with the spruce biomass. This catalyst is also the cheapest one as it is already available commercially. Al-MCM-41 type catalyst does not perform well with this biomass type, and furthermore, it has a weak hydrothermal stability. SBA-15 catalyst with aluminium incorporation can have a potential, but the performance and the price is probably not competitive with the FCC catalyst. The difference in catalyst performance is much greater than expected when the biomass is changed. With miscanthus, the unmodified Al-MCM-41 catalyst performs best and the FCC catalyst does not produce a good quality product. The SBA-15 catalyst's present performance is similar both with miscanthus and spruce.

| | Indexing Terms: English | Norwegian |
|-----------|-------------------------|-------------------|
| Group 1 | Heat engineering | Varmeteknikk |
| Group 2 | Biomass | Biomasse |
| Selected | Pyrolysis | Pyrolyse |
| by author | Catalysis | Katalyse |
| | Product distribution | Pyrolyseprodukter |

Preface

"Instead of our drab slogging forth and back to the fishing boats, there's a reason to life!

*We can lift ourselves out of ignorance,
we can find ourselves as creatures of excellence and intelligence and skill.*

We can be free! We can learn to fly!"

(Richard Bach, 'Jonathan Livingston Seagull,' 1970.)

First, I would like to thank my supervisors, Johan E. Hustad (NTNU) and Michael Stöcker (SINTEF), their guidance, suggestions and many good advices.

A great part of my work was done at Institute of Materials and Environmental Chemistry, Chemical Research Centre, Hungarian Academy of Sciences. I would like to thank Gábor Várhegyi and his research group, Marianne Blazsó, Emma Jakab and especially Erika Mészáros, for their excellent cooperation and many advices. This cooperation was extremely useful, I have learnt a lot from them.

The second parts of my experiments were carried out at Chemical Process Engineering Research Institute (CPERI), Centre for Research and Technology Hellas (CERTH). I would like to thank Eleni Antonakou and Angelos Lappas for making the cooperation possible and helping me during my stay in Greece.

My catalysts were made in Trondheim at Ugelstad Laboratory, Department of Chemical Engineering at NTNU, I had access to the lab, thanks to Johan Sjøblom and Gilse Øye. I also got a lot of good advices about the catalyst.

Thanks to Aud Bouzga and Merete H. Nilsen for characterising my catalysts, and answering many of my questions. They also made some of the catalysts I used.

I would like to acknowledge the Norwegian Research Council for the financial support. Gunhild and Anita was always available when I had problems, thanks for them to make my start in Norway easy and helping me whenever I needed.

Finally, I would like to thank my family and Fredrik for all their support.

Trondheim, September, 2005

Judit Adam

Abstract

The aim of this work has been to improve the characteristics of a liquid bio-fuel, the bio-oil, with the help of mesoporous materials. Seven different mesoporous materials have been tested; four Al-MCM-41 catalysts (K1-K4), a commercial FCC catalyst (K5) and two SBA-15 catalysts (K6-K7). The Al-MCM-41 catalyst group had a Si/Al ratio of 20 and consisted of an unmodified Al-MCM-41 (K1), two catalysts with enlarged pores (K2 and K3) and a transition metal (Cu) modified catalyst (K4). The pore enlargement in sample K2 was carried out with a spacer (mesitylene, C₉H₁₂), and in sample K3 by altering the template chain length from C₁₄ to C₁₈. The SBA-15 catalyst group consisted of a pure siliceous SBA-15 (K6) and an SBA-15 catalyst with aluminium incorporation (K7). The tests were carried out in three different pyrolysis systems, which were: analytical fast pyrolysis-GC/MS, TG/MS, and a fixed bed system. The used biomass was spruce, and in order to study the effect of the different biomass feedstocks, some experiments in the fixed bed reactor were carried out with miscanthus.

As a result of the catalytic cracking of the vapours, the amount of water increased compared to the non-catalytic experiments with all the catalysts in each of the reactors. When spruce was pyrolysed in the presence of unmodified Al-MCM-41 catalyst, the yields of furan ring containing compounds increased considerably. The yields of phenols, light phenol substitutes, hydrocarbons and PAHs increased, but the yields of alcohols, aldehydes, heavy phenol substitutes and heavy compounds decreased. With increasing pore diameter the changes show the same trends, but in a smaller degree. Metal incorporation into the parent Al-MCM-41 without any pore modifications shows similar yields as the catalyst with the largest pores, however, there can be small differences in the yields of a few compounds.

Spruce pyrolysis in the presence of SBA-15 catalyst shows similar yields as the uncatalysed experiments in most cases, however, the yields of furan-ring containing compounds increased and some other compounds varied slightly. Aluminium incorporation into the SBA-15 framework changed the product yields considerably. Both the desirable and the undesirable product yields increased. The SBA-15 catalysts compared to the MCM-41 catalysts, has lower surface areas, especially the aluminium

incorporated SBA-15, and considerably larger mesopores. During spruce pyrolysis in the presence of SBA-15 catalysts, compared to the Al-MCM-41 catalysts, the desirable product yield increased. In this case, however, the undesirable product yield increased considerably as well. According to the published results, among the studied catalysts, the FCC catalyst produced the best-quality bio-oil with the spruce biomass. This catalyst is also the cheapest one as it is already available commercially. The Al-MCM-41 type catalyst does not perform well with spruce, and furthermore, it has a weak hydrothermal stability. SBA-15 catalyst with aluminium incorporation can have a potential, but the performance and the price at present is not competitive with the FCC catalyst. The difference in catalyst performance was much greater than expected when the biomass feedstock was altered. With miscanthus, the unmodified Al-MCM-41 catalyst performed best and the FCC catalyst does not produce a good quality product. The SBA-15 catalyst performance was similar both with miscanthus and spruce.

Table of contents

| | |
|--|-----|
| PREFACE | I |
| ABSTRACT..... | II |
| TABLE OF CONTENTS..... | IV |
| LIST OF FIGURES | VI |
| LIST OF TABLES | VII |
| 1 OBJECTIVES, SUMMARY AND CONCLUSIONS | 1 |
| 1.1 <i>The aim of the work (PhD study)</i> | 1 |
| 1.2 <i>Materials and methods used</i> | 1 |
| 1.3 <i>Overall conclusions</i> | 8 |
| 1.4 <i>Summary and conclusions of the papers</i> | 10 |
| Paper I. | 10 |
| Paper II. | 11 |
| Paper III. | 11 |
| Paper IV. | 12 |
| 1.5 <i>Contribution to papers</i> | 13 |
| 2 INTRODUCTION..... | 14 |
| 2.1 <i>Energy from biomass</i> | 16 |
| 2.1.1 Biomass conversion technologies | 19 |
| 2.2 <i>Liquid biofuels</i> | 22 |
| 2.2.1 Biodiesel..... | 22 |
| 2.2.2 Bioethanol | 23 |
| 2.2.3 Pyrolysis liquid – bio-oil | 23 |
| 2.3 <i>Lignocellulosic materials</i> | 23 |
| 2.3.1 Extraneous materials..... | 24 |
| 2.3.2 Polysaccharides | 25 |
| 2.3.3 Lignin..... | 27 |
| 3 BIO-OIL..... | 28 |
| 3.1 <i>Bio-oil production</i> | 28 |
| 3.1.1 Reactor configuration | 30 |
| 3.1.2 Heat transfer and supply | 33 |
| 3.1.3 Feed preparation | 34 |
| 3.1.4 Char removal..... | 34 |
| 3.1.5 Liquid collection..... | 35 |

| | | |
|-------|--|----|
| 3.1.6 | Other processes to produce bio-oil | 35 |
| 3.2 | <i>Characterisation of bio-oils</i> | 36 |
| 3.2.1 | Chemical and physical methods for determination the bio-oil properties | 37 |
| 3.2.2 | Physical and chemical properties of bio-oils | 38 |
| 3.2.3 | The stability problem | 41 |
| 3.3 | <i>Processes to slow aging in bio-oils</i> | 43 |
| 3.3.1 | Upgrading of bio-oils..... | 43 |
| 3.3.2 | Catalytic pyrolysis..... | 45 |
| 3.4 | <i>Applications of bio-oils</i> | 47 |
| 3.4.1 | Combustion | 48 |
| 3.4.2 | Power generation | 48 |
| 3.4.3 | Chemicals..... | 49 |
| 4 | SYNTHESIS, CHARACTERISATION AND APPLICATIONS OF MESOPOROUS MATERIALS | 50 |
| 4.1 | <i>MCM-41</i> | 51 |
| 4.1.1 | Hydrothermal stability of mesoporous MCM-41 | 54 |
| 4.2 | <i>SBA-15</i> | 55 |
| 4.3 | <i>Applications of mesoporous materials</i> | 56 |
| 4.4 | <i>The use of metal-modified zeolite catalysts</i> | 57 |
| 5 | SUGGESTIONS FOR FURTHER WORK | 60 |
| | REFERENCES | 62 |
| | PAPER I. | |
| | PAPER II. | |
| | PAPER III. | |
| | PAPER IV. | |

List of Figures

| | |
|---|----|
| Figure 1-1. Pyrolysis-gas chromatography/mass spectrometry equipment. | 5 |
| Figure 1-2. Thermogravimetry/mass spectrometry equipment. | 6 |
| Figure 1-3. The fixed-bed reactor system. | 7 |
| Figure 2-1. Worlds primary energy consumption in 1990. | 14 |
| Figure 2-2. Actual use of bioenergy in the Nordic countries. | 16 |
| Figure 2-3. From multiple biomass resources to a variety of fuels and energy products. | 17 |
| Figure 2-4. Main conversion options for biomass to secondary energy carriers. | 18 |
| Figure 2-5. The process of bioethanol production from lignocellulosics. | 20 |
| Figure 2-6. Cellulose molecule. | 25 |
| Figure 2-7. Hardwood hemicellulose. | 26 |
| Figure 2-8. Softwood hemicellulose. | 26 |
| Figure 2-9. Lignin composition. | 27 |
| Figure 3-1. An example of a bio-oil production process. | 28 |
| Figure 3-2. Concept of the ablative pyrolysis. | 32 |
| Figure 3-3. The rotating cone reactor. | 33 |
| Figure 3-4. Links between pyrolysis oil production, quality and utilisation. | 37 |
| Figure 3-5. Bio-oil fractionation and characterisation. | 38 |
| Figure 3-6. Possibilities for bio-oil applications. | 48 |
| Figure 4-1. X-ray diffraction pattern of a high-quality calcined MCM-41. | 52 |
| Figure 4-2. Liquid-crystal templating (LCT) mechanism for the formation of MCM-41. | 53 |

List of Tables

| | |
|---|----|
| Table 1-1. The main catalyst properties..... | 3 |
| Table 1-2. The experiment and publication set up..... | 4 |
| Table 3-1. Typical bio-oil composition..... | 40 |
| Table 3-2. Physical properties of bio-oils..... | 40 |

1 Objectives, summary and conclusions

1.1 *The aim of the work (PhD study)*

The aim of this PhD study was to improve the bio-oil characteristics with the help of mesoporous materials. Further development and application tests of mesoporous catalysts were the main focus of the work. The tests were carried out with fresh catalysts only in order to obtain preliminary information about the products of catalytic conversion. Measurements to detect the changes of catalysts' activity and crystalline structure were beyond the scope of this work.

1.2 *Materials and methods used*

Barkless spruce wood (*Picea abies*) was milled and sieved and a fraction of a particle diameter of $>45\ \mu\text{m}$ was used in the microscale experiments and a particle diameter of 0.5-1.4 mm was used in the fixed bed experiments. The water content of the spruce wood was approximately 6 %.

To study the effect of biomass feedstock on the catalytic upgrading of bio-oil, some experiments were performed with miscanthus biomass (*Miscanthus sp.*) in the fixed bed reactor. The miscanthus was milled and sieved. The sample had a particle size of 1.0-1.5 mm and its moisture content was 6 %.

Seven different mesoporous materials have been tested; four Al-MCM-41 catalysts (K1-K4), a commercial FCC catalyst (K5) and two SBA-15 catalysts (K6-K7). The Al-MCM-41 catalyst group had a Si/Al ratio of 20 and consisted of an unmodified Al-MCM-41 (K1), two catalysts with enlarged pores (K2 and K3) and a transition metal (Cu) modified catalyst (K4). The pore enlargement in sample K2 was carried out with a spacer (mesitylene, C_9H_{12}), and in sample K3 by altering the template chain length from

C₁₄ to C₁₈. The SBA-15 catalyst group consisted of a pure siliceous SBA-15 (K6) and an SBA-15 catalyst with aluminium incorporation (K7).

Examples of Al-MCM-41 and SBA-15 preparations are the following:

Al-MCM-41

Molar composition: 1 Si : 0.06 Al : 0.4 C₁₄ : 68 H₂O.

The surfactant, C₁₄H₂₉(Me)₃NBr (tetradecyltrimethylammonium bromide, 15.15 g), was dissolved in water (95 g). Sodium-aluminate (0.43 g) was added and the solution was stirred overnight. Silica source, sodium-meta-silicate-5-hydrate (8.9 % Na₂O + 28 % SiO₂, 19.4 g), H₂SO₄ (10 %, 5.6 g) and water (15 g) was added, and the solution was stirred for 30 minutes. The pH was adjusted to ~10.

The solution was filled in a teflon-flask, heated at 100°C for 6 days, washed with distilled water or centrifuged until pH 5 was obtained. The white product was dried at 100°C overnight.

SBA-15

Molar composition: 1 Si : 0.02 EO₂₀PO₇₀EO₂₀ : 5 HCl + water.

The synthesis was carried out at 40 °C.

The surfactant (poly(ethylene glycol)-block-poly(propylene glycol)-block-poly(ethylene glycol): EO₂₀PO₇₀EO₂₀) was heated to 50 °C overnight.

Hydrochloric acid (120.6 g, 2M) was heated to 40 °C. Water (30 g) was added and the solution was heated until the temperature was stabilised at 40 °C. The surfactant (4.6 g) was added and this mixture was stirred for 5 hours. TEOS (tetraethoxysilan, 9 g) was added dropwise, and the clear solution was stirred overnight.

The homogenous, white solution was transferred to a Teflon flask, which was sealed with Teflon tape and heated at 100 °C for 48 hours.

The white solid was washed with warm distilled water or centrifuged until pH 5 was obtained. The white product was dried at 100°C overnight.

The main catalyst properties are summarised in Table 1-1.

Table 1-1. The main catalyst properties.

| CATALYST NAME | K1 | K2 | K3 | K4 | K5 | K6 | K7 |
|---|-----------|-----------|-----------|-----------|-----------|---------------|-----------|
| Catalyst type | MCM-41 | MCM-41 | MCM-41 | MCM-41 | FCC | SBA-15 | SBA-15 |
| Surface area (m²/g) | 917 | 947 | 928 | 816 | 178.4 | 817 | 536 |
| Total pore volume (ml/g) | 1.23 | 1.43 | 1.26 | 1.46 | N/A | 1.53 | 1.23 |
| Mesopore diameter (Å) | 24 | 28 | 30 | 24 | 24.26 | 68; 78- 95 | 63; 78 |

As Table 1–1. shows, the surface areas of most of these catalysts were high. The FCC (K5) catalyst has a much lower surface area. The total pore volume was similar in all cases. The pore enlargement of the Al-MCM-41 was successful, as Table 1–1. indicates (K2 and K3), it can also be seen that the SBA-15 catalyst group (K6 and K7) has considerable larger pore sizes than the MCM-41 catalysts.

These catalysts were tested in three different reactors, and the results are published, see Table 1–2.

Table 1-2. The experiment and publication set up.

| | Py-GC/MS | TG/MS | Fixed bed reactor |
|------------------------|-----------------|----------------|--------------------------|
| spruce | Paper I and II | Paper I and II | Paper III |
| spruce + K1 | Paper I and II | Paper I and II | Paper III |
| spruce + K2 | Paper I and II | Paper I and II | Paper III |
| spruce + K3 | Paper I and II | Paper I and II | Paper III |
| spruce + K4 | Paper I and II | Paper I and II | Paper III |
| spruce + K5 | Paper IV | Paper IV | Paper III |
| spruce + K6 | Paper IV | Paper IV | Paper III |
| spruce + K7 | Paper IV | Paper IV | Paper III |
| miscanthus | - | - | Paper III |
| miscanthus + K1 | - | - | Paper III |
| miscanthus + K4 | - | - | Paper III |
| miscanthus + K5 | - | - | Paper III |
| miscanthus + K7 | - | - | Paper III |

Pyrolysis-gas chromatography/mass spectrometry (Py-GC/MS, Fig. 1–1.) experiments were performed at 450 and 500 °C for 20 sec in a Pyroprobe 2000 pyrolyser (Chemical Data System) equipped with a platinum coil and quartz sample tube interfaced to a gas chromatograph (Agilent 6890) coupled with a mass selective detector (Agilent 5973) operating in electron impact mode (EI) at 70 eV. The temperature of the GC/MS interface was held at 250 °C. A helium carrier gas of 20 ml/min flow rate purged the pyrolysis chamber held at 250 °C. A split of the carrier gas (1:20) was applied. The GC separation was carried out on a fused silica capillary column (Hewlett-Packard 5MS), 30 m x 0.25 mm. A temperature program from 50 to 300 °C at 10 °C/min was applied with an isotherm period of 1 min at 50 °C and of 4 min at 300 °C. Identification of the GC/MS peaks was based on comparison to spectra of NIST 98 spectrum library.

With the help of the Py-GC/MS method we are able to separate and identify the gases and vapours produced during fast pyrolysis of wood and wood + catalyst samples.

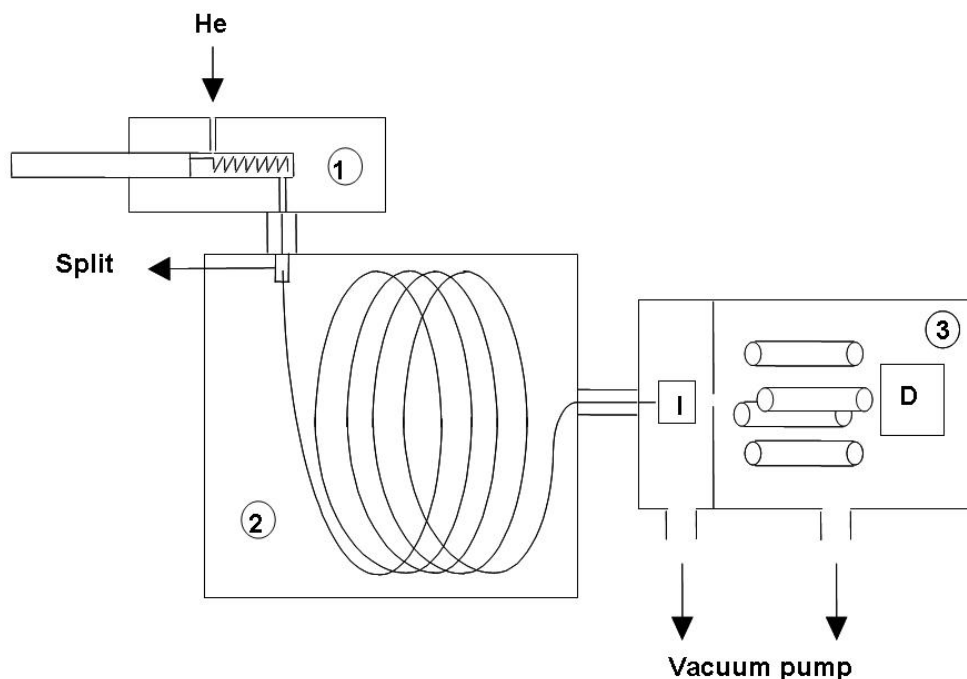


Figure 1-1. Pyrolysis-gas chromatography/mass spectrometry equipment. 1: pyrolysis chamber, 2: gas chromatograph, 3: mass spectrometer, I: ion source, D: detector.

The thermogravimetry/mass spectrometry (TG/MS) experiments (Fig. 1–2.) were carried out on a Perkin-Elmer TGS-2 thermobalance coupled to a HIDEN HAL 2/301 PIC quadrupole mass spectrometer through a glass-lined metal capillary heated to 300 °C. The temperature range of the experiments was 50-800 °C in argon atmosphere, and the heating rate was 20 °C/min. A portion of the evolved products (approximately 1 %) was introduced into the mass spectrometer operating in the electron impact ionization mode at 70 eV electron energy. The intensity of the products was normalised to the sample mass and the intensity of the ^{38}Ar isotope in order to avoid errors caused by the shift in sensitivity of the mass spectrometer. In this case the heating rate was lower compared to the Py-GC/MS method. Thus, a slow thermal decomposition of biomass could be studied. With the help of the thermobalance we got information concerning the sample mass, and we could monitor the profile of the arising volatile compounds, (by

their fragments) as a function of temperature (time) with the help of the mass spectrometer.

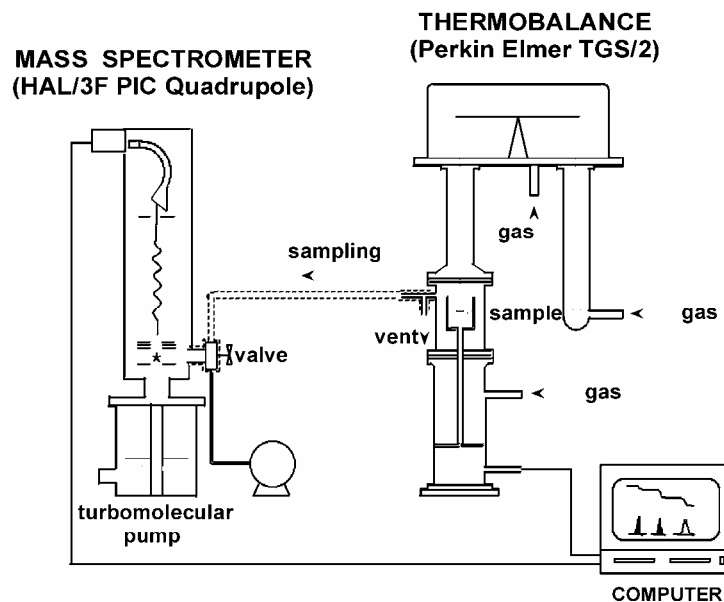


Figure 1-2. Thermogravimetry/mass spectrometry equipment.

The lab-scale experiments were performed in a fixed bed reactor (Fig. 1–3. and Fig. 1. in Paper III), with gas, fluid and char separation. In this reactor we got measurable amounts of pyrolysis gases and liquids, and it was possible to analyse the different phases separately. The reactor was filled with 0.7 g catalyst, or glassbeads for the non-catalytic tests and the piston was filled with biomass (1.5 g). Glasswool was placed in the bottom of the reactor, to the top of the piston and to separate the catalyst and the biomass bed. The system was always heated in the presence of N_2 (30 cc/min) and, by using a temperature controller, the temperature of each zone of the furnace was controlled. The reaction temperature was 500 °C. As soon as the reaction temperature was achieved, biomass entered the reactor and the experiment started. During the time of the experiment (15 min) the piston did not return to its original position in order to be checked after the end of the experiment. The experiments were performed in the presence of N_2 . The liquid products were collected in a liquid bath (-17 °C) and quantitatively measured in a pre-weighted glass receiver.

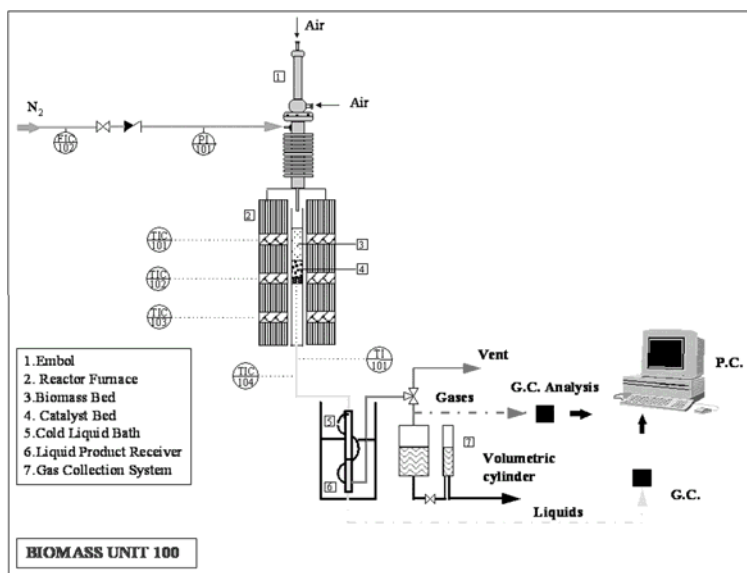


Figure 1-3. The fixed-bed reactor system.

The two phases of the liquid – the organic phase and the aqueous phase – were separated with an organic solvent. The gaseous products were collected and measured by water displacement. The amount of coke formed was measured by direct weighing. The liquid samples were analysed by GC/MS analysis in a HP 5989 MS ENGINE (Electron energy 70eV; Emission 300V; Helium flow rate: 0.7cc/min; Column: HP-5MS (30m x 0.25mmID x 0.25 μ m)) for the identification of compounds in the organic phase. The gaseous products were analysed in a HP 6890 GC, equipped with four columns (Precolumn:OV-101; Columns: Porapak N, Molecular Sieve 5A and Rt-Qplot (30m x 0.53mm ID) and two detectors (TCD and FID).

1.3 Overall conclusions

There are several reaction routes competing during biomass pyrolysis and after the pyrolysis in the hot vapour. Due to the catalysis, the particular reaction rates may change or new reaction routes occur, thus changing the product yields. The reactors used in this thesis have different configurations and heating rates which also affect the reaction rates during the pyrolysis and the upgrading process, and this is shown, for example, in the acids yield. The Py-GC/MS showed the highest acid yields, and the yields were higher than that of the non-catalytic sample. At the fixed bed reactor system, the aqueous phases were separated and not analysed. These probably contained most of the acids formed in the reaction. The TG/MS reactions showed a reduction in the acid yield compared to the non-catalytic sample, but here, the pyrolysis rate was slower and the residence time was longer, the acids might have reacted further. The amount of char increased in the microscale experiments (TG/MS and Py-GC/MS) but decreased in the fixed bed reactor.

However, some trends can be observed when catalysts are used. As a result of the catalytic cracking of the vapours, the amount of water increased compared to the non-catalytic experiments with all the catalysts in each of the reactors. When spruce was pyrolysed in the presence of unmodified Al-MCM-41 catalyst, the yields of furan ring containing compounds increased considerably. The yields of phenols, light phenol substitutes, hydrocarbons and PAHs increased, but the yields of alcohols, aldehydes, heavy phenol substitutes and heavy compounds decreased. With increasing pore diameter the changes show the same trends, but in a smaller degree. Metal incorporation into the parent Al-MCM-41 without any pore modifications shows similar yields as the catalyst with the largest pores, however, there can be small differences in the yields of a few compounds.

Spruce pyrolysis in the presence of SBA-15 catalyst shows similar yields as the uncatalysed experiments in most cases, however, the yields of furan-ring containing compounds increased and some other compounds varied slightly. Aluminium incorporation into the SBA-15 framework changed the product yields considerably. Both the desirable and the undesirable product yields increased. The SBA-15 catalysts

compared to the MCM-41 catalysts, has lower surface areas, especially the aluminium incorporated SBA-15, and considerably larger mesopores. During spruce pyrolysis in the presence of SBA-15 catalysts, compared to the Al-MCM-41 catalysts, increased the desirable product yield, mostly with Al-SBA-15, however, in this case, the undesirable product yield increased considerably as well.

According to the published results, among the studied catalysts, the FCC catalyst produces the best-quality bio-oil with the spruce biomass. This catalyst is also the cheapest one as it is already available commercially. Al-MCM-41 type catalyst does not perform well with this biomass type, and furthermore, it has a weak hydrothermal stability. SBA-15 catalyst with aluminium incorporation can have a potential, but the performance and the price is probably not competitive with the FCC catalyst. The difference in catalyst performance is much greater than expected when the biomass is changed. With miscanthus, the unmodified Al-MCM-41 catalyst performs best and the FCC catalyst does not produce a good quality product. The SBA-15 catalyst's present performance is similar both with miscanthus and spruce. The differences between these two biomasses can be attributed to the miscanthus' higher ash content (the miscanthus biomass contains approximately 4 % ash), which can contain metals that catalyse some reactions. The miscanthus has also higher cellulose and hemicellulose and lower lignin content, which can also contribute to the differences between the yields of obtained compounds.

1.4 Summary and conclusions of the papers

Paper I.

The effects of Al-MCM-41 catalysts on the thermal decomposition of barkfree spruce wood were studied in this paper. Samples of wood – catalyst mixtures were subjected to analytical pyrolysis at 500 °C for 20 seconds using on-line pyrolysis-gas chromatography/mass spectrometry (Py-GC/MS). Thermogravimetry (TG) experiments were performed to monitor the weight loss under slow heating rate conditions (20 °C/min) from 50 to 800 °C.

MCM-41 type mesoporous catalysts converted the pyrolysis vapours into lower molecular weight products, and hence, more desired bio-oil properties could be achieved. The catalytic properties of MCM-41 materials can be significantly improved when specific transition metal cations or metal complexes are introduced into the structure. Pore enlargement allows the processing of larger molecules. In this paper, four catalyst tests were published; all of them were Al-MCM-41 type catalysts with a Si/Al ratio of 20. These catalysts were: an unmodified Al-MCM-41, a transition metal (Cu) modified Al-MCM-41, and two Al-MCM-41 catalysts with enlarged pores. Different pore sizes were obtained by altering the chain length of the template and by applying a spacer.

Due to the activity of the catalysts, the product distribution of pyrolysis vapours changed significantly. In accordance with published reports, higher coke and water formation was observed during the reaction in the presence of the catalysts. The various catalysts showed different influences on the product distribution, and the greatest difference was achieved by using the unmodified Al-MCM-41 catalyst.

Thermogravimetric experiments indicated that the applied Al-MCM-41 catalysts increase the char and the water yield during the thermal decomposition of biomass. Nevertheless, the product distribution is altered due to the transformation of the volatile pyrolysis products by the catalysts.

Paper II.

In this paper, Al-MCM-41 type mesoporous catalysts were used for converting the pyrolysis vapours of spruce wood in order to obtain better bio-oil properties. Four Al-MCM-41 type catalysts with a Si/Al ratio of 20 were tested. The catalytic properties of Al-MCM-41 catalyst were modified by pore enlargement, which allows the processing of larger molecules and by introduction of Cu cations into the structure.

Spruce wood pyrolysis at 500 °C was performed and the products were analysed with the help of on-line pyrolysis-gas chromatography/mass spectrometry (Py-GC/MS). In addition, thermogravimetry/mass spectrometry (TG/MS) experiments were applied for monitoring the product evolution under slow heating conditions (20 °C/min) from 50 to 800 °C.

Levogluconan is completely eliminated, while acetic acid, furfural and furanes become quite important among cellulose pyrolysis products over the unmodified Al-MCM-41 catalyst. The dominance of phenolic compounds of higher molecular mass is strongly cut back among the lignin products. Both the increase of the yield of acetic acid and furan and the decrease of large methoxyphenols are repressed to some extent over catalysts with enlarged pores. The Cu modified catalyst performed similarly to the catalyst with enlarged pore size in converting the pyrolysis vapours of wood, although its pore size was similar to the unmodified Al-MCM-41.

Paper III.

Seven mesoporous catalysts were compared in this paper in how they can convert the pyrolysis vapours of spruce wood in order to obtain improved bio-oil properties. Four Al-MCM-41 type catalysts with a Si/Al ratio of 20, a commercial FCC catalyst, a pure siliceous SBA-15 and an aluminium incorporated SBA-15 materials were tested. The catalytic properties of Al-MCM-41 catalyst were modified by pore enlargement that allows the processing of larger molecules and by introduction of Cu cations into the structure.

Spruce wood pyrolysis at 500 °C was performed in a lab-scale fixed bed reactor, the solid, gaseous and liquid products were separated and the gases and the organic part of the liquids were analysed with the help of gas chromatography/mass spectrometry.

The gas yield increased in each catalytic case. The coke yield remained the same in some cases, whereas in other experiments a slight decrease could be observed compared to the non-catalytic experiments. The yield of the aqueous part in the liquid phase increased in the catalytic runs.

The obtained products in the organic phase were grouped into eight groups and further into desirable and undesirable product groups and the yields were evaluated. In the catalytic experiments the hydrocarbon and phenol yields increased, while the carbonyl yields decreased. All catalysts tested reduced the undesirable product yield, while the desirable product yield remained the same or, in some cases, increased.

To study the feedstock effect on the catalytic upgrading of the pyrolysis vapours, some tests were performed with miscanthus biomass. Comparing the bio-oil properties obtained from miscanthus and spruce it was found that the bio-oil produced from miscanthus has better characteristics. With spruce the FCC, with miscanthus the unmodified Al-MCM-41 are the best performing catalysts. Concerning the pyrolysed feedstocks, with miscanthus a better quality bio-oil has been obtained.

Paper IV.

Spruce wood was subjected to analytical pyrolysis at 500 °C for 20 sec using on-line pyrolysis-gas chromatography/mass spectrometry (Py-GC/MS). The volatile decomposition products were separated by gas chromatography and the components were analysed by mass spectrometry. In addition, thermogravimetry/mass spectrometry (TG/MS) experiments were applied for monitoring the weight loss and the product evolution under slow heating conditions (20 °C/min) from 50 to 800 °C.

New mesoporous materials (SBA-15) and a commercial FCC catalyst were tested in this work. During the pyrolysis experiments, the biomass and the catalyst were placed in two layers, with the catalyst on top in order to ensure that the pyrolysis vapours pass through the catalyst.

Due to the catalytic activity, the product distribution of pyrolysis vapours changed significantly. As expected, higher coke and water formation was observed during the reaction, and the yields of several compounds were altered. The amount of the evolved organic acids and aldehydes decreased, while the amount of hydrocarbons increased.

The studied catalysts showed different influences on the product distribution and the largest effect was achieved by using the commercial FCC catalyst. The results show that catalyst usage can be advantageous in the production of better quality bio-oils.

1.5 Contribution to papers

Judit Adam has contributed to the papers as follows:

Paper I and II.

Judit Adam has prepared the catalyst particles under the guidance of Michael Stöcker, Merete H. Nilsen and Aud Bouzga and performed part of the experiments. Evaluation and analysis of the experimental results were performed in cooperation with Marianne Blazsó and Erika Mészáros.

Paper III.

Judit Adam has prepared the catalyst particles in cooperation with Michael Stöcker, Merete H. Nilsen and Aud Bouzga, performed all the experiments and carried out the evaluation and analysis of the experimental results in cooperation with Eleni Antonakou.

Paper IV.

Judit Adam has prepared the catalyst particles in cooperation with Michael Stöcker, Merete H. Nilsen and Aud Bouzga and performed part of the experiments. Evaluation and analysis of the experimental results were performed in cooperation with Marianne Blazsó and Erika Mészáros.

2 Introduction

The largest single portion of the energy used is derived from petroleum, the renewable energy usage is 13-14 % from biomass and 6 % from hydro (Fig. 2-1.).

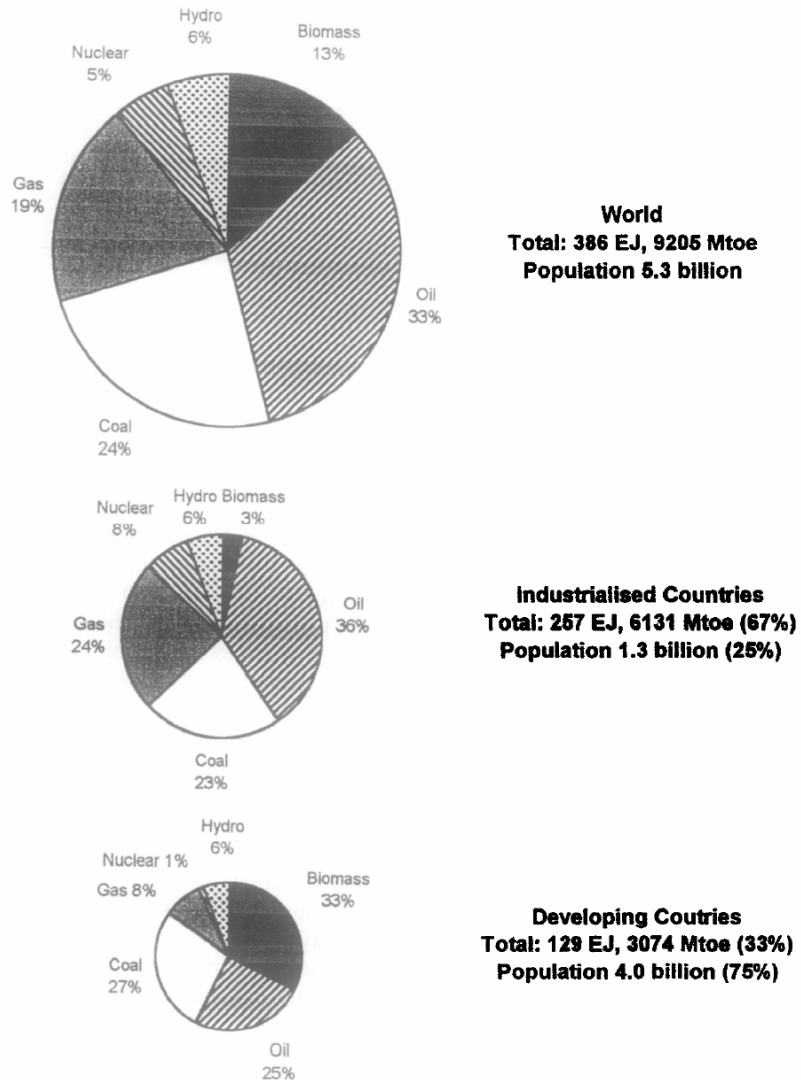


Figure 2-1. Worlds primary energy consumption in 1990 [1]. Industrialised countries: all OECD countries plus E. Europe and ex-USSR.

Because much of the oil is produced in unstable regions of the world, the high dependence on outside sources of oil resulted in several price shocks and caused considerable damage to the economy in the 1970s. As a result, many countries ought to develop new sources of energy that would reduce oil imports and improve their strategic and economic strength. Besides these economic issues, in the near future we are also faced with potentially even greater environmental consequences if we do not change our energy use patterns. Renewable energy is of growing importance in satisfying environmental concerns compared to the use of fossil fuel and its contribution to the greenhouse effect. A future lack of fuel resources and the environmental effects related to energy conversion of these fuels have put focus on renewable energy sources. Utilisation of wind, solar and biomass for energy purposes are areas with extensive R&D activities. Biomass is regarded as the most important renewable energy source in the nearest future. In 1990, the EU member states had a target of an increase of the use of renewable energy from 6 % to 12 % by the end of 2010, and bioenergy will contribute for a major part (approximately 2/3) of this increase. The large role biomass is expected to play in the future energy supply can be explained by the fact that biomass fuels can substitute more or less directly for fossil fuels in the existing energy supply infrastructure. Intermittent renewables such as wind and solar energy are more challenging to the ways we distribute and consume energy.

The total use of biomass in the Nordic countries is about 235 TWh (Fig. 2–2.), which is even more than the total hydropower electricity and approximately 40 % of the total use of biomass energy in Europe. In Finland and Sweden, the major consumers of biofuels are the pulp and paper industry, using bark peat and black liquor. In Denmark, it is essential the combustion of straw bales in small boilers for district heating. In Norway, use of wood stoves is very common.

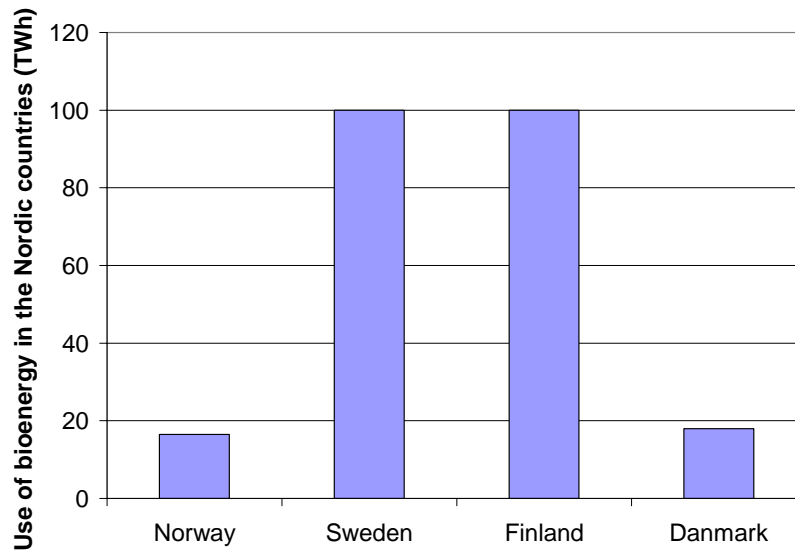


Figure 2-2. Actual use of bioenergy in the Nordic countries [2].

In Norway, the total energy consumption is 219 TWh of which the total stationary energy consumption makes 165 TWh. The use of bioenergy is 16.5 TWh and half of it is consumed in private households. In Sweden the bioenergy use is about 17 %, in Denmark 8 % and in Finland 25 % of total energy consumption [2].

2.1 Energy from biomass

Biomass is a complex resource that can be processed in many ways leading to a variety of products. This is reviewed by Chum and Overend [3] and in Fig. 2–3. However, for renewable processing of biomass the cost of technologies still needs to be decreased through research, development, demonstrations, and diffusion of commercialised new technologies. Valuing the environmental and social contributions that biomass inherently makes can also help to increase its use. Broad societal consensus on land and water use issues is needed. Each route requires integrated efforts across federal agencies, multiple industrial sectors, academia, national laboratories, non-profit organisations, professional societies etc.

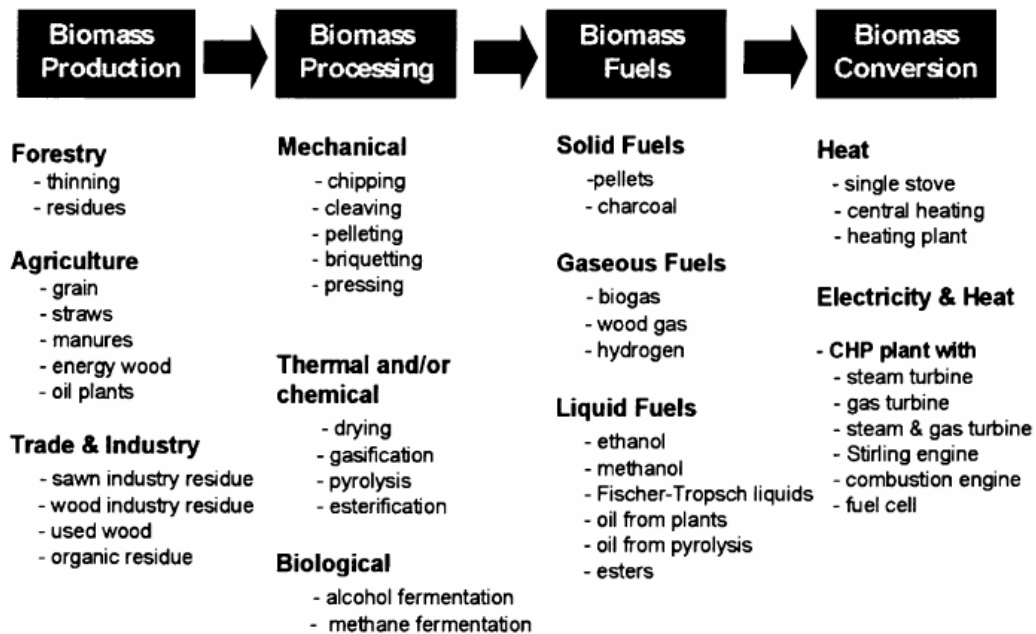


Figure 2-3. From multiple biomass resources to a variety of fuels and energy products [3].

As we can see in Fig. 2–3. and [4] the biomass conversion technologies are mostly grouped as the following:

- physical/chemical processing
- thermochemical (via heat treatment)
- biological (via microbiological action)

There are several ways we consume energy. Basically, we need heat, electricity and fuel for transportation. Production of these services from biomass has to meet the possibilities. Faaij [5] has reviewed the different biomass applications and the different conversion technologies. This is summarized in Fig. 2–4.

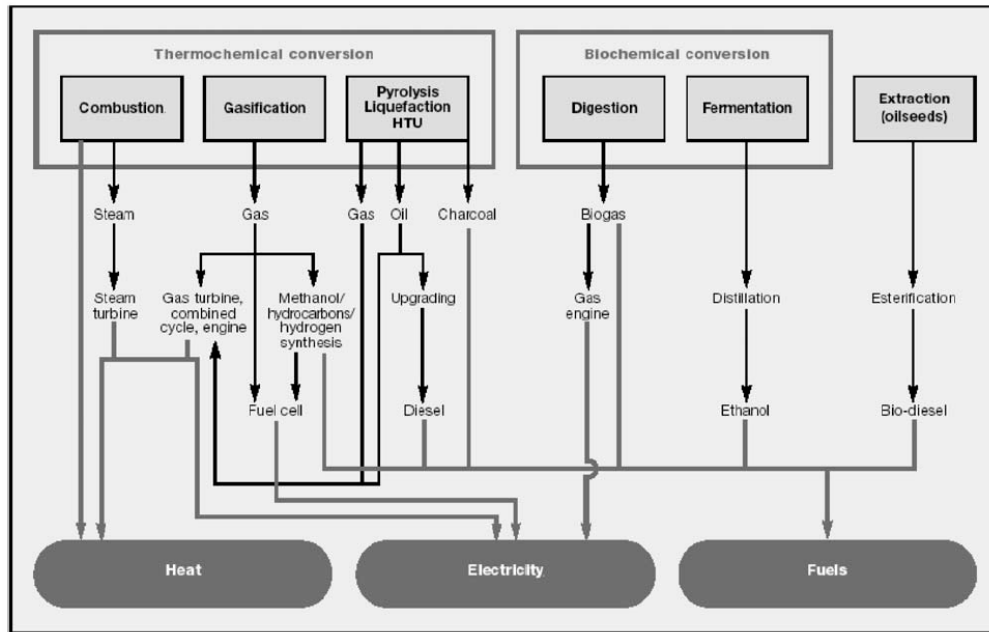


Figure 2-4. Main conversion options for biomass to secondary energy carriers [5].

Bridgwater et al. [6] reviewed and evaluated the projects on how biomass conversion technologies can meet environmental requirements. The gaseous emissions were studied, and the recommended emission controls were discussed using biofuel (solid, liquid bio-oil and biogas from gasification) in combustion applications (engines, boilers and gas turbines). They concluded that the solid fuel combustion is the most established technology for biomass utilisation. Bio-oil needs new fuel injection systems to control NO_x and bio-oils further need to be standardised to be regarded as a commercial fuel. The problem with biofuel combustion is the size: how to control emissions while ensuring that the technologies involved do not bankrupt the overall process. Biomass-based systems have traditionally small system capacities, which limit both scale economies and system efficiencies, making it difficult to absorb the extra costs of emission control.

2.1.1 Biomass conversion technologies

Some examples of the biomass conversion technologies are the following:

Direct combustion to provide heat

Biomass combustion is commercially available and it is convenient to produce heat and power at high (80-90 %) efficiency, however in this case the efficiency of the power production is rather low (15-30 %). Production of heat in district heating systems increases the overall efficiency. The technology represents a minimum risk to investors.

Gasification to provide fuel gas

Biomass gasification with turbine or engine to power production has an efficiency of about 40-50 %. This technology is also commercially available. The biomass gasification process is also referred as 'pyrolysis by partial oxidation'. It intends to maximise the gaseous product, and generally takes place between 800 and 1000 °C. The product is fuel gas, which can be upgraded to methanol by synthesis, combusted to generate heat, or can be used in engines, high temperature turbines or fuel cells to generate power. The gas is very costly to store or transport because of the low energy density so it has to be used locally.

Biological gasification to produce hydrogen

The main objective of this process is to produce hydrogen from crops and wastes employing anaerobic, thermophilic or hyperthermophilic microorganisms in order to supply the fuel cell industry with clean hydrogen gas derived from renewable resources. The final product is hydrogen.

Extraction and production of esters from oilseeds

Oilseeds, like rapeseed can be extracted and converted to esters and are well suited to replace diesel. Rapeseed production and subsequent esterification (using methanol to produce rapeseed methyl ester, RME) and distribution is an established technology in Europe. However, RME fuel chains are unfavourable when compared to perennial crops, meaning the net energy production per hectare is low. [5]

Biological degradation to produce ethanol

Ethanol is world-wide produced from sugar and starch, this is a well established technology. Ethanol is generally used mixed with gasoline which at low percentages (up to 20 %) can be done without adaptations to the current vehicle fleet. Ethanol has the advantage to lower NO_x and dust emissions compared to gasoline use only. However ethanol production from food crops is far from competitive when compared to gasoline and diesel prices.

Hydrolysis of lignocellulosic biomass can open the way toward low cost and efficient ethanol production. This method uses cellulase enzymes and yeast to convert the wood, however, cheap and efficient hydrolysis processes are still under development and some fundamental issues need to be resolved.

Biomass can be converted to ethanol by acid- or enzymatic-based approaches (Fig. 2–5.).

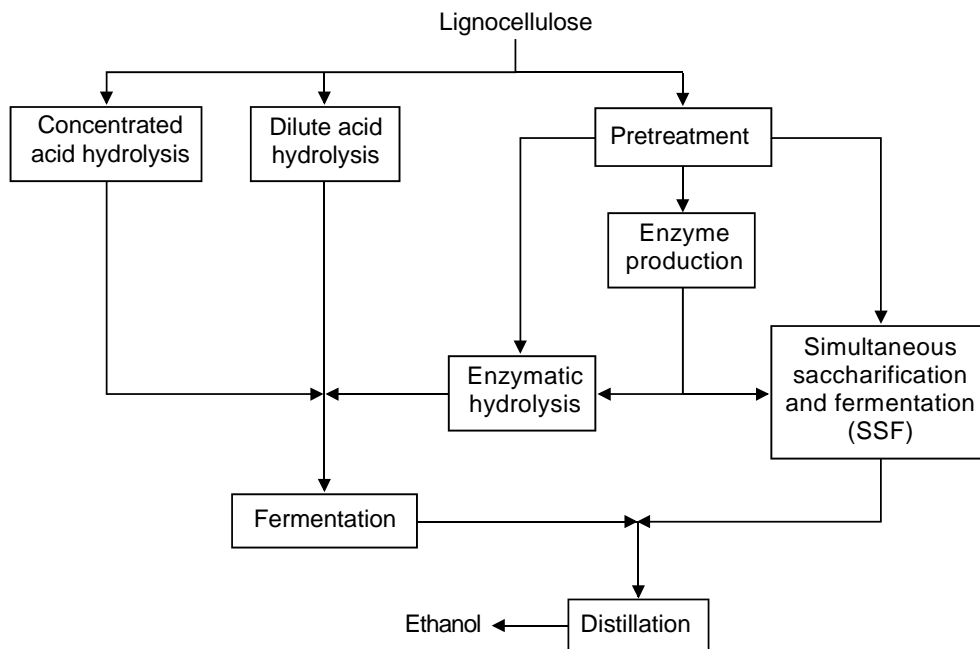


Figure 2-5. The process of bioethanol production from lignocellulosics.

In either option, the material must first be processed in some way to reduce its size and facilitate subsequent handling. Then acids or enzymes are used to break apart or

hydrolyse the hemicellulose and cellulose chains to form their monomeric sugars. If enzymes are used, a pretreatment step is necessary to render the cellulose fraction accessible to the cellulase enzymkomplex. The reason is that the native biomass is recalcitrant to the action of cellulase enzymes due to its crystallinity, presence of lignin and hemicellulose, acetylation of hemicellulose and inaccessible surface area. The formed monomeric sugars are fermented to ethanol by adding yeast, bacteria, or other suitable organisms, and the ethanol is recovered by distillation or with other separation technologies for use as fuel. The lignin from the biomass can be burned to provide all the heat and electricity for the process or converted into valuable chemicals or fuels.

Pyrolysis

Pyrolysis is the thermal degradation of biomass in the absence of oxydising agent at 200-500°C. Depending on the method used, the process leads to a mixture of tar vapours, gases and highly reactive carbonaceous char of different proportions. Using high heating rates, moderate temperatures and very short residence times the tar compound can be maximised (bio-oil production), while using low temperatures and long residence times the char yield can be maximised. The char produced can be upgraded to activated carbon, domestic cooking fuel or barbecuing.

Heat and power is being produced in stationary power plants which, due to their size, have many opportunities to deal with several types of (problematic) feed, and to clean gases. Production of transportation fuels is more challenging. As the transportation fuel is used in many vehicles, any modifications in the engine need to take place in each of the vehicles, which makes a new fuel application expensive. Biofuels that can be used without engine modifications have great opportunities in the near future. These are for example biodiesel and bioethanol/gasoline blends.

2.2 Liquid biofuels

The advantage of producing a liquid fuel is the improved transport possibilities (i.e. lower costs) that is, when the fuel is not used at the production site, but it needs to be stored and transported. Liquid fuels are cheapest and easiest to transport, as they have the largest energy density. Solid fuels are easy and safe to transport, but it can be more expensive, as they have lower energy density. Gaseous fuels are expensive, difficult and more dangerous to transport, these should be used at the production site. Heat can only be transported at short distances and must be used at the production site.

Global interest in liquid fuels has increased considerably over the last decade despite the fall in oil prices after 1981. The EU Commission has set a target of up to 5 % of the liquid transport fuel market could be supplied by biodiesel and bioethanol by 2010 [1].

Examples of liquid bio fuels with potential are biodiesel, bioethanol and bio-oil.

2.2.1 Biodiesel

Biodiesel comprises ethyl or methyl esters of edible oils. Rape methyl ester (RME) produced from oilseed rape is the main source in Europe and Canada, while soya oil is used in the USA [1]. Biodiesel can be used pure or blended with mineral diesel in existing engines with only minor modifications and a small reduction in engine performance. Lapuerta et al. [7] investigated the emissions from a diesel engine running on diesel, biodiesel and blends. They concluded that the particular matter emissions were reduced for every mode tested as the concentration of any of the tested biodiesel fuels were increased in the blend. Additionally, the presence of oxygen on the ester molecules did not lead to increase in NO_x formation. On the contrary certain decrease was observed at high load.

2.2.2 Bioethanol

Ethanol has a number of very favourable properties that are desirable for use as a neat or pure fuel. Its high heat of vaporisation, low flame temperature, greater gas volume change, high specific energy, high octane, and other characteristics make it possible to achieve about a 15 % higher efficiency for ethanol than for gasoline in properly optimised spark-ignition engines. This improvement can largely compensate for the fact that ethanol has about two-thirds of the volumetric energy content of gasoline, and a vehicle should be able to travel about 75 % to 80 % of the distance on a given volume of ethanol as on the same volume of gasoline. From an economic perspective, this means neat or pure ethanol is worth about 75 % to 80 % of the pump price of gasoline. Using ethanol-gasoline blended fuel instead of gasoline alone, especially under fuel rich conditions, can lower HC, CO and NO_x emissions [8]. Hansen et al. [9] reviewed the tests on ethanol-diesel fuel blends. They stated that ethanol in the fuel reduces the particulate matter in each case, but its effect on CO, hydrocarbon and NO_x emission was not clear. Furthermore, ethanol can be blended in diesel up to 10 % without any significant effect on the engine performance.

2.2.3 Pyrolysis liquid – bio-oil

Pyrolysis liquid is referred to many names including pyrolysis oil, bio-oil, bio-crude oil, biofuel-oil, wood liquids, wood oil, liquid smoke, wood distillates, pyroligneous tar, pyroligneous liquid and liquid wood. The crude bio-oil is dark brown and approximates to biomass in elemental composition. The application possibilities and the combustion tests are described in Chapter 3.4.

2.3 *Lignocellulosic materials*

Lignocellulosic materials are of interest as a raw material for bioenergy production since they are available in large amounts and are relatively cheap. Since the chemical composition and physical characteristics differ between various raw materials, the processing of the materials to produce energy differs as well as the yield obtained.

Lignocellulosic materials consist of three major components, typically, about 35 % to 50 % is composed of cellulose, and another 20 to 35 % is made up of hemicellulose. Lignin is the third major constituent and the rest is typically much smaller amounts of ash, soluble phenolics and fatty acids called extractives, and other minor components. Generally, softwoods contain more lignin than other lignocellulosic materials.

The wood system is classified for convenience into three major components, extraneous substances, polysaccharides, and lignin.

2.3.1 Extraneous materials

The extraneous component refers to all non-cell wall materials. This component consists of an astonishingly wide variety of chemicals. Based on their solubilities in water and neutral organic solvents, these chemicals can be classified as extractives or non-extractives. The extractives can be crudely divided into three groups, namely, terpenes, resins and phenols. The terpenes are regarded as isoprene polymers and are a source of turpentine in industrial processes. Related to terpenes are terpene alcohols and ketones. The resins include a wide variety of non-volatile compounds, including fats, fatty acids, alcohols, resin acids, phytosterols, and less known neutral compounds in small amounts. The phenols consist of a large number of compounds, the most important among them are tannins, heartwood phenols, and related substances. In addition, low molecular weight carbohydrates, alkaloids, and soluble lignin are extracted.

The non-extractives mainly consist of inorganics mostly present in ash minerals. The dominating components are alkali and alkali earth carbonates, and oxalates. Silica deposited as crystals is especially abundant in straws; furthermore, small amounts of non-cell-wall substrates, such as starch, pectin, and protein are not extractable.

In spite of their small quantity, the role of extraneous compounds is very significant in that they render cellulose not only resistant to decay and insect attack but also inhibitive to pulping and bleaching.

2.3.2 Polysaccharides

The polysaccharide component consists of high-molecular weight carbohydrates, namely, cellulose and hemicellulose, which amount to 60 to 80 % of the total wood.

Cellulose

Cellulose is the major component of cell walls of wood fibre and is a linear polymer of D-glucose molecules bound together by β (1,4)-glycosidic linkages. Strictly speaking, the repeating units are cellobiose molecules. The degree of polymerisation (the number of glucose molecules in a cellulose chain) is normally in the range of 7500-15000 for plant cellulose. The cellulose molecule is shown in Fig. 2-6.

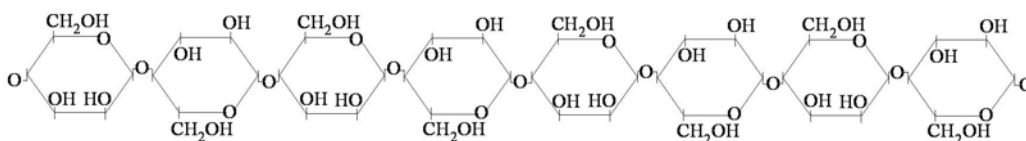


Figure 2-6. Cellulose molecule.

The cellulose chains are bound together by hydrogen bonds to form a very rigid macromolecular structure, microfibrils, with diameters in the range of 10-25 nm. Microfibrils are built up to fibrils and finally to cellulose fibres. Most of the cellulose chains are highly ordered or crystalline, due to hydrogen bonding occurring between linear molecules, but small parts of the cellulose are amorphous. The degree of crystallinity varies within different plants.

Hemicellulose

Hemicellulose, an amorphous heterogeneous group of branched polysaccharides, surrounds the cellulose fibres and intrudes into the cellulose through pores. Xylose, arabinose, mannose, glucose, glucuronic acid and galactose are the major sugar residues. The role of this component is to provide a linkage between lignin and cellulose. In its natural state, it exists in an amorphous form and can be divided into two categories, cellulosans and polyuronides. Cellulosans include all those hemicelluloses, which are polymers, whose building blocks are monomers of single sugars, including

hexosans, such as mannan, galactan, and glucosan, and pentosans such as xylan and arabinan. Polyuronides are hemicelluloses, which contain large amounts of hexuronic acids and some methoxyl, acetyl, and free carboxylic groups. Hemicellulose structure is characterised by a long, linear backbone of one repeating sugar type, with short, branched side chains composed of acetate and sugars. The degree of polymerisation is about 200 for hemicellulose. The composition of hemicellulose varies between species and particularly between soft- and hardwoods.

Hemicellulose is composed of shorter chain polysaccharides, and it is the principal non-cellulosic fraction of polysaccharides. Hardwood hemicellulose is rich in xylan polymers with small amounts of mannan, and is shown in Fig. 2-7., whereas softwood hemicellulose is rich in mannan polymers and contains significant quantities of xylans, as shown in Fig. 2-8.

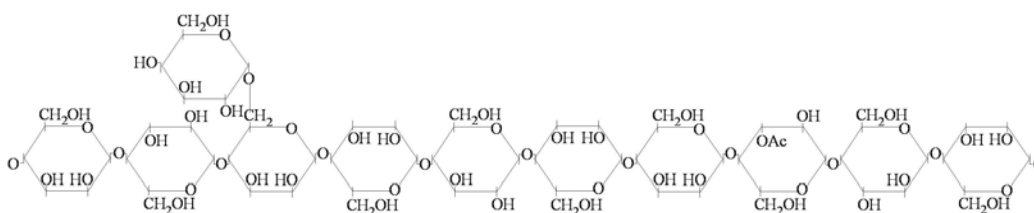


Figure 2-7. Hardwood hemicellulose: O-acetyl-galacto-glucomannan.

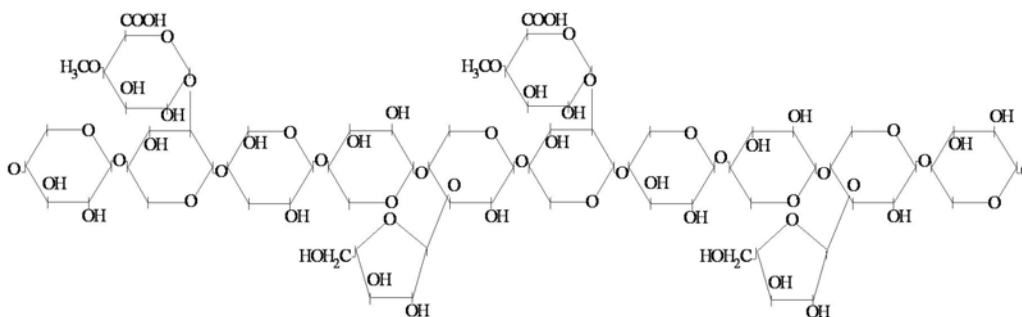


Figure 2-8. Softwood hemicellulose: arabino-4-O-methylglucuronoxylan.

2.3.3 Lignin

Lignin is a highly complex, probably the most complex and least well characterised molecular group among wood components, three-dimensional polymer of different phenyl-propane units (which are mainly guaiacyl, syringyl and p-hydroxy-phenyl), and which are bound together by ether and carbon-carbon bonds (Fig. 2-9.). It possesses a high molecular weight and is amorphous in nature. In wood, the lignin network is concentrated between the outer layers of fibres. The lignin gives structural rigidity by stiffening and holding the fibres of polysaccharides together. Lignin amounts to 20-35 % of the wood structure.

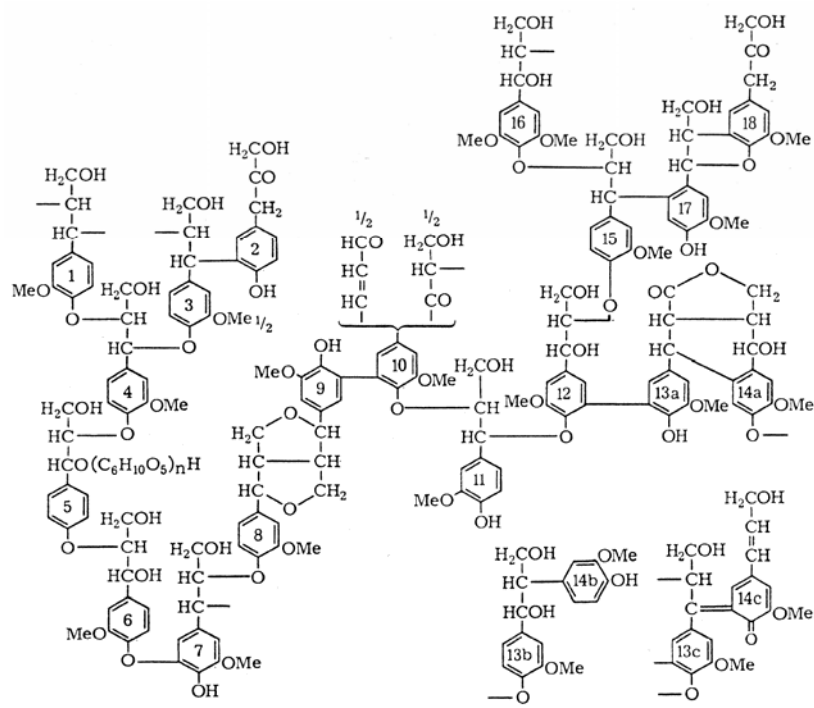


Figure 2-9. Lignin composition [10].

3 Bio-oil

3.1 Bio-oil production

Pyrolysis is by definition thermal decomposition occurring in the absence of oxygen. It is always the first step in combustion and gasification processes where it is followed by total or partial oxidation of the primary products.

In order to maximise the liquid yield of the pyrolysis process short residence times and moderate temperatures should be chosen. The pyrolysis process under such conditions is called fast pyrolysis. An example of such a process is shown in Fig. 3-1.

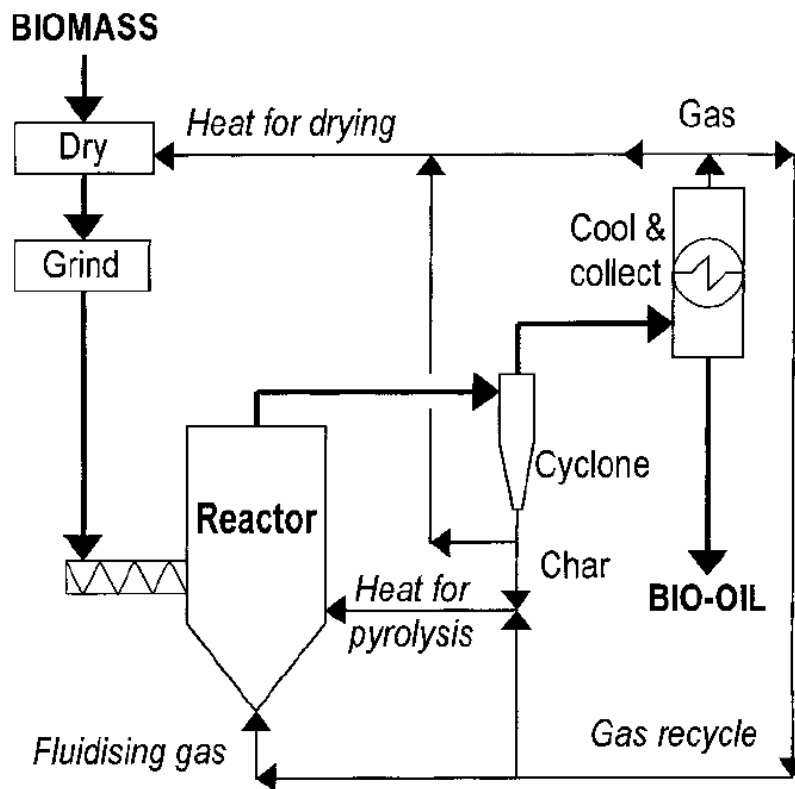


Figure 3-1. An example of a bio-oil production process [11].

Fast pyrolysis is a process where biomass is rapidly heated in the absence of oxygen. As a result biomass decomposes to generate mostly vapours and aerosols and some charcoal. After cooling and condensation, a dark brown mobile liquid is formed which has a heating value about half that of conventional fuel oil. Fast pyrolysis is not an equilibrium process. During fast pyrolysis dramatic changes occur in specific volume between the reactants (biopolymers) and the products causing the volatile products leave the pyrolysis zone at considerable velocities. This results in the entrainment of solid particles and aerosols, which normally would not volatilise at the process temperature. Bridgwater and Peacocke [11] reviewed the key features of fast pyrolysis, technology, status and liquid production processes in 2000.

The essential features of fast pyrolysis process for producing liquids are:

- Reactor configuration
- Heat transfer
- Heat supply
- Feed preparation
- Temperature of the reaction
- Vapour residence time
- Secondary vapour cracking
- Liquids collection
- Char separation
- Ash

3.1.1 Reactor configuration

The heart of a fast pyrolysis is the reactor, almost all research and development has focused on this part.

Rapid thermal processing reactors are processing at a temperature between 400-600 °C and have a very short residence time (up to 2 s). These types of reactors are fluidised bed reactors, ablative pyrolysis, entrained flow and rotating cone.

Fluidised bed reactors

Bubbling fluid beds

Bubbling fluidised bed reactors have a simple construction and operation, they have good temperature control and very efficient heat transfer to biomass particles due to high solids density. They are also easy to scale. This is a well understood technology, the reactor has good and consistent performance with high liquid yields: typically 70-75 wt% from wood on a dry feed basis.

In the reactor, heating can be achieved in a variety of ways (direct, indirect and use of indifferent media), the residence time of solids and vapours is controlled by the fluidising gas flow rate and is higher for char than vapours. Char acts as an effective vapour cracking catalyst at fast pyrolysis reaction temperatures, so rapid and effective char separation/elutriation is important using this technology. Small biomass particle sizes (less than 2-3 mm) are needed to achieve a high heating rate.

Circulating and transported fluid beds

In the circulating fluidised bed reactor the solids are entrained in a vertical tubular reactor (riser). The biomass is fed in the riser section of the bed, where it is pyrolysed [12]. After the pyrolysis zone, the solids (char and sand mixture) are separated from the gas (organic vapours + combustion and fluidising gases) stream and recycled to the combustion chamber (second reactor, often bubbling fluidised bed), where fluidising gas is fed. The char combustion provides the heat necessary for devolatilisation. The pyrolysis vapours leave the reactor through a system of cyclones and are supplied to the downstream processing equipment for quenching and recovery.

These reactors are characterised by high heat transfer rates, high char abrasion from biomass and char erosion leading to high char in product, so effective char/solid heat carrier separation is required. Furthermore solids recycle is required as well. This system has an increased complexity compared to bubbling fluidised bed reactors. The maximum feedstock particle sizes are up to 6 mm. Possibly the liquids crack by hot solids, and secondary liquid cracking is also possible by hot char. Scale-up problems may occur due to very large quantity of hot gas is required.

Good temperature control can be achieved in reactor. The residence time for char is almost the same as for vapours and gas. These reactors are suitable for very large throughputs, and perform a well understood technology, hydrodynamics are more complex, and char is more attrited due to higher gas velocities. Char separation is done by cyclone, and a closely integrated second reactor (for char combustion and sand reheating) requires careful control. The system has a liquid yield at about 60-70 % wt.

Ablative pyrolysis

Ablative pyrolysis is substantially different in concept compared to the other methods of fast pyrolysis. The mode of reaction in ablative pyrolysis is analogous to melting butter in a frying pan, when the rate of melting can be significantly enhanced by pressing down and moving the butter over the heated pan surface. In ablative pyrolysis heat is transferred from the hot reactor wall to "melt" wood that is in contact with it under pressure (Fig. 3-2.). As the wood is mechanically moved away, the residual oil film both provides lubrication for successive biomass particles and also rapidly evaporates to give pyrolysis vapours for collection in the same way as other processes. The rate of reaction is strongly influenced by pressure, the relative velocity of wood on the heat exchange surface and the reactor surface temperature. It has a liquid yield of 60-65 % wt.

This technology accepts large size feedstocks, as the hot solid abrades the product char off the particle exposing fresh biomass for reaction, and performs very high mechanical char abrasion. It has a compact design, but the heat supply can be a problem.

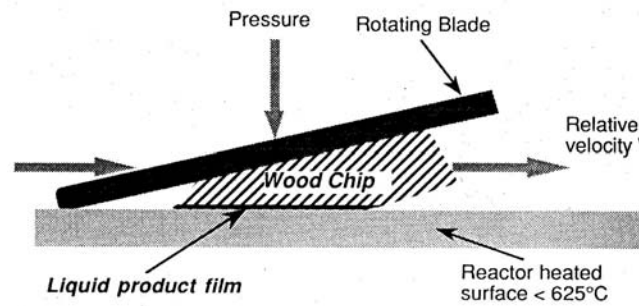


Figure 3-2. Concept of the ablative pyrolysis.

High pressure of particle on hot reactor wall due to centrifugal force or mechanically and high relative motion between particle and reactor wall is achieved. The reactor wall temperature is less than 600 °C. These reactors use large feed sizes, and inert gas is not required so the processing equipment is smaller (in case of mechanically applied pressure). The reaction system is more intensive. The process is limited by the rate of heat supply to the reactor rather than the rate of heat absorption by the pyrolysing biomass as in other reactors and the reaction rates are limited by heat transfer to the reactor not to the biomass. This process is mechanically driven so the reactor is more complex. [13]

Entrained flow

This technology is characterised by low heat transfer rates. The particle size limit is < 2 mm, and there is limited gas/solid mixing. Liquid yields of 50-60 wt% on dry feed have been obtained. [13]

Rotating cone

The rotating cone fast pyrolysis reactor has been developed at the University of Twente (The Netherlands) based on particles being transported up a heated rotating cone mixed with heated sand [14]. This rotating cone reactor enables high solids throughput without requiring any transport gas (except for secondary equipment). Inside the rotating cone, biomass particles are mixed intensively with an excess of hot sand particles. The concept can be seen in Fig. 3-3.

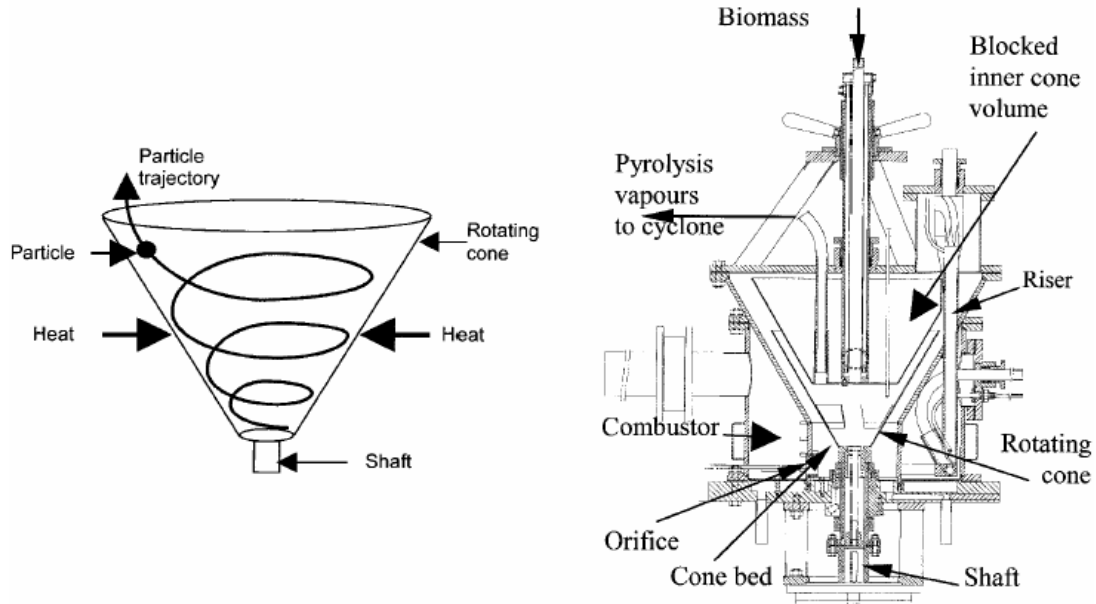


Figure 3-3. The rotating cone reactor.

The rotating speed is 600 rpm, which drives hot sand and biomass up a rotating heated cone, vapours are collected and processed conventionally, the char is burned in a secondary bubbling fluid bed combustor and the hot sand is recirculated to the pyrolyser. Carrier gas requirements in the pyrolysis reactor are much less than for fluid bed and transported bed systems (however more gases are needed for char burn off and for sand transport). Typical yields obtained are about 60-70 wt%. This technology means complex integrated operation of three subsystems: rotating cone pyrolyser, bubbling bed char combustor and riser for sand recycling.

3.1.2 Heat transfer and supply

There are two important requirements of heat supply:

- to the reactor heat transfer medium
- from the heat transfer medium to the pyrolysing biomass

and there are three main ways of heating biomass particles in a fast pyrolysis system:

- gas-solid heat transfer, where the heat is transferred from the hot gas to the solid biomass
- particle heating by primarily convection
- solid-solid heat convection with mostly conductive heat transfer.

Fluid bed pyrolysis utilises the inherently good solids mixing to transfer approximately 90 % of the heat by solid-solid heat transfer. Circulating fluid bed and transport reactors rely on both gas-solid convective heat transfer from the fluidising gas and solid-solid heat transfer from the hot fluidising solid. Some radiation effects occur in all reactors.

Since the thermal conductivity of the biomass is very poor, biomass particles have to be very small to fulfil the requirements of rapid heating to achieve high liquid yields. As particle size increases, liquid yield reduces as secondary reactions within the particle become increasingly significant.

The high heat transfer rate is necessary to heat the particles sufficiently rapid imposes a major design requirement on achieving the high heat fluxes required to match the high heating rates and endothermic pyrolysis reactions.

3.1.3 Feed preparation

The heat transfer rate requirements described above impose particle size limitations on the feed for some reactors. Drying is usually required to achieve less than 10 wt% water unless a naturally dry material (for example straw) is available.

3.1.4 Char removal

Char acts as a vapour cracking catalyst so effective char removal (separation from the vapours) is essential during the pyrolysis process. Cyclones are the usual method of char removal and two cyclones are usually provided, the first to remove the bulk of the material, and a second to remove as much of the residual fines as possible. Some fines, however, always pass through the cyclones and are collected in the liquid product where they accelerate aging and contribute the instability problem. Some success has been

achieved by hot gas filtration, but liquid filtration has proved difficult as the liquid can have a gel-like consistency.

3.1.5 Liquid collection

Collection of liquids from biomass pyrolysis has long been a major difficulty in biomass pyrolysis research. The pyrolysis vapours have similar properties to cigarette smoke and capture by almost all collection devices is normally very inefficient. The product vapours are not true vapours but rather a mist or fume and are typically present in an inert gas at relatively low concentrations which increases cooling and condensation problems.

Electrostatic precipitators are effective and are used by many researchers, but can create problems from the polar nature of product and arcing of the liquids as they flow, causing the electrostatic precipitator to short out. Larger scale liquid collecting processes employ some type of quenching or contact with the cooled liquid product. In these quenches, a very rapid cooling of the product takes place, which is effective, especially in direct contact quench.

The temperature of the transfer lines from the reactor through the cyclones to the liquid collection system should be maintained at $> 400\text{ }^{\circ}\text{C}$ to minimise liquid deposition on the walls.

3.1.6 Other processes to produce bio-oil

Vacuum pyrolysis

Vacuum pyrolysis is not a true fast pyrolysis as the heat transfer rate to and through the solid biomass is much slower than in the previously described reactors, but the vapour residence time is comparable. Contrary to the fast pyrolysis approach, vacuum pyrolysis is a slow heating process with a long contact time of the solid residues inside the reactor and a short residence time of the condensable organic vapours formed during the pyrolysis reactions. Operating the reactor under vacuum minimises the occurrence of secondary decomposition reactions. Typical liquid yields obtained during vacuum

pyrolysis of wood reach 65 wt%, and the preferred operating pressure of a vacuum pyrolysis plant is 15 kPa [15].

The vacuum pyrolysis process can accept larger particles than most pyrolysis reactors, there is less char in the liquid product due to lower gas velocities and there is no requirement for a carrier gas. The process is relatively complicated mechanically. Vacuum pyrolysis appeared to be less economical than fast pyrolysis for the production of primary fuel oil.

HTU process

In the HTU process the feedstock is treated in liquid water at temperatures ranging from 300 to 350 °C, the pressure is between 100-180 bar (it has no effect, just should keep the water in liquid phase) and the residence time is 5-20 minutes. Oxygen is removed from the biomass mainly as CO₂, which results in a product with low oxygen content (10-18 wt%). This product, the biocrude, is not miscible with water and has a relatively high heating value (LHV=30-35 MJ/kg) [16].

3.2 Characterisation of bio-oils

The analysis and the characterisation of the fast pyrolysis bio-oils are important areas of research. Data on the physical and chemical properties of these liquids can give important indications about the pyrolysis process parameters and information about quality, toxicity and stability of the product [13]. There are several papers available on characterisation of fast pyrolysis liquids [17-21] and they agreed on that there is no standard bio-oil, the properties of the liquid are strongly dependent on the feedstock and the production conditions. The desired properties vary on the utilisation (Fig. 3–4.). For example for chemical purposes the bio oil must be very clean, however, there are less demands for fuel purposes.

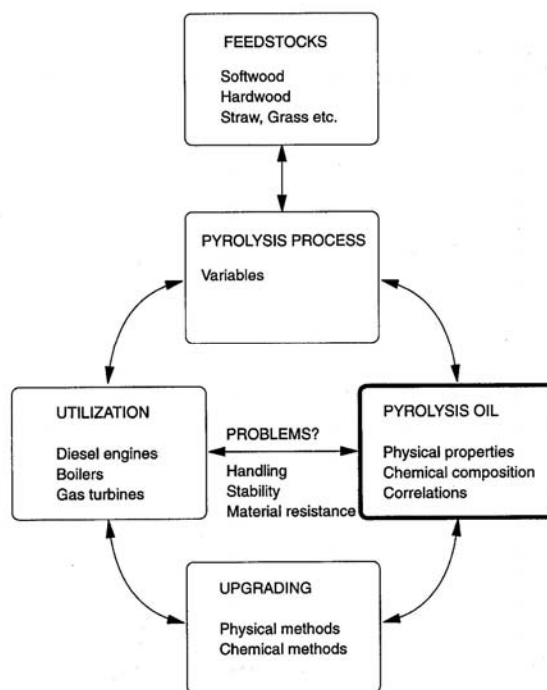


Figure 3-4. Links between pyrolysis oil production, quality and utilisation.

3.2.1 Chemical and physical methods for determination the bio-oil properties

The status of the test methods for characterisation of pyrolysis liquids are entirely described by Meier et al. [22] and the chemical analysis methods of bio-oils are described by Meier [23]. Sampling methods as well as review of the five key areas as physical/chemical properties, combustion technology, safety technology, composition and new tests are described. It is often useful to fractionate the bio-oil and characterise each fraction (Fig. 3–5.) [21].

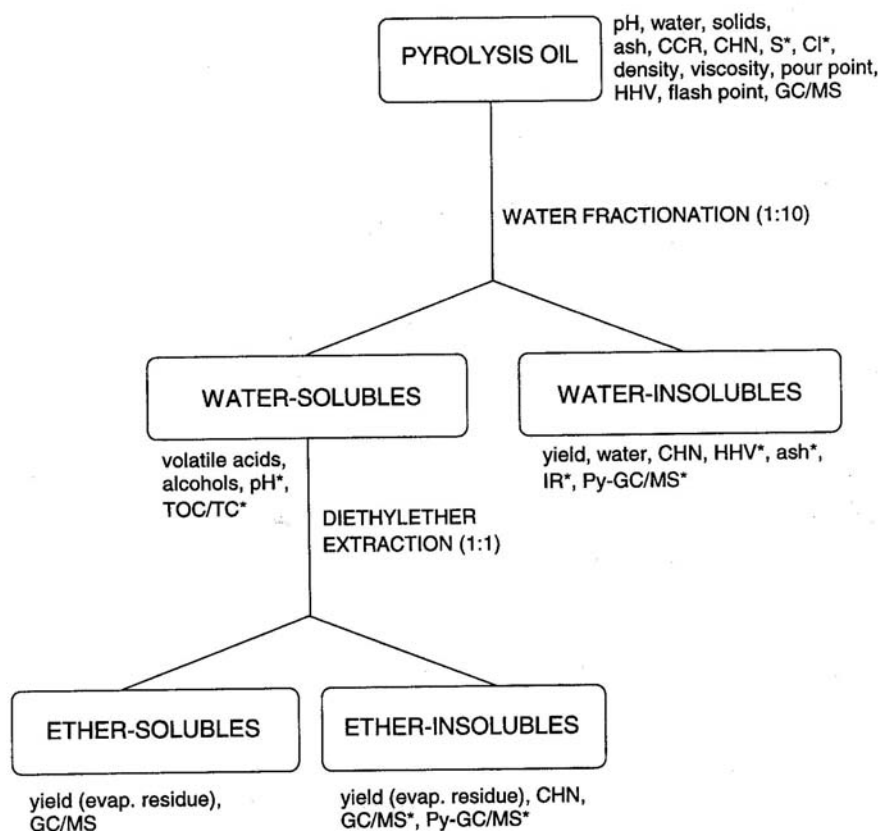


Figure 3-5. Bio-oil fractionation and characterisation.

3.2.2 Physical and chemical properties of bio-oils

The chemical composition of biomass-based pyrolysis oils is complex – and therefore complicated to analyse in all its details. The main components comprising mainly of water, carboxylic acids, carbohydrates and lignin derived substances [18]. Faix et al. [24-27] published a detailed compilation of the pyrolysis products of wood including gas chromatographic retention data and mass spectra.

The composition of bio-oils results form a complex interrelationship of [28]:

- The biomass species used as feedstock (organic and inorganic compositions, including dirt and moisture).
- Organic nitrogen or protein content of the feedstock.
- The heat transfer rate and final char temperature during pyrolysis.

- The extent of vapour dilution in the reactor.
- The time and temperature history of the vapours in the reactor.
- The time and temperature history of the vapours in the heated transfer lines from the pyrolysis reactor through the char removal equipment to the quench zone.
- Whether the vapours pass through accumulated char (i.e., in hot-gas char filtration between backflushing operations).
- The efficiency of the char recovery system to separate the char from the bio-oil vapours before condensation.
- The efficiency of the condensation equipment to recover the volatile components from the non-condensable gas stream, e.g., water and low molecular weight esters, ethers, acetals, alcohols, and aldehydes.
- Whether the condensates have been filtered to remove suspended char fines.
- The water content of the bio-oil.
- The extent of contamination of the bio-oil during storage by corrosion or leaching of the containers.
- Exposure to air during storage.
- The length of storage time.
- The storage temperature.
-

The typical chemical composition of a bio-oil is given in Table 3–1. [18].

Table 3-1. Typical bio-oil composition.

| Major components | Percent by mass wt% |
|-------------------------|----------------------------|
| Water | 20-30 |
| Lignin fragments | 15-20 |
| Aldehydes | 10-20 |
| Carboxylic acids | 15-20 |
| Carbohydrates | 5-10 |
| Ketones | 1-5 |
| Phenols | 2-5 |
| Alcohols | 2-5 |
| Char | 2-3 |
| Ash | 0.7-0.14 |

There is also a range of articles, trying to summarise the physical characteristics of pyrolysis oils. These characteristics are made for flash pyrolysis bio-oils (see Table 3–2.) and the different type of oils are distinguished by feedstock material, or by the pyrolysis method, based on literature data [18-19, 21, 29].

Table 3-2. Physical properties of bio-oils.

| | |
|----------------------------------|-----------|
| HHV, MJ/kg | 15-19 |
| LHV, MJ/kg | 14-19 |
| Density, kg/m³ | 1200-1300 |
| Flash point °C | 50-100 |
| Viscosity @50°C, cSt | 45-70 |
| pH | 2.5-3.5 |

Heating value: The literature distinguishes between the higher heating value (HHV) and lower heating value (LHV). Higher heating value gives the heating value of the dry part of the fuel. Lower heating value is the higher heating value minus the lost energy due to vapour formation during combustion.

Flash point: There is a wide variation in the content of volatiles and it represents a wider range flash point values. Above temperatures of 70-75 °C, water vapours from the pyrolysis oils start to disturb the analysis and a reproducible value is hard to obtain.

Density: The density of bio-oils are much higher than petroleum derived oils (0.85-1.0 kg/m³), which reflect the high oxygen content in bio-oils. Bio-oils, which have higher densities typically have lower water contents.

pH: This is a strong hinder of bio-oil applications compared to petroleum derived oils, as the low pH values mean high corrosion.

The physico-chemical composition of bio-oils is reviewed in detail by Milne et al. [20] and by Diebold [28]. Several bio-oils were analysed and the contents reported by Oasmaa et al. [30] as well.

3.2.3 The stability problem

The stability problem and the possible reasons of it are studied by many researchers. This is reviewed by Diebold [28] and James and Diebold [31]. Pyrolysis of biomass under conditions of rapid heating and short reactor residence times can produce a low-viscosity, single-phase pyrolysis liquid (bio-oil) in yields reported higher than 70 %. Most projected uses of bio-oil require that it retain these initial properties during storage, shipment and use. The pyrolysis oils are chemically reactive with themselves and will polymerise with time, usually with the formation of addition water as a byproduct of the reactions. After prolonged storage, the oils tend to increase their molecular weight owing to chemical reactions, hence increase the viscosity, and also it has a tendency to separate into a thin oil phase and a thick tar phase. This process is called aging, and makes storage difficult. Aging is much faster at increased temperatures. The loss of volatiles also increases the viscosity.

Fast pyrolysis is not an equilibrium process, hence the product, the bio-oil, is not in thermodynamic equilibrium at storage temperatures. Bio-oil contains a large number of oxygenated organic compounds with a wide range of molecular weights, typically in small percentages. During storage, the chemical composition of the bio-oil changes toward thermodynamic equilibrium, resulting in changes in viscosity, molecular weight and co-solubility of its many compounds. In addition, the simple phase bio-oil can

separate into various tarry, sludgy, waxy, and thin aqueous phases during aging. Tarry sludges and waxes still in suspension cause rapid plugging of fuel filters.

Most important reactions that occur within bio-oil probably involve:

- Organic acids with alcohols to form esters and water.
- Organic acids with olefins to form esters.
- Aldehydes and water to form hydrates.
- Aldehydes and alcohols to form hemiacetals, or acetals and water.
- Aldehydes to form oligomers and resins.
- Aldehydes and phenolics to form resins and water.
- Aldehydes and proteins to form oligomers.
- Organic sulfur to form oligomers.
- Unsaturated compounds to form polyolefins.
- Air oxidation to form more acids and reactive peroxides that catalyze the polymerization of unsaturated compounds.

These reactions are described in details by Diebold [28].

During aging, chemical reactions change the polarity of the bio-oil components. For example esterification converts highly polar organic acid and alcohol molecules into esters with relatively low polarity and extremely polar water. This increasing difference in polarity among the compounds in the aged bio-oil increases the tendency for phase separation. This phase separation will occur into a light, highly polar aqueous phase and a less polar heavier organic phase. Additional lighter waxy phases and heavier sludge phases also form during storage because of decrease in mutual solubility during aging.

The headspace gases that evolve during aging could be pyrolysis gases (depending on the production procedure) that were selectively absorbed by the bio oil in the condensation train during production. The pyrolysis gases would be desorbed with a rise in temperature or with a chemical change in the bio-oil that reduced their solubility.

Boucher et al. [32-33] aged bio-oil samples by heating up to 40 and 80 °C. They found that the viscosity increased with the residence time and heating temperature. They

observed no phase separation while heating the raw bio-oil samples. They observed a significant change in the bio-oil solid content only after one week of heating at 80 °C. Previous literature reported that the water concentration in the bio-oil increased with the length of storage period, but Boucher et al. found no clear tendency to conclude this. They observed an irreversible phase separation after heating the samples to 80 °C. They reported that the average molecular weight of the bio-oil increased with the length and the temperature of storage.

3.3 Processes to slow aging in bio-oils

3.3.1 Upgrading of bio-oils

Upgrading of bio-oils can be done with solvents and with catalytic processes. The upgrading possibilities are reviewed by Czernik et al. [34].

Sharma and Bakhshi [35] studied upgrading of the non-phenolic fraction of bio-oil with HZSM-5 catalyst in a dual-reactor system. Their objective was to maximise the amount of organic distillate with high aromatic hydrocarbon yields. The organic distillate from the effluent they obtained from the second reactor showed a yield up to 22 wt% of the non-phenolic fraction and it contained up to 78 % of aromatic hydrocarbons. Comparison of results with those from a single reactor system revealed that by using the dual reactor system, the total amount of coke and char mostly decreased whereas the amount of organic distillate product increased, especially when the temperature in the first reactor was below 370 °C.

They further studied the upgrading of the pyrolytic lignin with the same reaction system [36]. The objective was the same – to maximise the amount of organic distillate with high aromatic hydrocarbon yields. Due to the highly viscous nature of the pyrolytic lignin fraction, it was co-processed with tetralin. The amount of organic distillate in the effluent from the second reactor was between 22-31 wt% of the pyrolytic lignin fraction and contained up to 84 wt% aromatic hydrocarbons.

Adjaye and Bakshi [37-38] studied the upgrading of fast pyrolysis bio-oils with different catalysts in a fixed bed micro-reactor. The objective was to obtain high yields of hydrocarbons. The yields of hydrocarbons (based on the amount of bio-oil fed) were 27.9 wt% with HZSM-5, 14.1 wt% with H-Y, 4.4 wt% with H-mordenite, 5 wt% with silicate and 13.2 wt% with silica-alumina. They found that HZSM-5 and H-mordenite produced more aromatic than aliphatic hydrocarbons, while H-Y, silicate and silica-alumina produced more aliphatic than aromatic hydrocarbons. Furthermore they observed a significant amount of char production during upgrading, which indicates the unstable nature of the bio-oil. The char formation decreased with increasing both the space velocity and temperature, but then deoxydation and hydrocarbon formation decreased as well. They found that upgrading of bio-oils with silicate was highly undesirable, and the most effective catalysts to upgrade bio-oil to hydrocarbons were the acidic zeolite catalysts (HZSM-5, H-Y and silica-alumina), and the catalyst acidity affect the coke formation. The catalyst effectiveness to reduce the coke formation decreased with increase in the pore size of the acidic zeolite catalysts.

Boucher et al. [32-33] produced bio-oil by vacuum pyrolysis and blended it with methanol and pyrolytic aqueous phase. The aqueous phase is a dark brown liquid consisting of 84 wt% water and 16 wt% organic compounds. According to previous literature, methanol is an effective additive due to the stability and viscosity of the resulting biofuel. Moreover, methanol is inexpensive. Boucher et al. found that the surface tension rises with an increase of the aqueous phase concentration in the bio-oil mixture. The viscosity of the aqueous phase/oil mixtures was slightly higher than that of the raw bio-oil, but they found no important influence, either positive or negative on the viscosity. Methanol, by its contribution to form lower particle size droplets, will considerably reduce the sedimentation velocity in the mixture and thus increase the stability. During heating, the viscosity of the system decreases, resulting in an accelerated sedimentation process. The water droplets, even if they are small attract each other and form larger ones and this agglomeration leads to sedimentation. Both methanol and the aqueous phase decreased the heating value, but both reduced the density and methanol reduced the viscosity as well. They reported also that a bio-oil to be used as a liquid fuel should not contain more than a total of 15 % aqueous phase, and the aqueous phase lowers the stability even at a weak concentration.

Diebold has reviewed [28] the effect of solvent addition in detail.

3.3.2 Catalytic pyrolysis

One approach to improve the quality of the liquid bio-oil is stabilisation by mild catalytic pyrolysis.

Rolin et. al [39] investigated the influence of various catalysts on fast pyrolysis of biomass at short residence times. They examined also the effect of the biomass moisture content. They impregnated the wood in aqueous solution of catalyst. KCl, NaCl, ZnCl₂, H₃PO₄ and (NH₄)₂HPO₂ appeared to be good flame retardants at 900 °C. They observed a decrease in the mass yield of gasification, and an increase in residue and a gas phase was less flammable as more CO₂ and H₂O and less CO are evolved. They found that CaCl₂ Ni(CH₃COO)₂ and H₂O, at 900 °C and carbonates and hydrogen-carbonates at 800 and 900 °C favour the gasification reaction. They observed an increase in the mass yield of gasification and in the volume of gas evolved (with more H₂ and CO) and a decrease in residue. These effects were further enhanced in the presence of water.

Gregorski and Pavlath [40] studied the influence of various acidic, basic and neutral catalysts on the pyrolysis of pure carbohydrates present in agricultural products. They applied thermogravimetry coupled with gas chromatography and mass spectrometry to identify the products. They found that the volatile products decrease with catalytic pyrolysis and more with acidic than basic catalysts.

Zaror et al. [41] investigated the secondary char formation in catalytic pyrolysis of wood and pure cellulose. The pyrolysed biomass was untreated or impregnated with salt (Na₂CO₃, K₂CO₃, NaCl, KCl). They concluded that salt impregnation modified weight loss rates and increased the charcoal yield in the presence of an inert carrier gas. Longer residence times of volatiles in the hot zone gave rise to larger charcoal yields from untreated substrates. However, long residence times of volatile matter over Na₂CO₃-impregnated cellulose were found to be detrimental to char formation. The results indicated that primary volatiles may undergo secondary reactions through competitive pathways, either polymerising to form char or cracking to form lighter volatiles.

Simionescu et al. [42] investigated the effect of catalysts on the pyrolysis of various hydrocarbon polymers such as aliphatic saturated, olefinic and aromatic compounds. The following types of catalysts were used: pure metals, metal oxides, zeolites and amorphous or crystalline silicates. The order of efficiency was: aluminium bronze < MnO_2 < Cr_2O_3 < CuO < microporous mordenite < macroporous mordenite < amorphous aluminasilica (13 % Al_2O_3) < amorphous aluminasilica (25 % Al_2O_3) < crystalline silicates (10 % molecular sieves) < ZSM-5 zeolites.

In 1994 Bridgwater summarised the possibilities of catalytic biomass pyrolysis [43]. He claims that catalysis with zeolites is less understood and less developed than other upgrading possibilities for example hydrotreatment. The catalysts and the processes need to be developed and optimised, but this is an interesting method to upgrade the bio-oil to fuel or chemicals.

Laurant and Delmon [44] investigated hydrodeoxygenation of the reactive carbonyl, carboxylic and guaiacyl groups. They used model oxygenated compounds, namely 4-methylacetophenone, diethyldecanedioate and guaiacol to test them simultaneously in one reaction test in the presence of sulfided cobalt-molybdenum and nickel-molybdenum supported on γ -alumina catalysts in a batch system. They found that the ketonic group is easily and selectively hydrogenated into a methylene group at temperatures higher than 200 °C. Carboxylic groups are also hydrogenated to methyl groups, but a parallel decarboxylation occurs at comparable rates. A temperature around 300 °C is required for the conversion of carboxylic groups as well as for the conversion of the guaiacyl groups. The main reaction scheme of guaiacol is its transformation in hydroxyphenol which is subsequently converted to phenol. But at batch reactor conditions, guaiacol gives a high proportion of heavy products. They also concluded that CoMo and NiMo catalysts had comparable activities and selectivities. However, the NiMo catalyst had a higher decarboxylating activity than CoMo and also leads to a higher proportion of heavy products during the conversion of guaiacol.

Samolada and Vasalos [45] evaluated various catalysts for biomass flash pyrolysis. They evaluated selected commercial catalysts in a fixed bed reactor using solid biomass. They found that catalytic biomass pyrolysis supplies lower liquid yields containing higher water content. They also evaluated the Fluid Catalytic Cracking (FCC) in a circulating fluid bed reactor of a pilot plant unit. Catalytic and non-catalytic runs were

effectively performed in the unit. The stability of the obtained liquid product was effectively improved using catalysts, even though no major changes in the chemical composition were detected.

Dobele et al. [17] used analytical pyrolysis combined with gas chromatography (Py-GC) to study the composition of volatile products of different commercial celluloses impregnated with various amounts of phosphoric acid. The influence on the yields of levoglucosan and levoglucosenone was studied taking into account the supramolecular structure, degree of polymerisation, hydrophilic properties and pretreatment conditions of the celluloses. It was found that levoglucosenone predominates in the volatiles of acid catalysed pyrolysis. However, the relative total amount of both 1,6-anhydrosaccharides varied only in a narrow range of 75–85 % regardless of the impregnation and pretreatment conditions of the celluloses.

Salter et al. [46] carried out some experiments with catalytic pyrolysis to produce a better quality bio-oil. They used pelleted zeolite catalysts (ZSM-5 and Y zeolite) and found that addition of these catalysts significantly changed the chemical composition of the pyrolysis-oil. They observed reduced viscosity of the liquid product and low gas yield. The low gas yield indicates that the mechanism of catalytic pyrolysis is not by cracking or that the gas is being used or absorbed by the catalyst. They obtained similar yields both at catalysed and non-catalysed pyrolysis reactions. This may be a function of the low percentage (10 %) of catalyst used or may confirm that quenching rather than cracking occurred.

3.4 Applications of bio-oils

Bio-oil applications have several possibilities (Fig. 3–6.). Bio-oil can substitute for fuel oil or diesel in many stationary applications including boilers, furnaces, engines and turbines for electricity generation. There is also a range of chemicals (food flavourings, resins, agri-chemicals, fertilisers, etc.) that can be extracted or derived from the bio-crude oil. [11, 13]

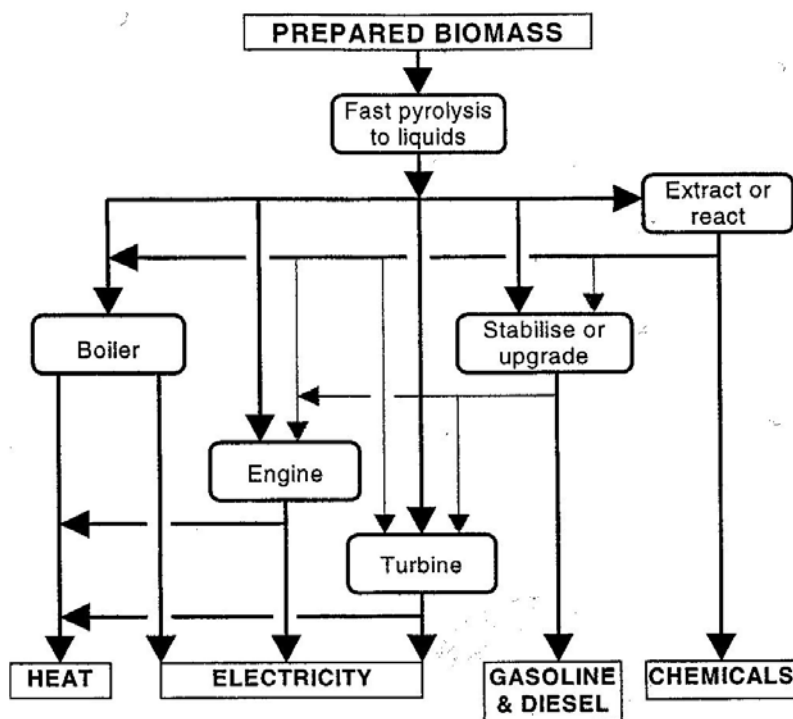


Figure 3-6. Possibilities for bio-oil applications [13].

3.4.1 Combustion

Existing oil-fired burners cannot be fuelled directly with solid biomass without major reconstruction of the unit. Liquid products are easier to handle and transport in combustion applications and this is important in retrofitting existing equipment. Bio-oils are likely to require only minor modifications or even none in some cases. The problems that have been predicted in handling the fuel (high viscosity and suspended char) have not been found to be as severe or serious as first thought, and many organisations are proceeding with successful developments.

3.4.2 Power generation

Bio-oil has been successfully fired in a diesel test engine, where it behaves very similar to diesel in terms of engine parameters and emissions. Over 300 h operation have been achieved. A diesel pilot fuel is needed, typically 5 % in larger engines, and no

significant problems are foreseen in power generation up to 15 MWe per engine. A 2.5 MWe gas turbine has also been successfully tested although for not many hours operation to date

[13]. However, the current method of utilising bio-oil in a diesel engine requires three fuels and a complex start-up and shut down procedure. Chiaramonti et al. [47-48] worked on the development of emulsions from biomass pyrolysis liquid and diesel to feed immediately diesel engines, and tested the combustion. They found that the emulsion was more stable than the pure bio-oil, and the viscosity dependent on the bio-oil percentage. Fresh bio-oil should be used as the aged one is making the emulsification process more difficult. After the combustion tests they concluded that the injector as well as the fuel pump should be made of stainless steel, or similar corrosive resistant material.

3.4.3 Chemicals

A range of chemicals can also be produced from bio-oils. Chemicals that have been reported as recovered include polyphenols for resins with formaldehyde, calcium and/or magnesium acetate for biodegradable de-icers, fertilisers, levoglucosan, hydroxyacetaldehyde and food flavourings that are commercially produced from wood pyrolysis products in many countries. All chemicals have attractive possibilities due to their much higher added value compared to fuels and energy products. An integrated approach to chemicals and fuels production offers interesting possibilities for better total economy production in a plant.

4 Synthesis, characterisation and applications of mesoporous materials

Designing heterogeneous catalysts involve both the proper control of the surface chemistry and a rigorous control of the surface geometry at the micro-, meso- and macroscales. This is because high surface areas or high active phase dispersions as well as fast mass transfer of the reactants and products to and from the catalytic sites are required from any active catalyst.

Porous solids are used technically as adsorbents, catalysts and catalytic supports owing to their high surface areas. According to the IUPAC definition, porous materials are divided into three classes according to their diameter: Microporous (< 2 nm), mesoporous (2-50 nm) and macroporous (> 50 nm) [49].

The following three kinds of relevant mesoporous materials were obtained by different synthetic procedures [50]. The first one is the so-called M41S family of silica and aluminosilicates introduced by the Mobil group which includes hexagonal MCM-41, cubic MCM-48 and lamellar MCM-50 phases. One of the unique features of the M41S molecular sieve family is the sorption of molecules within a uniform mesopore channel of dimensions from 15 to ~ 100 Å. The uniform pore size of the molecular sieve can be finely tuned by the selection of the appropriate chain length of the alkyltrimethylammonium cationic surfactant and auxiliary organics used in the synthesis. The preparation of M41S materials involves ionic surfactants, exemplified by cetyltrimethyl ammonium bromide (CTAB), as structure directing agents. It may be conducted in basic conditions in which case it follows an ionic assembly mechanism schematically represented as S^+I^- .

The second one was introduced by the group of Pinnavaia who produced mesoporous molecular sieves (MMSs) using two neutral routes based on hydrogen bonding and self assembly of non-ionic primary amines such as hexadecyl amine or polyethylene oxide (EO) surfactants and neutral oligomeric silica precursors schematically represented as S^0I^0 . The hexagonal mesoporous silica (HMS) produced by this technique is less ordered, showing a wormhole like pore structure, than MMS's produced with ionic

surfactants. HMS has a monodispersed pore diameter, thicker pore walls and therefore higher degree of condensation and higher thermal stability. In addition, the mesopores of HMS being shorter allow a faster diffusion of reactants.

Stucky and co-workers [51-52] introduced a new synthesis route involving amphiphilic di- and tri-block copolymers as organic structure directing agents. These materials, exemplified by hexagonal (p6 mm) SBA-15, have long range order, large monodispersed mesopores (up to 50 nm) and thicker silica walls (typically between 3 and 9 nm) which make them more thermally and hydrothermally stable than previous materials.

4.1 MCM-41

With MCM (Mobil Composition of Matter) -41 the first mesoporous solid was synthesised that showed a regularly ordered pore arrangement and a very narrow pore-size distribution. After the discovery of MCM-41 in 1992 [49], the research interest focused on the following main subjects:

- characterisation
- mechanism of formation
- synthesis of new materials based on the MCM-41 synthesis concept
- morphology control
- technical applications

The MCM-41 material is amorphous and has a honeycomb structure that is a result of hexagonal packing of unidimensional cylindrical pores. The XRD pattern of MCM-41 shows typically three to five reflections between $2\theta = 2^\circ$ and 5° [49 and Fig. 4-1.].

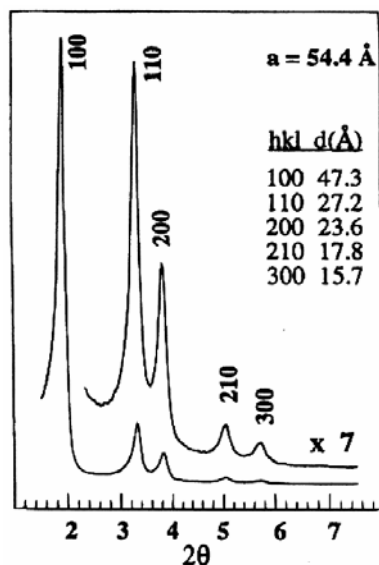


Figure 4-1. X-ray diffraction pattern of a high-quality calcined MCM-41 [49].

The four main components in the M41S syntheses are structure-directing surfactants, a source of silica, a solvent and a catalyst (acid or base). In the cases of aluminosilicate materials, an aluminium source is added as well. In their pioneering work on the M41S materials the Mobil researchers used alkyl-trimethyl ammonium halides as the structure-directing surfactants and combinations of sodium silicate, tetraethoxy silicate (TEOS), fumed silica and Ludox as the silica source. Sodium hydroxide or tetraethyl ammonium hydroxide was used as basic additives to the aqueous synthesis solutions. The synthesis solutions were kept at temperatures ranging from 100 to 150 °C for 24-144 h. Then the solid products were filtered washed and dried. Finally, the materials were calcined at 540 °C under a gas flow or alternately nitrogen and air, resulting in porous structures [53].

The original MCM-41 synthesis was carried out in water under alkaline conditions (Fig. 4-2). Similar to zeolite syntheses, organic molecules – surfactants – function as templates forming an ordered organic – inorganic composite material. However, in contrast to zeolites the templates are not single organic molecules but liquid-crystalline self-assembled surfactant molecules. The formation of the inorganic-organic composites is based on electrostatic interactions between the positively charged surfactants and the

negatively charged silica species. Via calcination the surfactant is removed, leaving the porous silicate network.

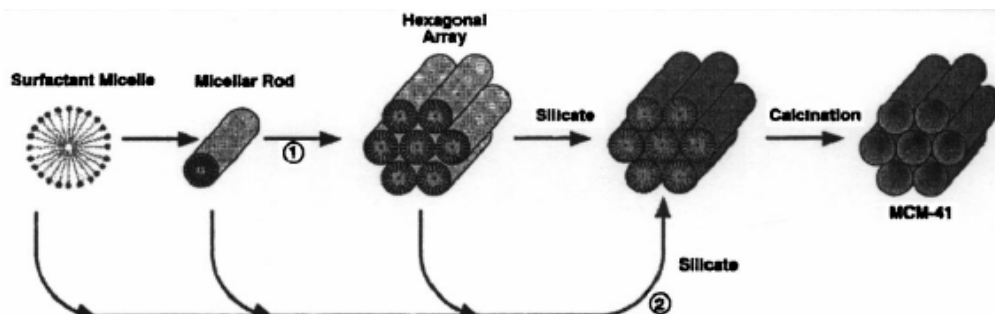


Figure 4-2. Liquid-crystal templating (LCT) mechanism for the formation of MCM-41: (1) liquid-crystal-initiated and (2) silicate initiated pathways [49].

The pore size is primarily a function of the alkyl chain length of the templating surfactant, but it can be further manipulated by other synthesis parameters [54].

Because of the formation of catalytically active acid sites, the incorporation of aluminium into silica frameworks is of special interest. Schmidt et al. [55] synthesised and characterised MCM-41 materials with bulk Si/Al ratios of 18, 9 and 4 with different pore sizes. They concluded that it is possible to synthesise MCM-41 mesoporous materials with a high content of tetrahedrally co-ordinated aluminium ions. Adding aluminium to the synthesis gel increases the long range ordering of the materials obtained. The template interacts with silanol groups and Al-species in different ways. Removal of the template using liquid phase extraction instead of calcination had significant effect on the characteristics of the final material. Template associated with silanol groups can be washed out completely by liquid extraction, whereas the removal of the Al-associated template was incomplete.

4.1.1 Hydrothermal stability of mesoporous MCM-41

Mokaya [56] tested Al-grafted MCM-41 with respect to their hydrothermal stability by heat treatment at 800 or 900 °C for 4 hours in a flow of nitrogen saturated with water vapour at room temperature. All tested samples were relatively stable at 800 °C, however, after treatment at 900 °C, the samples severely degraded.

According to a report by Ryoo et al. [57], MCM-41 withstands hydrothermal treatment using heated water at 65 °C for 12 hours, however, treatment with boiling water for 12 hours cause degeneration of the mesoporous structure.

The addition of cations (TPA⁺, TEA⁺ and TMA⁺) to the synthesis gel of MCM-41 lead to an improvement of the hydrothermal stability. The resulting materials as stable against water in closed bottles at 100 °C for 4 days [58].

Ti- containing MCM-41 was treated in boiling water for 120 hours, however, the structure was destroyed after this treatment, which was also observed for SBA-15 [59].

MCM-41 samples were subjected to 20 % water vapour in a nitrogen stream at 800 °C for 5 hours, with the result of a collapse of the mesopores upon this treatment [60]. The nitrogen stream was bubbled through a water bath at a controlled temperature to achieve the desired partial pressure of water vapour.

The hydrothermal stability of mesoporous materials was improved by coating the material with ZSM-5 zeolite [61]. The test was performed with boiling water at 100 °C and with 20 % water vapour in nitrogen at 800 °C. The mesoporous structure of the parent material collapsed after this treatment at 48 hours, whereas no significant collapse of the mesopore structure was observed for the ZSM-5 coated mesoporous material after 48 hours under the same treatment conditions.

1.5 % Al containing MCM-41 materials were subjected to steam treatment for 5 hours at 600 and 800 °C, respectively [62]. Whereas the structure was partly in shape after treatment at 600 °C (however, certain decrease in cell size, surface area, pore volume and pore diameter was observed), treatment at 800 °C resulted in a complete collapse of the mesoporous structure.

Recently, the synthesis of a mesoporous aluminosilicate (MAS-5), consisting of both mesopores and micropores has been reported [63]. The material is classified to be similar to Al-MCM-41, and has been described as stable after treatment with boiling

water for more than 300 hours. At 600 °C the sample tolerates steam for 6 hours, whereas at 800 °C in the presence of steam the sample does not degrade for 2 – 3 hours, however, the resultant samples present Si/Al ratios too high for many catalytic applications.

Better results have been achieved by Zhao et al. [64], who prepared a disordered mesoporous aluminosilicate similar to MCM-41, using a polymer of aluminium and silicon as precursor and a cationic surfactant. The material withstands boiling water for 12 hours without losing the mesoporous structure, however, after 70 hours in boiling water, the samples start to degrade.

4.2 SBA-15

SBA-15 is a hexagonally ordered mesoporous material synthesised by the self-assembly between an inorganic silica source, tetraethyl orthosilicate, and an organic amphiphilic triblock copolymer.

Use of amphiphilic triblock copolymers to direct the organisation of polymerising silica species has resulted in the preparation of well-ordered hexagonal mesoporous silica structures (SBA-15) with uniform pore sizes up to approximately 300 Å. The SBA-15 materials are synthesised in acidic media to produce highly ordered, two-dimensional hexagonal silica-block copolymer mesophases. Calcination at 500 °C gives porous structures with unusually large interlattice d spacings of 74.5 to 320 Å between the (100) planes, pore sizes from 46 to 300 Å, pore volume fractions up to 0.85, and silica wall thicknesses of 31 to 64 Å. SBA-15 can be readily prepared over a wide range of uniform pore sizes and pore wall thicknesses at low temperature (35 to 80 °C), using a variety of poly(alkylene oxide) triblock copolymers and by the addition of cosolvent organic molecules. The block copolymer species can be recovered for reuse by solvent extraction with ethanol or removed by heating at 140 °C for 3 hours, in both cases yielding a product that is thermally stable in boiling water [52].

Yue et al. [65] obtained aluminium incorporated SBA mesoporous materials by direct synthesis. The resulting materials retained the hexagonal order and physical properties

of purely siliceous SBA-15 and presented higher catalytic activities in the cumene cracking reaction than Al-MCM-41 materials.

Sumiya et al. [66] synthesised mesoporous siliceous SBA-15 molecular sieve and carried out post-synthesis alumination with trimethylaluminium (TMA). They found that the aluminium could be easily incorporated into the siliceous framework of SBA-15 without serious structure deformation. From detailed characterisation of the prepared aluminium-containing SBA-15 it was also found that it is difficult to keep the aluminium in the framework position after calcination. The hydrothermal stability of SBA-15 was considerably improved by the TMA processing.

4.3 Applications of mesoporous materials

The enormous interest in these materials, especially zeolites, is due to their wide catalytic applications within industrial areas, such as oil refining, petrochemistry and synthesis of chemicals. The materials are also important as adsorbents.

Despite their large pore dimensions compared to that of microporous zeolites, mesoporous materials are restricted in their use as catalysts for large organic molecules by their relatively poor thermal stability and broad distribution of acid sites. A combination of the large pore dimensions of mesoporous materials with the strong acid sites present in zeolite-like structures would be highly advantageous leading to a novel and probably useful catalytic material. Hydrocarbon reactions involving large organic molecules that cannot enter the small pores of a zeolite catalyst may be catalyzed by the new material having a mesoporous framework structure with accessible strong acid sites on the surface of these large pores.

When MCM-41 was first discovered there were great expectations for applications in the petroleum industry, for instance in processing of heavy residues.

One of the first areas considered for application of M41S materials was catalytic cracking of large molecules. Corma et al. [67] have compared Al-MCM-41, amorphous silica-alumina and USY zeolite (Zeolite Y) in the catalytic cracking of *n*-heptane. In the cracking of *n*-heptane, the activity of the USY zeolite was approximately 140 times that of Al-MCM-41. This was ascribed to more and stronger Brønsted acid sites in the

zeolite. The Al-MCM-41 activity was higher than for the amorphous silica-alumina and approached that for the USY zeolite in the processing of large oil molecules. The selectivity of Al-MCM-41 in the gas oil cracking resulted in more liquid fuels and less gases and coke compared to the amorphous silica-alumina. Compared with the USY zeolite, the diesel formation was higher and gives less gasoline and more coke.

Vartuli et al. [68] compared the benzene sorption capacity of the MCM-41 and MCM-48 catalysts. They found that the hydrocarbon sorption increases with pore diameter for the calcined versions. The sorption of hydrocarbons by as-synthesised M41S materials is a unique feature not observed with microporous molecular sieves.

Mesoporous aluminosilicas can serve as solid acid catalysts by introducing negative charges into the silica framework by substituting trivalent aluminium for tetravalent silicon. Aluminated SBA-15 material can catalyse reactions with large bulky aromatic molecules. One example is the Friedel-Crafts benzylation of toluene [69].

Other applications as redox catalysis, support material, films and membranes are reviewed by Trong On et al. [50] and Øye et al. [53].

4.4 The use of metal-modified zeolite catalysts

Bezouhanova [70] replaced the classical acid catalysts with zeolites in acylation of benzene ring. The activity of zeolite CeY was compared with that cation exchanged montmorillonite. The yield of acylation products varied upon the nature of interlayer cation. Al-montmorillonite was more active compared with other pillared clays containing H, Ni, Zr, Ce, Cu or La cations. From the experiment with the toluene introduction the coordination complex of acetyl chloride with Zn seemed to be more reactive, but actually Zn-MCM-41 was less active than H-MCM-41. Zeolite encaged transition metallophthalocyanines, for instance CoPcX activated the air oxidation of ethylbenzene to acetophenone. In the presence of Ti-zeolite TS-1 or V-containing VAPO-5 hydrogen peroxide or alkylperoxides were used as oxidants. Benzylic oxidation was performed also by alkylhydroperoxide in the presence of chromium pillared clays. Under these conditions the branched hydrocarbons were not oxidised at the tertiary carbon atom.

Bonelli et al. [71] were testing as-synthesized Na-bearing MCM-41 sample with Si/Al=20, together with several Cs or K exchanged samples in the isomerisation of 1-butene. They used Al-MCM-41 in protonic form as a reference. The totally siliceous sample was not active. Al-MCM-41 was the most active catalyst, with conversions close to thermodynamic equilibrium between cis/trans 2-butene. All examples with the likely exception of Al-MCM-41 showed some deactivation during the time of reaction.

Catani et al. [72] tested Al-MCM-41 type catalysts containing small amounts of metal (Ni, Rh or Pt) in the synthesis of clean diesel fuels by oligomerisation of light alkenes and alkanes. High Si/Al ratios had a negative effect on both activity and catalyst stability. Si/Al ratio at 20 was observed to be optimal. The presence of small amount of metal inside the mesoporous structure did not significantly modify the catalytic activity, although specific effects were detected for each element.

Fujishima et al. [73] studied the catalytic performances of *bis*- and *tris*(bipyridine) Ru complexes grafted on mesoporous FSM-16 in the photooxidation of benzene to phenol using H₂O₂ as an oxidant. [Ru(bpy)₃]Cl₂/FSM-16 showed a high activity under UV-irradiation, and the turnover number (TON) of phenol was 430 based on Ru in 24 h, and the selectivity to phenol among the products was 98 %.

Lewandowska et al. [74] worked with siliceous, aluminosilicate and niobosilicate mesoporous MCM-41 in hydrogenation of benzene. They found that at a low temperature the catalytic activity in the hydrogenation of benzene increases with Ni dispersion, whereas at higher temperatures (150–200 °C) it is possibly determined by H₂ chemisorption strength and the reducibility of Ni-species.

Noreña-Franco et al. [75] studied the oxidation reaction of phenol in aqueous and acetonitrile media under mild conditions, employing Cu-modified MCM-41 mesoporous catalysts. They found that the highest activity was obtained with copper acetate–MCM-41 catalysts.

Yuan et al. [76] synthesised manganese modified MCM-41 catalysts under mild alkaline conditions under the absence of alkaline metal ions, and characterised them. They found that after calcination the nanostructure of the silicate possessed a high thermal stability. The total pore volume of the MnMCM-41 sample was 1.30 cm³/g with a corresponding surface area of 1510 m²/g.

Sheldon et al. [77] wrote a review article about applications of zeolite catalysts in several chemical reactions. These reactions include acid, base and redox catalysis.

5 Suggestions for further work

Catalysts. The MCM-41 type catalysts did not perform well during this work with spruce biomass. On the other hand, they do not have a satisfactory hydrothermal stability. Therefore, it is not recommended to use them if the biomass is wood. In case of grassy biomass, it is recommended to develop an MCM-41 catalyst with improved hydrothermal stability first.

As we could see, metal incorporation into Al-MCM-41 structure improved the catalyst properties, and it is possible that we get a better catalyst with modification of Al-SBA-15 with metals as well. It is recommended to perform a literature study of the suitable metals for biomass pyrolysis with this type of catalyst.

Catalyst degradation study. In order to get a better picture of the catalysts' properties and how the activities change during long-term operation, it is recommended to test them after several regeneration cycles, together with measuring the activity loss and the changes in crystalline structure after the experiments and the regeneration processes.

Waste pyrolysis. One of our greatest environmental problems is the amount of waste, which is very complex and difficult to handle. Some experiments could be done on waste, to see if catalysts make the products from waste pyrolysis more suitable for energy purposes. Wastes from pulp and paper industry can have a great potential, if cheap drying is possible [78-80].

References

1. D. O. Hall (1997) Biomass energy in industrialised countries – a view of the future *Forest Ecology and Management* **91** p 17.
2. Norwegian Bioenergy Association homepage, www.nobio.no
3. H. L. Chum, R. P. Overend (2001) Biomass and renewable fuels *Fuel Processing Technology* **71** p 187.
4. A. V. Bridgwater, D. Meier, D. Radlein (1999) An overview of fast pyrolysis of biomass *Organic Geochemistry* **30** p 1479.
5. A. P. C. Faaij, Bio-energy in Europe: changing technology choices *Energy Policy*, article in press, available online at www.sciencedirect.com
6. A. V. Bridgwater, D. C. Elliott, L. Fagernäs, J. S. Gifford, K. L. Mackie, A. J. Toft, (1995) The nature and control of solid, liquid and gaseous emissions from the thermochemical processing of biomass *Biomass and Bioenergy* **9** p 325.
7. M. Lapuerta, O. Armas, R. Ballesteros, J. Fernández (2005) Diesel emissions from biofuels derived from Spanish potential vegetable oils *Fuel* **84** p 773.
8. F. Yüksel, B. Yüksel (2004) The use of ethanol-gasoline blend as a fuel in an SI engine *Renewable Energy* **29** p 1181.
9. A. C. Hansen, Q. Zhang, P. W. L. Lyne (2005) Ethanol-diesel fuel blends – a review *Bioresource Technology* **96** p 277.
10. M. J. Antal Jr., (1983) Biomass pyrolysis: A review of the literature Part 1 - carbohydrate pyrolysis *Advances in Solar Energy* (Edited by K. W. Boer and J. A. Duffie, Am. Solar Energy Soc, N. Y.) p 61.
11. A. V. Bridgwater, G. V. C. Peacocke (2000) Fast pyrolysis processes for biomass *Renewable and Sustainable energy Reviews* **4** p 1.
12. I. Boukis, K. Maniatis, A. V. Bridgwater, V. Vassilatos, S. Kyritsis (1993) Design concept and hydrodynamics of an air-blown circulating fluidized bed reactor for biomass flash pyrolysis *Advances in thermochemical biomass conversion* (edited by A. V. Bridgwater) **2** p 1151.
13. V. Bridgwater (1999) Principles and practice of biomass fast pyrolysis processes for liquids *Journal of Analytical and Applied Pyrolysis* **51** p 3.

14. A. M. C. Janse, W. Prins, W. P. M. van Swaaij (1997) Development of a small integrated pilot plant for flash pyrolysis of biomass *Developments in thermochemical biomass conversion (edited by A. V. Bridgwater and D. G. B. Boocock)* **1** p 368.
15. C. Roy, D. Blanchette, B. de Caumia, B. Labrecque (1993) Conceptual design and evaluation of a biomass vacuum pyrolysis plant *Advances in thermochemical biomass conversion (edited by A. V. Bridgwater)* **2** p 1165.
16. F. Goudriaan, B. van de Beld, F. R. Boerefijn, G. M. Bos, J. E. Naber, S. van de Wal, J. A. Zeevalkink (2001) Thermal efficiency of the HTU[®] process for biomass liquefaction *Progress in thermochemical biomass conversion (edited by A. V. Bridgwater)* **2** p 1312.
17. G. Dobele, D. Meier, O. Faix, S. Radtke, G. Rossinskaja, G. Telysheva (2001) Volatile products of catalytic flash pyrolysis of celluloses *Journal of Analytical and Applied Pyrolysis* **58-59** p 453.
18. D. R. Huffman, A. J. Vogiatzis, A. V. Bridgwater (1993) The characterization of fast pyrolysis bio-oils *Advances in thermochemical biomass conversion (edited by A. V. Bridgwater)* **2** p 1095.
19. R. Maggi, B. Delmon (1993) Characterization of bio-oils produced by pyrolysis *Advances in thermochemical biomass conversion (edited by A. V. Bridgwater)* **2** p 1086.
20. T. Milne, F. Agblevor, M. Davis, S. Deutch, D. Johnson (1997) A review of the chemical composition of fast-pyrolysis oils from biomass *Developments in thermochemical biomass conversion (edited by A. V. Bridgwater and D. G. B. Boocock)* **1** p 409.
21. K. Sipilä, E. Kuoppala, L. Fagernäs, A. Oasmaa (1998) Characterization of biomass-based flash pyrolysis oils *Biomass and Bioenergy* **14** p 103.
22. D. Meier, A. Oasmaa, G. V. C. Peacocke (1997) Properties of fast pyrolysis liquids: Status of test methods *Developments in thermochemical biomass conversion (edited by A. V. Bridgwater and D. G. B. Boocock)* **1** p 391.
23. D. Meier (2002) Summary of the analytical methods available for chemical analysis of pyrolysis liquids *Fast Pyrolysis of biomass: A Handbook Vol. 2. (edited by A V Bridgwater)* p 59.

24. O. Faix, I. Fortmann, D. Meier (1990) Thermal degradation products of wood: Gas chromatographic separation and mass spectrometric characterization of monomeric lignin derived products *Holz als Roh- und Werkstoff* **48** p. 281.
25. O. Faix, I. Fortmann, D. Meier (1990) Thermal degradation products of wood: A collection of electron-impact (EI) mass spectra of monomeric lignin derived products *Holz als Roh- und Werkstoff* **48** p. 351.
26. O. Faix, I. Fortmann, J. Bremer, D. Meier (1991) Thermal degradation products of wood: Gas chromatographic separation and mass spectrometric characterisation of polysaccharide derived products *Holz als Roh- und Werkstoff* **49** p 213.
27. O. Faix, I. Fortmann, J. Bremer, D. Meier (1991) Thermal degradation products of wood: A collection of electron impact (EI) mass spectra of polysaccharide derived products *Holz als Roh- und Werkstoff* **49** p 299.
28. J. P. Diebold (2000) A review of the chemical and physical mechanisms of the storage stability of fast pyrolysis bio-oils *NREL subcontractor report*
29. J. P. Diebold, T. A. Milne, S. Czernik, A. Oasmaa, A. V. Bridgwater, A. Cuevas, S. Gust, D. Huffman, J. Piskorz (1997) Proposed specifications for various grades of pyrolysis oils *Developments in thermochemical biomass conversion (edited by A. V. Bridgwater and D. G. B. Boocock)* **1** p 433.
30. A. Oasmaa, D. Meier (2002) Pyrolysis liquids analyses, the results of IEA-EU round robin *Fast Pyrolysis of biomass: A Handbook Vol. 2. (edited by A V Bridgwater)* p 41.
31. P. James, P. E. Diebold (2002) A review of the chemical and physical mechanisms of the storage stability of fast pyrolysis bio-oils *Fast Pyrolysis of biomass: A Handbook Vol. 2. (edited by A V Bridgwater)* p 243.
32. M. E. Boucher, A. Chaala, C. Roy (2000) Bio-oils obtained by vacuum pyrolysis of softwood bark as a liquid fuel for gas turbines. Part I: Properties of bio-oil and its blends with methanol and a pyrolytic aqueous phase *Biomass and Bioenergy* **19** p 337.

33. M. E. Boucher, A. Chaala, C. Roy (2000) Bio-oils obtained by vacuum pyrolysis of softwood bark as a liquid fuel for gas turbines. Part II: Stability and ageing of bio-oils and its blends with methanol and a pyrolytic aqueous phase *Biomass and Bioenergy* **19** p 351.
34. S. Czernik, R. Maggi, G. V. C. Peacocke (2002) Review of methods for upgrading biomass-derived fast pyrolysis oils *Fast Pyrolysis of biomass: A Handbook Vol. 2. (edited by A V Bridgwater)* p 141.
35. R. K. Sharma, N. N. Bakhshi (1993) Conversion of non-phenolic fraction of biomass-derived pyrolysis oil to hydrocarbon fuels over HZSM-5 using a dual reactor system *Bioresource Technology* **45** p 195.
36. R. K. Sharma, N. N. Bakhshi (1993) Upgrading of pyrolytic lignin fraction of fast pyrolysis oil to hydrocarbon fuels over HZSM-5 in a dual reactor system *Fuel Processing Technology* **35** p 201.
37. J. D. Adjaye, N. N. Bakhshi (1995) Production of hydrocarbons by catalytic upgrading of a fast pyrolysis bio-oil: Part I: Conversion over various catalysts *Fuel processing technology* **45** p 161.
38. J. D. Adjaye, N. N. Bakhshi (1995) Production of hydrocarbons by catalytic upgrading of a fast pyrolysis bio-oil: Part II: Comparative catalyst performance and reaction pathways *Fuel processing technology* **45** p 185.
39. Rolin, C. Richard, D. Masson, X. Deglise (1983) Catalytic conversion of biomass by fast pyrolysis *Journal of Analytical and Applied Pyrolysis* **5** p 151.
40. K. S. Gregorski, A. E. Pavlath (1985) Study of the catalytic pyrolysis of carbohydrates through thermogravimetry *Thermochimia Acta* **93** 395.
41. C. A. Zaror, I. S. Hutchings, D. L. Pyle, H. N. Stiles, R. Kandiyoti (1985) Secondary char formation in the catalytic pyrolysis of biomass *Fuel* **64** p 990.
42. Cr. I. Simionescu, C. Vasile, P. Onu, M. Sabliovschi, G. Moroi, V. Barboiu, D. Ganju, M. Florea (1988) Modification in thermal decomposition products of polymers by catalytic pyrolysis *Thermochimia Acta* **134** p 301.
43. A. V. Bridgwater (1994) Catalysis in thermal biomass conversion *Applied Catalysis A: General* **116** p 5.

44. E. Laurent, B. Delmon (1994) Study of the hydrodeoxygenation of carbonyl, carboxylic and guaiacyl groups over sulfided CoMo/ γ -Al₂O₃ and NiMo/ γ -Al₂O₃ catalysts. I. Catalytic reaction schemes *Applied Catalysis A* **109** p 77.
45. M. Samolada, I. A. Vasalos: Catalytic pyrolysis of biomass for improved liquid fuel quality. Final report of the contract: JOR3-CT95-0081
46. E. H. Salter, N. M. Robinson, G. C. Peacocke, D. Ristorcelli, H. Sheena, A. V. Bridgwater (1998) Catalytic fast pyrolysis of biomass *IChemE Res. Event, Two-Day Symp.*, p 89.
47. D. Chiaramonti, M. Bonini, E. Fratini, G. Tondi, K. Gartner, A. V. Bridgwater, H. P. Grimm, I. Soldaini, A. Webster, P. Baglioni (2003) Development of emulsions from biomass pyrolysis liquid and diesel and their use in engines – Part 1: emulsion production *Biomass and Bioenergy* **25** p 85.
48. D. Chiaramonti, M. Bonini, E. Fratini, G. Tondi, K. Gartner, A. V. Bridgwater, H. P. Grimm, I. Soldaini, A. Webster, P. Baglioni (2003) Development of emulsions from biomass pyrolysis liquid and diesel and their use in engines – Part 2: test in diesel engines *Biomass and Bioenergy* **25** p 101.
49. U. Ciesla, F. Schüth (1999) Ordered mesoporous materials (Review) *Microporous and Mesoporous Materials* **27** p 131.
50. D. Trong On, D. Desplandier-Giscard, D. Danumah, S. Kaliaguine (2001) Perspectives in catalytic applications of mesostructured materials *Applied Catalysis A: General* **222** p 299.
51. G. D. Stucky, D. Zhao, P. Yang, W. Lukens, N. Melosh, B. F. Chmelka, (1998) Using the Organic-Inorganic Interface to Define Pore and Macroscale Structure *Studies in Surface Science and Catalysis* **117** p 1.
52. D. Zhao, J. Feng, Q. Huo, N. Melosh, G. H. Fredrickson, B. F. Chmelka, G. D. Stucky (1998) Triblock copolymer syntheses of mesoporous silica with periodic 50 to 300 angstrom pores *Science* **279** p 548.
53. G. Øye, J. Sjöblom, M. Stöcker (2001) Synthesis, characterisation and potential applications of new materials in the mesoporous range *Advances in Colloid and Interface Science* **89-90** p 439.

54. G. L. Haller (2003) New catalytic concepts from new materials: understanding catalysis from a fundamental perspective, past, present and future *Journal of Catalysis* **216** p 12.
55. R. Schmidt, D. Akporiaye, M. Stöcker, O. H. Ellestad (1994) Synthesis of Al-containing MCM-41 materials: Template interaction and removal *Zeolites and Related Microporous Materials: State of the art 1994 (Edited by J. Weitkamp, H. G. Karge, H. Pfeifer, W. Hölderich) Studies in Surface Science and Catalysis* **84** p 61.
56. R. Mokaya (2001) Influence of pore wall thickness on the steam stability of Al-grafted MCM-41 *Chemical Communications* p 633.
57. R. Ryoo, J. M. Kim, C. H. Shin, J. Y. Lee (1997) Synthesis and hydrothermal stability of a disordered mesoporous molecular sieve *Zeolites and Related Microporous Materials: State of the art 1994 (Edited by J. Weitkamp, H. G. Karge, H. Pfeifer, W. Hölderich) Studies in Surface Science and Catalysis* **105** p 45.
58. D. Das, C. M. Tsai, S. Cheng (1999) Improvement of hydrothermal stability of MCM-41 mesoporous molecular sieve *Chemical Communications* p 473.
59. F. S. Xiao, Y. Han, Y. Yu, X. Meng, M. Yang, S. Wu (2002) Hydrothermally stable ordered mesoporous titanosilicates with highly active catalytic sites *J. Am. Chem. Soc.* **124** p 888.
60. T. R. Pauly, V. Petkov, Y. Liu, S. J. L. Billinge, T. J. Pinnavaia (2002) Role of framework sodium versus local framework structure in determining the hydrothermal stability of MCM-41 mesostructures *J. Am. Chem. Soc.* **124** p 97.
61. D. Trong On, S. Kaliaguine (2002) Ultrastable and highly acidic, zeolite-coated mesoporous aluminosilicates *Angew. Chem. Int. Ed* **41** p 1036.
62. A. Corma, M. T. Navarro (2002) From micro to mesoporous molecular sieves: adapting composition and structure for catalysis *Studies in surface science and catalysis (edited by R. Aiello, G. Giordano, and F. Testa; Elsevier Science B.V.)* p 487.

63. Z. Zhang, Y. Han, F. S. Xiao, S. Qiu, L. Zhu, R. Wang, Y. Yu, Z. Zhang, B. Zou, Y. Wang, H. Sun, D. Zhao, Y. Wei (2001) Mesoporous aluminosilicates with ordered hexagonal structure, strong acidity, and extraordinary hydrothermal stability at high temperatures *J. Am. Chem. Soc.* **123** p 5014.
64. D. Zhao, C. Nie, Y. Zhou, S. Xia, L. Huang, Q. Li (2001) Comparison of disordered mesoporous aluminosilicates with highly ordered Al-MCM-41 on stability, acidity and catalytic activity *Catalysis Today* **68** p 11.
65. Y. Yue, A. Gédéon, J. L. Bonardet, N. Melosh, J. B. D'Espinoza, J. Fraissard (1999) Direct synthesis of AISBA mesoporous molecular sieves: characterisation and catalytic activities *Chemical Communications* p 1967.
66. S. Sumiya, Y. Oumi, T. Uozumi, T. Sano (2001) Characterisation of AISBA-15 prepared by post-synthesis alumination with trimethylaluminium *Journal of Materials Chemistry* **11** p 1111.
67. Corma, M. S. Grande, V. Gonzalez-Alfaro, A. V. Orchilles (1996) Cracking activity and hydrothermal stability of MCM-41 and its comparison with amorphous silica-alumina and USY zeolite *Journals of Catalysts* **159** p 375.
68. J.C. Vartuli, A. Malek, W. J. Roth, C. T. Kresge, S. B. McCullen (2001) The sorption properties of as-synthesised and calcined MCM-41 and MCM-48 *Microporous and Mesoporous Materials* **44-45** p 691.
69. J. J. Chiu, D. J. Pine, S. T. Bishop, B. F. Chmelka (2004) Friedel-Crafts alkylation properties of aluminosilica SBA-15 meso/macroporous monoliths and mesoporous powders *Journal of Catalysis* **221** p 400.
70. C. P. Bezouhanova (2002) Synthesis of aromatic ketones in the presence of zeolite catalysts *Applied Catalysis A: General* **229** p 127.
71. B. Bonelli, M.F. Ribeiro, A.P. Antunes, S. Valange, Z. Gabelica, E. Garrone (2002) Al-MCM-41 systems exchanged with alkali-metal cations: FT-IR characterization and catalytic activity towards 1-butene isomerization *Microporous and Mesoporous Materials* **54** p 305.
72. R. Catani, M. Mandreoli, S. Rossini, A. Vaccari (2002) Mesoporous catalysts for the synthesis of clean diesel fuels by oligomerisation of olefins *Catalysis Today* **75** p 125.

73. K. Fujishima, A. Fukuoka, A. Yamagishi, S. Inagaki, Y. Fukushima, M. Ichikawa (2000) Photooxidation of benzene to phenol by ruthenium bipyridine complexes grafted on mesoporous silica FSM-16 *Journal of Molecular Catalysis A: Chemical* **166** p 211.
74. Lewandowska, S. Monteverdi, M. Bettahar, M. Ziolk (2002) MCM-41 mesoporous molecular sieves supported nickel—physico-chemical properties and catalytic activity in hydrogenation of benzene *Journal of Molecular Catalysis A: Chemical* **188** p 85.
75. L. Noreña-Franco, I. Hernandez-Perez, J. Aguilar-Pliego, A. Maubert-Franco (2002) Selective hydroxylation of phenol employing Cu–MCM-41 catalysts *Catalysis Today* **75** p 189.
76. Z-Y. Yuan, H-T. Ma, Q. Luo, W. Zhou (2002) Synthesis and characterization of manganese-modified MCM-41 *Materials Chemistry and Physics* **77** p 299.
77. R.A. Sheldon, R.S. Downing (1999) Heterogeneous catalytic transformations for environmentally friendly production *Applied Catalysis A: General* **189** p 163.
78. Y. H. Yu, S. D. Kim, J. M. Lee, K. H. Lee (2002) Kinetic studies of dehydration, pyrolysis and combustion of paper sludge *Energy* **27** p 457.
79. A. van der Drift, J. van Doorn, J. W. Vermeulen (2001) Ten residual biomass fuels for circulating fluidized-bed gasification *Biomass and Bioenergy* **20** p 45.
80. Zs. Kádár, Zs. Szengyel, K. Réczey, (2004) Simultaneous saccharification and fermentation (SSF) of industrial wastes for the production of ethanol *Industrial Crops and Products* **20** p 103.

Paper I.

Presented as a poster presentation in the conference of "Science in Thermal and Chemical Biomass Conversion", Victoria BC, Canada, August 2004.

Published in the conference proceedings.

Catalytic pyrolysis of biomass

Judit Adam^a, Marianne Blazsó^b, Erika Mészáros^b, Michael Stöcker^c,
Merete H. Nilsen^c, Aud Bouzga^c, Johan E. Hustad^a, Morten Grønli^a,
Gisle Øye^d

^a*Department of Energy and Process Engineering, Norwegian University of Science and Technology, Trondheim, Norway*

^b*Institute of Materials and Environmental Chemistry, Chemical Research Center, Hungarian Academy of Sciences, Budapest, Hungary*

^c*SINTEF Materials and Chemistry, Oslo, Norway*

^d*Ugelstad Laboratory, Department of Chemical Engineering, Norwegian University of Science and Technology, Trondheim, Norway*

ABSTRACT: The effects of Al-MCM-41 catalysts on the thermal decomposition of barkfree spruce wood were studied. Samples of wood – catalyst mixtures were subjected to analytical pyrolysis at 500 °C for 20 seconds using on-line pyrolysis-gas chromatography/mass spectrometry (Py-GC/MS). Thermogravimetry (TG) experiments were performed to monitor the weight loss under slow heating rate conditions (20 °C/min) from 50 to 800 °C.

MCM-41 type mesoporous catalysts converted the pyrolysis vapours into lower molecular weight products, and hence more desired bio-oil properties can be achieved. The catalytic properties of MCM-41 materials can be significantly improved when specific transition metal cations or metal complexes are introduced into the structure. Pore enlargement allows the processing of larger molecules. In the present work, four catalysts were tested; all of them were Al-MCM-41 type catalysts with a Si/Al ratio of 20. These catalysts were: an unmodified Al-MCM-41, a transition metal (Cu) modified Al-MCM-41, and two Al-MCM-41 catalysts with enlarged pores. Different pore sizes were obtained by altering the chain length of the template and by applying a spacer. Due to the activity of the catalysts, the product distribution of pyrolysis vapours changed significantly. In accordance with published reports, higher coke and water formation was observed during the reaction in the presence of the catalysts. The various catalysts showed different influences on the product distribution, and the greatest difference was achieved by using the unmodified Al-MCM-41 catalyst. Thermogravimetric experiments indicated that the applied Al-MCM-41 catalysts increase the char and the water yield during the thermal decomposition of biomass. Nevertheless, the product distribution is altered due to the transformation of the volatile pyrolysis products by the catalysts.

INTRODUCTION

Wood and biomass can be used in a variety of ways to provide energy. Bio-oil is mainly produced by fast pyrolysis and its heating value is about half of that of the conventional fuel oil. Bio-oil can substitute fuel or diesel oil in many applications including boilers, furnaces, engines and turbines for electricity generation. There is also a range of chemicals (food flavourings, resins, agrochemicals, fertilisers, etc.) that can be extracted or derived from bio-oils [1].

Unfortunately, some bio-oils rapidly become more viscous under storage. The pyrolysis oils are chemically reactive with themselves and will polymerise with time, usually with the formation of additional water as a byproduct of the reactions. After prolonged storage, the oils tend to increase their molecular weight owing to chemical reactions, viscosity, and also tendency to separate into a thin oil phase and a thick tar phase. This process is called aging, and makes storage and usage difficult [2].

Stabilisation of bio-oils and slowing of their aging can be achieved by upgrading them either with solvents or with the help of catalysts. The upgrading possibilities are reviewed by Czernik et al [3]. Vitolo et al. [4] studied different types of zeolites to upgrade bio-oil to fuel. They studied the influence of residence time and temperature in a fixed bed microreactor, too. Simionescu et al. [5] investigated the catalytic pyrolysis of various hydrocarbon products. They concluded that the catalysts cause an increase in the amount of gas, and 5-10% coke deposits on the catalyst. Gregorski et al. [6] found that the volatile products decrease with catalytic pyrolysis and more with acidic than basic catalysts. Adjaye et al. [7,8] investigated the upgrading of fast pyrolysis bio-oils with different catalysts in a fixed bed micro-reactor. They found that upgrading of bio-oils with silicate was highly disadvantageous, and the most effective catalysts to upgrade bio-oil to hydrocarbons were acidic zeolite catalysts. They reported a significant amount of char production during upgrading. The catalyst effectiveness to reduce the coke formation decreased with increase in the pore size of the acidic zeolite catalysts.

Catani et al. [9] tested Al/Si MCM-41 type catalysts containing small amounts of metal (Ni, Rh or Pt) in the synthesis of clean diesel fuels by oligomerisation of orphan olefin streams. High Si/Al ratios had a negative effect on both activity and catalyst stability. Si/Al ratio at 20 was observed to be optimal. The presence of small amount of metal inside the mesoporous structure did not significantly modify the catalytic activity, although specific effects were detected for each element.

Noreña-Franco et al. [10] studied the oxidation reaction of phenol in aqueous and acetonitrile media under mild conditions, employing Cu-modified MCM-41 mesoporous catalysts. They found that the highest activity was obtained with copper acetate-MCM-41 catalysts.

The hydrothermal stability of MCM-41 catalysts depends on the preparation method, the aluminium content and the thickness of pore walls. Up to now the results are still not satisfactory [11-13].

The aim of the present work is to study the thermal decomposition of spruce wood in the presence of MCM-41 type catalysts. These catalysts were tested as possible materials capable of modifying the thermal decomposition products of spruce, which is a waste material of wood industry in northern countries. In this work the product distributions were compared to each other and the catalyst influences were evaluated by the different yields of the chosen compounds.

EXPERIMENTAL

MATERIALS

Barkless spruce wood was milled and sieved and a fraction of particle diameter $<45\mu\text{m}$ was used in the experiments. The water content of the sample was approximately 6%. Four different mesoporous MCM-41 catalysts with Si/Al ratio of 20 have been tested: an unmodified one (K1 sample), two different with enlarged pores (K2 and K3 samples) and a transition metal (Cu) modified one (K4 sample). The pore enlargement in sample K2 was carried out with a spacer (mesitylene, C_9H_{12}), and in sample K3 by altering the template chain length from C_{14} to C_{18} .

The catalyst preparation

K1: Al-MCM-41

The surfactant, $\text{C}_{14}\text{H}_{29}(\text{Me})_3\text{NBr}$ (tetradecyltrimethylammonium bromide, 15.15 g), is dissolved in water (95 g). Sodium-aluminate (0.43 g) is added and the solution is stirred overnight. Silica source, sodium-meta-silicate-5-hydrate (8.9% Na_2O + 28% SiO_2 , 19.4 g), H_2SO_4 (10%, 5.6 g) and water (15 g) is added, and the solution is stirred for 30 minutes. The pH is adjusted to ~ 10 .

The solution is filled in a teflon-flask, heated at 100°C for 6 days, washed with distilled water and centrifuged until pH 5 is obtained. The white product is dried at 100°C overnight.

K2: MCM-41 with a spacer

The surfactant, $\text{C}_{14}\text{H}_{29}(\text{Me})_3\text{NBr}$ (tetradecyltrimethylammonium bromide, 15.5 g) is dissolved in water (50 g) and stirred for 30 minutes. Sodium-aluminate (54% Al_2O_3 , 41% Na_2O , 0.43 g) is dissolved in water (40 g) and H_2SO_4 (95%, 1.4 g) is added to the solution, then it is stirred for 30 minutes. The solution of aluminium is then added dropwise to the solution of surfactant and the mixture is stirred for one hour. Sodium-meta-silicate-5-hydrate (8.9% Na_2O + 28% SiO_2 , 19.7 g) is dissolved in water (15 g) and stirred for 30 minutes before it is added dropwise to the solution described above and stirred for 1 hour. The spacer, mesitylene, (C_9H_{12} , 14.4 g) is added dropwise, and stirred for 24 hours. The final solution is treated as described above.

K3: MCM-41 with C₁₈ as surfactant

The synthesis is carried out at 50°C. The surfactant, C₁₈H₃₇(Me)₃NBr (octadecyltrimethylammonium bromide, C₁₈, 15.7 g) is added to water (100 g) and stirred for 1 hour. Sodium-aluminat (54% Al₂O₃, 41% Na₂O, 0.44 g) is added to the solution and stirred for 4 hours, then H₂SO₄ (10%, 5.7 g) is added to it. Sodium-meta-silicate-5-hydrate (8.9% Na₂O + 28% SiO₂, 18.7 g) is added to water (40 g), and stirred for a few minutes. The mixture is added dropwise to the acidic solution of C₁₈ and aluminium. A yellow-coloured product is formed. After stirring for 30 minutes, a homogenous, light pink solution is obtained. The final solution is treated as described above.

K4: Cu-Al-MCM-41

The surfactant C₁₄H₂₉(Me)₃NBr (tetradecyltrimethylammonium bromide, 7.1 g) is dissolved in water (50 g) and stirred for 1 hour. Sodium-aluminate (54% Al₂O₃, 41% Na₂O, 0.45 g) is dissolved in water (40 g) and H₂SO₄ (95%, 1.5 g) and is added to the solution, which is stirred for 45 minutes. Copper acetate (2.0 g) is added to the solution of aluminium, and stirred for 1 hour. The solution obtained is then added dropwise to the solution of template. The light blue solution is stirred for one hour. Sodium-meta-silicate-5-hydrate (8.9% Na₂O + 28% SiO₂, 18,7 g) is dissolved in water (15 g) and stirred for 50 minutes before it is added dropwise to the solution described above and stirred for 2 hours. The pH in the final solution is 10. The final solution is treated as described above. The product is light-blue.

THERMOGRAVIMETRY

TG experiments were carried out in a Perkin-Elmer TGS-2 thermobalance. Samples of 3-6 mg depending on catalyst usage were placed into a platinum sample pan and heated at a rate of 20 °C/min in argon atmosphere. The background due to the given catalyst is subtracted from the TG curves of the catalyst containing samples in all cases.

PYROLYSIS-GC/MS

Py-GC/MS (pyrolysis-gas chromatography/mass spectrometry) experiments were performed at 500°C for 20 sec in a Pyroprobe 2000 pyrolyser (Chemical Data System) equipped with a platinum coil and quartz sample tube interfaced to a gas chromatograph (Agilent GC 6890) coupled to a mass selective detector (Agilent MSD 5973) operating in electron impact mode (EI) at 70 eV. The temperature of the GC/MS interface was held at 280 °C.

The same amounts (1.5-2.0 mg) of wood and catalyst, respectively were weighed into the pyrolysis tube. The wood was placed in the middle of the pyrolysis tube and the catalyst next to the wood at both ends of the tube. A comparative experiment was carried out with a pre-mixed sample of the same wood to catalyst ratio (1:1). The product pattern of the pyrolysis did not change due to variations in the sampling procedure, however, their relative yields showed considerable differences. Sampling without mixing was chosen for better control of the wood to catalyst ratio.

A helium carrier gas of 20 ml/min flow rate purged the pyrolysis chamber held at 250°C. A split of the carrier gas (1:20) was applied. The GC separation was carried out on a fused silica capillary column (Hewlett-Packard 5MS), 30m x 0.25mm. A temperature program from 50 to 300 °C at 10 °C/min heating rate was applied with an isothermal period of 1 min at 50°C and of 4 min at 300°C. The pyrolysis temperature was chosen for optimal bio-oil production as earlier reported [1].

Identification of the GC/MS peaks was based in most cases on comparison with spectra of the NIST 98 spectrum library. The semi-quantitative analysis of the products was based on the peak areas of selected characteristic molecular or fragment ion gas chromatograms. No internal standard was used, since the production of the same compounds were compared in various experiments, in order to follow the influence of the catalysts on the formation of the selected oil components.

RESULTS AND DISCUSSION

TG EXPERIMENTS

We applied thermogravimetry to monitor mass changes of the samples during thermal decomposition at relatively low heating rate (20°C/min).

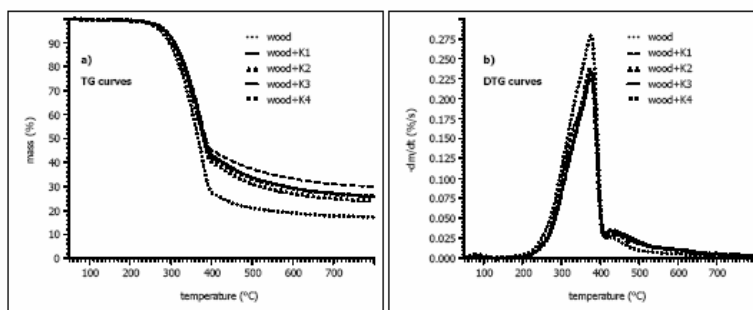


Fig. 1 TG (a) and DTG (b) curves of spruce wood and mixtures of wood and Al-MCM-41 catalysts.

Fig. 1/a shows the variation of TG curves of spruce heated together with the studied catalysts. The changes observed clearly indicate that the total amount of volatile products is decreased, while the char yield is increased in the presence of catalysts. This is in good agreement with previous studies [3,7,8]. The char residue is the highest for the sample catalysed with the unmodified catalyst (K1).

As the DTG curves indicate in Fig. 1/b, the maximal rate of decomposition occurs at about the same temperature (370 °C) in all cases, in spite of the presence of the catalysts. Only the height of DTG curves is decreased due to catalyst, corresponding to the lower yield of volatile products compared to that of wood. The similar decomposition temperatures mean that the main wood decomposition reactions leading

to volatile formation are not much influenced by these catalysts, however it should be noted that the catalysts were not impregnated on the wood particles, only the decomposition products of wood contacted with them in the vapour phase. Pure catalysts samples were studied with TG and DTG also, and we found no sign of thermal degradation of the catalysts.

PY-GC/MS EXPERIMENTS

Py-GC/MS has been applied to clarify the effect of different catalytic materials on the pyrolysis product distribution obtained under fast heating conditions.

Pyrolysis water yields

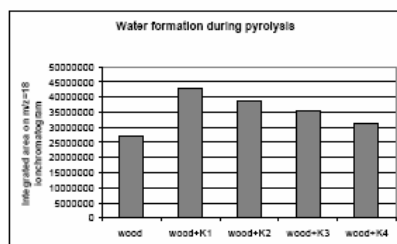


Fig. 2 Yields of pyrolytic water.

As it is shown in Fig. 2, the water yield is higher in all cases from catalyst containing samples compared to that from the wood sample. Catalyst K1 has the strongest effect on the yield of water. The major polymeric constituents of wood, cellulose, hemicellulose and lignin contain a lot of hydroxyl functional groups. The cleavage of these groups is promoted by the zeolite catalysts resulting in the increased water evolution.

Formation of furan derivatives

The pyrolysis of polysaccharide components of wood results mainly in the formation of levoglucosan, pyran-, and furan derivatives as well as smaller molecules (e.g., hydroxyacetaldehyde, acetic acid). Furan derivatives originate from both cellulose and hemicellulose components of wood [14]. The intensity of the furan-ring containing products is shown in Fig. 3.

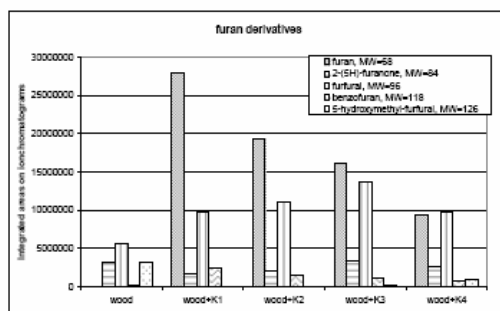


Fig. 3 Amounts of furan and its derivatives during pyrolysis.

As Fig. 3 shows, the MCM-41 type catalyst favors the formation of furan ring. As the result of catalysis, the product distribution changes, unsubstituted furan appeared among the pyrolysis products. As the catalysts worked in the secondary reactions, the levoglucosan yield decreased, its dehydrated product, furan, appeared, and water yield increased. K1 sample produced the highest yield and K4 the least amount of furan. Furfural yield increased with increasing pore size of the catalyst, while the furanone yield did not change significantly. There was a slight increase in benzofuran yield and the furan derivative of the highest molecular mass (5-hydroxymethyl-furfural) decreased in the presence of catalysts.

CONCLUSIONS

As measured by thermogravimetry, the decomposition temperatures of wood sample with and without catalysts are similar, indicating that the catalysts do not influence the primary reactions of wood pyrolysis. This was expected, the catalysts were not impregnated on the wood. However, the char yield increased in the presence of catalyst, which is a drawback of the catalytic pyrolysis. The modified MCM-41 catalysts increased the char yield to a lesser degree than the original catalyst.

During flash pyrolysis, the intensity of volatile products decreases and the water yield increases in the presence of catalysts. It should be noted that the increased yield of furan derivatives is accompanied by the increased water yield and by the reduced amount of levoglucosan, which is one of the most significant pyrolysis products of pure cellulose.

The catalysts promote the formation of the furan ring. The yield of furan decreases and the yield of furfural increases with increasing pore size. Cu-metal incorporation increases the furan and furanone yield also, but compared to catalysts with increased pore sizes the yields are decreased. The effect of MCM-41 type catalyst on the pyrolysis products of spruce seem to be related to the size of the pores of the catalyst and to the transition metal incorporation.

ACKNOWLEDGEMENTS

J. Adam is indebted to the Norwegian Research Council for her Ph. D. grant and M. H. Nilsen thanks the Norwegian University of Science and Technology for the Post-doc grant. M. Stöcker and A. Bouzga acknowledge the financial support of the European Union (ENK 6-CT2001-00049). The work of E. Mészáros and M. Blazsó was supported by the Hungarian National Research Fund (OTKA T037704).

REFERENCES

- 1 A.V. Bridgwater, D. Meier, D. Radlein (1999) An overview of fast pyrolysis of biomass *Organic Geochemistry* **30** 1479-1493
- 2 P. James, P. E. Diebold (2002) A review of the chemical and physical mechanisms of the storage stability of fast pyrolysis bio-oils *Fast Pyrolysis of Biomass: A Handbook Vol. 2. (edited by A. V. Bridgwater; CPL Press, Newbury, UK;)* 243-292
- 3 S. Czernik, R. Maggi, G. V. C. Peacocke (2002) Review of methods for upgrading biomass-derived fast pyrolysis oils *Fast Pyrolysis of Biomass: A Handbook Vol. 2. (edited by A. V. Bridgwater; CPL Press, Newbury, UK;)* 141-145
- 4 S. Vitolo, M. Seggiani, P. Frediani, G. Ambrosini, L. Politi (1999) Catalytic upgrading of pyrolytic oils to fuel over different zeolites *Fuel* **78** 1147-1159
- 5 Cr. I. Simonescu, C. Vasile, P. Omu, M. Sabliovschi, G. Moroi, V. Barboiu, D. Ganju, M. Florea (1988) Modification in thermal decomposition products of polymers by catalytic pyrolysis *Thermochimica Acta* **134** 301-305
- 6 K. S. Gregorski, A. E. Pavlath (1985) Study of the catalytic pyrolysis of carbohydrates through thermogravimetry *Thermochimica Acta* **93** 395-396
- 7 J. D. Adjaye, N. N. Bakhshi (1995) Production of hydrocarbons by catalytic upgrading of a fast pyrolysis bio-oil: Part I: Conversion over various catalysts *Fuel Processing Technology* **45** 161-183
- 8 J. D. Adjaye, N. N. Bakhshi (1995) Production of hydrocarbons by catalytic upgrading of a fast pyrolysis bio-oil: Part II: Comparative catalyst performance and reaction pathways *Fuel Processing Technology* **45** 185-202
- 9 R. Catani, M. Mandreoli, S. Rossini, A. Vaccari (2002) Mesoporous catalysts for the synthesis of clean diesel fuels by oligomerisation of olefins *Catalysis Today* **75** 125-131
- 10 L. Noreña-Franco, I. Hernandez-Perez, J. Aguilar-Pliego, A. Maubert-Franco (2002) Selective hydroxylation of phenol employing Cu-MCM-41 catalysts *Catalysis Today* **75** 189-195
- 11 R. Mokaya (2001) Influence of pore wall thickness on the steam stability of Al-grafted MCM-41 *Chem. Commun.* 633-634
- 12 T. R. Pauly, V. Petkov, Y. Liu, S. J. L. Billinge, T. J. Pinnavaia (2002) Role of framework sodium versus local framework structure in determining the hydrothermal stability of MCM-41 mesostructures *J. Am. Chem. Soc.* **124** 97-103

- 13 A. Corma, M. T. Navarro (2002) From micro to mesoporous molecular sieves: adapting composition and structure for catalysis *Studies in surface science and catalysis* (edited by R. Aiello, G. Giordano, and F. Testa; Elsevier Science B.V.) 487-501
- 14 M. J. Antal Jr (1983) Biomass pyrolysis: A review of the literature Part 1 – carbohydrate pyrolysis *Advances in Solar Energy* (American Solar Energy Society Inc. and Plenum Press)

Paper II.

Published in "Fuel".



Pyrolysis of biomass in the presence of Al-MCM-41 type catalysts

Judit Adam^{a,*}, Marianne Blazsó^b, Erika Mészáros^b, Michael Stöcker^c, Merete H. Nilsen^c,
Aud Bouzga^c, Johan E. Hustad^a, Morten Grønli^a, Gisle Øye^d

^aDepartment of Energy and Process Engineering, Faculty of Engineering Science and Technology, Norwegian University of Science and Technology, K. Hejesvei 1A, N-7491 Trondheim, Norway

^bInstitute of Materials and Environmental Chemistry, Chemical Research Centre, Hungarian Academy of Sciences, P.O. Box 17, H-1525 Budapest, Hungary

^cSINTEF Materials and Chemistry, P.O. Box 124 Blindern, N-0314 Oslo, Norway

^dUgelstad Laboratory, Department of Chemical Engineering, Norwegian University of Science and Technology, Sem Sælandsvei 4, N-7491 Trondheim, Norway

Received 11 November 2004; received in revised form 5 February 2005; accepted 8 February 2005
Available online 17 March 2005

Abstract

Al-MCM-41 type mesoporous catalysts were used for converting the pyrolysis vapours of spruce wood in order to obtain better bio-oil properties. Four Al-MCM-41 type catalysts with a Si/Al ratio of 20 were tested. The catalytic properties of Al-MCM-41 catalyst were modified by pore enlargement that allows the processing of larger molecules and by introduction of Cu cations into the structure.

Spruce wood pyrolysis at 500 °C was performed and the products were analysed with the help of on-line pyrolysis-gas chromatography/mass spectrometry (Py-GC/MS). In addition, thermogravimetry/mass spectrometry (TG/MS) experiments were applied for monitoring the product evolution under slow heating conditions (20 °C/min) from 50 to 800 °C.

Levoglucosan is completely eliminated, while acetic acid, furfural and furanes become quite important among cellulose pyrolysis products over the unmodified Al-MCM-41 catalyst. The dominance of phenolic compounds of higher molecular mass is strongly cut back among the lignin products. Both the increase of the yield of acetic acid and furan and the decrease of large methoxyphenols are repressed to some extent over catalysts with enlarged pores. The Cu modified catalyst performed similarly to the catalyst with enlarged pore size in converting the pyrolysis vapours of wood, although its pore size was similar to the unmodified Al-MCM-41.

© 2005 Elsevier Ltd. All rights reserved.

Keywords: Al-MCM-41; Catalyst; Biomass; Bio-oil; Pyrolysis

1. Introduction

During pyrolysis, wood decomposes and generates gases, condensable vapours and charcoal. Bio-oil is mainly produced by fast pyrolysis—high heating rate and low residence times—obtaining higher yields of condensable vapours than upon slow heating [1].

Analysis and characterisation of fast pyrolysis bio-oils is an important area of research. Data on the physical and chemical properties of these liquids can give important indications about the pyrolysis process parameters and information about quality, toxicity and stability of

the product [1]. There are several papers available on characterisation of fast pyrolysis liquids [2–6] and they agreed on that there is no standard bio-oil, the properties of the liquid are strongly dependent on feedstock and production circumstances. The chemical composition of biomass-based pyrolysis oils is complicated, comprising mainly of water, carboxylic acids, carbohydrates and lignin derived substances [3]. Faix et al. [7–10] published a detailed compilation of the pyrolysis products of wood including gas chromatographic retention data and mass spectra.

The effective usage of bio-oil requires that it retains the initial properties during storage, shipment and use. Unfortunately, some bio-oils rapidly deteriorate under storage. Some components of the pyrolysis oils are chemically reactive and will undergo polymerisation with time, usually with the formation of additional water as a by-product of the reactions. After prolonged storage, the oils become more viscous, and separate into a thin oil phase and a thick tar

* Corresponding author. Tel.: +47 7 359 0623; fax: +47 7 359 8390.
E-mail address: judit.adam@ntnu.no (J. Adam).

phase. This process is called aging, and makes the storage and pumping difficult. Aging is much faster at elevated temperatures [11]. The loss of volatiles also increases the viscosity. The instability of pyrolysis bio-oils and the possible reasons of it have been studied by many researchers, and reviewed by James and Diebold [12].

Taking into consideration the compounds present, chemical reactions may occur within bio-oil: i.e. organic acids form esters with alcohols eliminating water, aldehydes form oligomers and resins, aldehydes and phenolics form resins and water, aldehydes and proteins form oligomers, organic sulphur forms oligomers and unsaturated compounds form polyolefins.

Upgrading of bio-oils can be achieved with solvents and with catalysis. The upgrading possibilities are reviewed by Czernik et al. [13]. Boucher et al. [11,14] produced bio-oil by vacuum pyrolysis and blended it with methanol and a pyrolytic aqueous phase. Adjaye and Bakhshi [15,16] studied the upgrading of fast pyrolysis bio-oils with different catalysts in a fixed bed micro-reactor. They found that upgrading of bio-oils with silicate was highly disadvantageous, and the most effective catalysts to upgrade bio-oil to hydrocarbons were acidic zeolite catalysts (e.g. HZSM-5, H-mordenite H-Y, silicalite and silica-alumina). Furthermore, they observed a significant amount of char production during upgrading. The catalyst effectiveness to reduce the coke formation decreased with increase in the pore size of the acidic zeolite catalysts. Garcia et al. [17] used different inorganic materials in steam reforming of bio-oils for hydrogen production. Dobele et al. [18] studied the volatile products of catalytic flash pyrolysis of celluloses with Py-GC method using phosphoric acid as catalyst. They found that the impregnation of cellulose with an acidic catalyst such as phosphoric acid and subsequent heat treatment results in a decrease of degree of polymerisation by hydrolysis preferably in less ordered microregions of cellulose, and they found evidence that heating also gives rise to intermolecular cross-linking reactions leading to a decrease in the total yield of volatiles.

Trong On et al. [19] reviewed the preparation properties and application of mesostructured materials. Catani et al. [20] tested Al-MCM-41 type catalysts containing small amounts of metal (Ni, Rh or Pt) in the synthesis of clean diesel fuels by oligomerisation of light alkenes and alkanes. High Si/Al ratios had a negative effect on both the activity and the catalyst stability. Si/Al ratio of 20 was observed to have the strongest catalytic effect. The presence of small amounts of metal inside the mesoporous structure did not significantly modify the catalytic activity, although specific effects were detected for each element. Noreña-Franco et al. [21] studied the catalytic oxidation reaction of phenol in aqueous and acetonitrile media under mild conditions. The highest activity was obtained with copper modified mesoporous MCM-41 catalysts. Sheldon and Downing [22] reviewed the usage of zeolite catalysts in several chemical reactions including acid, base and redox catalysis.

In the present work spruce wood was pyrolysed and the vapours were led through a catalyst layer which was placed on the wood. This set was chosen to avoid condensation of the pyrolysis products and to ensure that the formed volatiles pass through the catalyst for upgrading of the bio-oil before undergoing secondary reactions. Four MCM-41 type catalysts, an unmodified, a transition metal (Cu) modified, and two with enlarged pores were applied in order to find out whether aluminosilicate mesoporous catalysis can improve the quality of bio-oils. The quality of oil is characterised by the aldehyde yield, since it is responsible for many reactions in the aging procedure, and by the organic acid yield, since low pH values make combustion in engines difficult due to corrosion. The phenol yield is also interesting because of its price: high phenol yield makes the process relatively cheaper. Spruce was chosen as a raw material, as it is available in the northern countries as waste in large amounts.

2. Experimental

2.1. Materials

Barkfree spruce wood was milled and sieved and a fraction of particle diameter $< 45 \mu\text{m}$ was used for the experiments. The water content was approximately 6%.

Four different samples of mesoporous MCM-41 catalysts with a Si/Al ratio of 20 have been synthesized, an unmodified one (K1), two with enlarged pores (K2 and K3) and a transition metal (Cu) modified (K4). The pore enlargement in one case was carried out with a spacer (K2) and in the other case (K3) by altering the template chain length. The catalysts were calcined in air at 600°C for 6 h. The XRD characteristics of the studied catalysts are listed in Table 1, which demonstrates that the synthesized materials have MCM-41 structure. K2 is the only material that seems to consist of different phases, probably two MCM-41 phases with different pore sizes. The intensity of the (100)-reflection is lower for the K4 than for the parent MCM-41 (K1), which indicates that the metal cation is located in the MCM-41 framework. The catalysts did not contain any

Table 1
XRD characterisation of the prepared Al-MCM-41 materials

| Sample | | d (Å) (100) | d (Å) (110) | d (Å) (200) | d (Å) (210) | Ad- ditional peaks | Lattice constant a_0 (Å) |
|--------------------------------|----|------------------|------------------|------------------|------------------|--------------------------|----------------------------------|
| Al-MCM-41 (Si:Al 20) | K1 | 37 | 21 | 19 | 14 | 12 | 42 |
| MCM-41 with spacer | K2 | 39 | 23 | 20 | 15 | 49 | 45 |
| MCM-41 with C_{18} | K3 | 45 | 25 | 22 | – | – | 52 |
| Cu–Al- MCM-41 | K4 | 38 | 22 | 19 | – | – | 43 |

organic contamination or degradable material (except some adsorbed water) giving detectable background either in GC/MS or in TG/MS. The experiments were carried out to obtain preliminary information about the products of catalytic conversion on an analytical scale. The change of catalyst's activity and crystalline structure are beyond the scope of this work.

2.2. The catalyst preparation

2.2.1. K1: Al-MCM-41

The surfactant, $C_{14}H_{29}(Me)_3NBr$ (tetradecyltrimethylammonium bromide, 15.15 g), is dissolved in water (95 mL). Sodium aluminate (0.43 g) is added and the solution is stirred overnight. Silica source, sodium metasilicate 5 hydrate (8.9% $Na_2O + 28\% SiO_2$, 19.4 g), H_2SO_4 (10%, 5.6 g) and water (15 mL) is added, and the solution is stirred for 30 min. The pH is adjusted to ~ 10 .

The solution is filled in a teflon-flask, heated at $100^\circ C$ for 6 days, washed with distilled water and centrifuged until pH 5 is obtained. The white product is dried at $100^\circ C$ overnight.

2.2.2. K2: Al-MCM-41 with a spacer

The surfactant, $C_{14}H_{29}(Me)_3NBr$ (tetradecyltrimethylammonium bromide, 15.5 g) is dissolved in water (50 mL) and stirred for 30 min. Sodium aluminate (54% Al_2O_3 , 41% Na_2O , 0.43 g) is dissolved in water (40 mL) and H_2SO_4 (95%, 1.4 g) is added to the solution, then it is stirred for 30 min. The solution of aluminate is then added dropwise to the solution of surfactant and the mixture is stirred for 1 h. Sodium metasilicate 5 hydrate (8.9% $Na_2O + 28\% SiO_2$, 19.7 g) is dissolved in water (15 mL) and stirred for 30 min before it is added dropwise to the solution described above and stirred for 1 h. The spacer, mesitylene, (C_9H_{12} , 14.4 g) is added dropwise, and stirred for 24 h. The final solution is treated as described above.

2.2.3. K3: MCM-41 with C_{18} as surfactant

The synthesis is carried out at $50^\circ C$. The surfactant, $C_{18}H_{37}(Me)_3NBr$ (octadecyltrimethylammonium bromide, C_{18} , 15.7 g) is added to water (100 mL) and stirred for 1 h. Sodium aluminate (54% Al_2O_3 , 41% Na_2O , 0.44 g) is added to the solution and stirred for 4 h, then H_2SO_4 (10%, 5.7 g) is added. Sodium metasilicate 5 hydrate (8.9% $Na_2O + 28\% SiO_2$, 18.7 g) is added to water (40 mL), and stirred for a few minutes. The mixture is added dropwise to the acidic solution of C_{18} and aluminate. A yellow-coloured product is formed. After stirring for 30 min, a homogenous, light pink solution is obtained. The final solution is treated as described above.

2.2.4. K4: Cu-Al-MCM-41

The surfactant $C_{14}H_{29}(Me)_3NBr$ (tetradecyltrimethylammonium bromide, 7.1 g) is dissolved in water (50 mL) and stirred for 1 h. Sodium aluminate (54% Al_2O_3 , 41% Na_2O ,

0.45 g) is dissolved in water (40 mL) and H_2SO_4 (95%, 1.5 g) is added to the solution, which is stirred for 45 min. Copper acetate (2.0 g) is added to the solution of aluminate, and stirred for 1 h. The solution obtained is then added dropwise to the solution of template. The light blue solution is stirred for 1 h. Sodium metasilicate 5 hydrate (8.9% $Na_2O + 28\% SiO_2$, 18.7 g) is dissolved in water (15 mL) and stirred for 50 min before it is added dropwise to the solution described above and stirred for 2 h. The pH in the final solution is 10. The final solution is treated as described above. The product is light blue.

2.3. Py-GC/MS

Py-GC/MS (pyrolysis-gas chromatography/mass spectrometry) experiments were performed in a Pyroprobe 2000 pyrolyser (Chemical Data System) interfaced to a gas chromatograph (Agilent 6890) coupled to a mass selective detector (Agilent 5973) operating in electron impact mode (EI) at 70 eV. The pyrolysis was carried out at 450 and $500^\circ C$, for 20 s using a platinum coil probe and quartz sample tubes.

The same amounts (1.5–2.0 mg) of wood and catalyst were weighed into the pyrolysis tube. The wood was placed in the middle of the pyrolysis tube and the catalyst next to the wood at both ends of the tube. A comparative experiment was carried out with a pre-mixed sample of the same wood to catalyst ratio (1:1). The product profile and yields of the pyrolysis were the same irrespective to the sampling procedure. Sampling without mixing was chosen for better control of the wood to catalyst ratio and the arrangement of sample between two catalyst layers guarantees that all vapours produced from wood travel through the catalyst and cannot pass by.

A helium carrier gas of 20 mL/min flow rate purged the pyrolysis chamber which was held at $250^\circ C$. A split of the carrier gas (1:20) was applied. The temperature of the GC/MS injector was held at $280^\circ C$. The GC separation was carried out on a fused silica capillary column (Hewlett-Packard 5MS), 30 m \times 0.25 mm. A temperature program from 50 to $300^\circ C$ at $10^\circ C/min$ was applied with an isotherm period of 1 min at $50^\circ C$ and of 4 min at $300^\circ C$.

2.4. TG/MS

TG/MS experiments were carried out on a Perkin-Elmer TGS-2 thermobalance coupled to a HIDEN HAL 2/301 PIC quadrupole mass spectrometer through a glass-lined metal capillary heated to $300^\circ C$. Samples of 3 mg wood were placed into a platinum pan and the catalyst (3 mg) was layered on it, to ensure that vapours pass through the catalyst. The samples were heated at a rate of $20^\circ C/min$ in argon atmosphere. The flow rate of the argon purge gas was 140 mL/min. A portion of the evolved products was introduced into the mass spectrometer operating in the electron impact ionization mode at 70 eV electron energy.

The intensity of the products was normalized to the sample mass and the intensity of the ^{38}Ar isotope in order to avoid errors caused by the shift in sensitivity of the mass spectrometer.

3. Results and discussion

3.1. Py-GC/MS

Py-GC/MS has been applied to clarify how far the different catalytic materials can modify the pyrolysis product distribution. The fast pyrolysis temperature was chosen to be 500 °C, which was found optimal in earlier works [1,5]. One comparative experiment with the wood+K1 sample was carried out at 450 °C. The deviation between the product distribution obtained at 450 and 500 °C was not larger than that of parallel experiments. Condensed tar was found on the ends of the pyrolysis tube at the uncatalysed experiments, which disappeared when catalyst was placed at both ends of the tube next to the wood. This confirms that the used experiment set-up is necessary to avoid the condensation of pyrolysis products in the catalysed experiments. Gas chromatography/mass spectrometry was applied to separate and identify the products. Identification of the GC/MS peaks was based in most cases on comparison with spectra of the NIST 98 spectrum library. More than 100 peaks were displayed in the GC/MS chromatograms. The perfect separation of all the peaks was not possible due to the complex composition of the pyrolysis vapours. Only those separated products were semi-quantitatively evaluated which arose in considerable amounts. The semi-quantitative analysis of the products was based on the peak areas of selected characteristic molecular or fragment ion chromatograms.

Fig. 1 shows the volatile products of the pyrolysis of spruce wood separated by gas chromatography and detected by mass spectrometry. The identification of the peaks marked by numbers are listed in Table 2. The main pyrolysis product of the cellulose is levoglucosan (20), while the lignin component of wood produces several substituted phenolic compounds (10–13, 15–19, 21). The major effect of the catalyst is conspicuous; levoglucosan disappeared and the yields of heavier components decreased significantly in all cases where catalysts were used. The overall yield of pyrolysis vapours decreased as well. (Note, the corresponding peak areas in the different chromatograms in Fig. 1 are comparable, because the mass of the pyrolysed wood sample was the same within 10 wt% in the different experiments.) The yields of heavier components were relatively higher with K3 and K4 catalysts compared to those with K1 and K2. The chromatograms in Fig. 1(b) and (c) are alike, indicating similar effects of the corresponding catalysts (K1 and K2) on the products of thermal decomposition of wood. The chromatograms in Fig. 1(b), (d)–(e) exhibit dissimilar product distributions, indicating

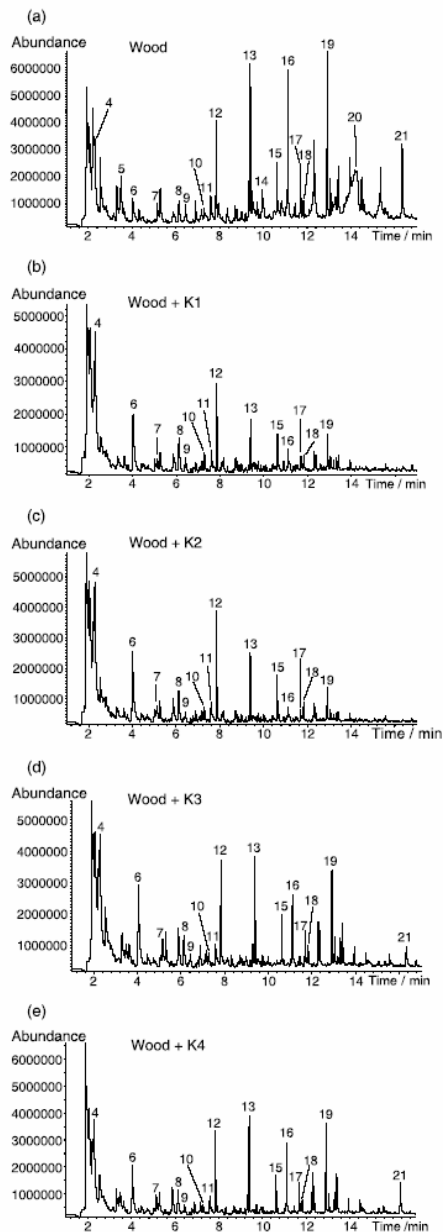


Fig. 1. Total ion chromatograms of spruce wood pyrolysis products: (a) wood, (b) wood+K1, (c) wood+K2, (d) wood+K3 and (e) wood+K4 samples in Py-GC/MS experiments.

Table 2
Identification of the peaks of total ion chromatograms displayed in Fig. 1

| Peak no. | Retention time (min) | Compound name |
|----------|----------------------|----------------------------------|
| 1 | 1.9 | Water ^a |
| 2 | 2.0 | Furan ^a |
| 3 | 2.2 | Hydroxyacetaldehyde ^a |
| 4 | 2.3 | Acetic acid |
| 5 | 3.4 | Propanal |
| 6 | 4.0 | Furfural |
| 7 | 5.2 | 2(5H)-Furanone |
| 8 | 6.1 | Phenol |
| 9 | 6.4 | Benzofuran |
| 10 | 7.3 | 2-Methylphenol |
| 11 | 7.6 | 4-Methylphenol |
| 12 | 7.8 | 2-Methoxyphenol |
| 13 | 9.5 | 2-Methoxy-4-methylphenol |
| 14 | 10.0 | 5-Hydroxymethylfurfural |
| 15 | 10.6 | 4-Ethyl-2-methoxyphenol |
| 16 | 11.1 | 4-Ethenyl-2-methoxyphenol |
| 17 | 11.7 | 6-Methoxy-3-(2-propenyl)-phenol |
| 18 | 11.8 | 2-Methoxy-4-propylphenol |
| 19 | 12.4 | 2-Methoxy-4-(1-propenyl)-phenol |
| 20 | 14.2 | Levoglucofan |
| 21 | 16.4 | 2-Methoxy-4-propenalphenol |

^a Unresolved peak in TIC.

different influence of K3 and K4 compared to that of K1 catalyst on the pyrolysis vapours.

Fig. 2 shows the phenol and substituted phenol yields obtained in the pyrolysis experiments. It can be concluded

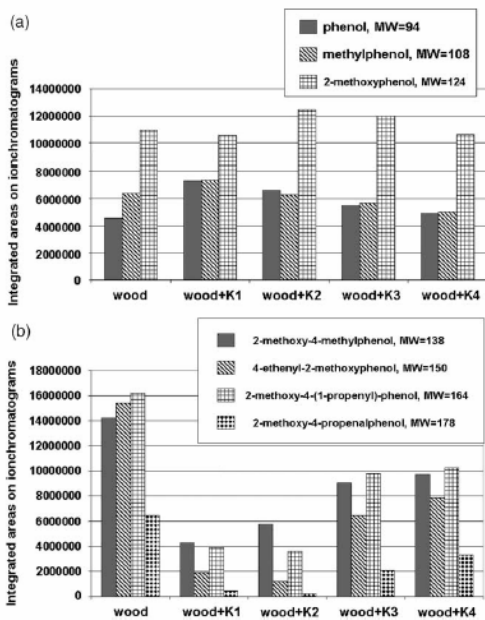


Fig. 2. Yields of (a) phenol and substituted phenols $MW \leq 124$ and (b) substituted phenols $MW \geq 138$ in Py-GC/MS experiments.

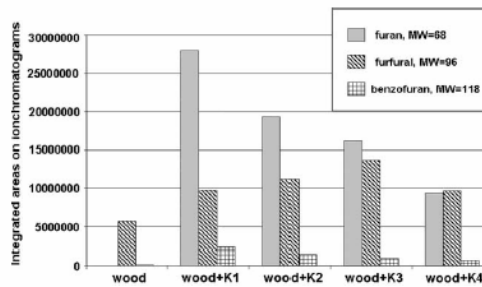


Fig. 3. Comparison of the yields of furan and its derivatives formed in Py-GC/MS experiments.

that as a result of the application of catalysts, the yield of pure phenol increased (Fig. 2(a)) and the yields of heavier substituted phenols (4-alkyl- and 4-alkenylphenols) decreased (Fig. 2(b)), i.e. the catalysts promote the scission of the aliphatic side chains of phenol derivatives. This effect is most expressed in the presence of the K1 and the K2 catalysts. The observed changes are smaller when the pyrolysis vapours contact the K3 and the K4 catalysts. They provoked higher yields of heavier phenol derivatives compared to the other catalysts; however, this yield is still lower compared to the pyrolysis products of the original wood sample. The phenol yield was lower when K3 and K4 catalysts were applied than in the wood+K1 or wood+K2 mixtures. The yields of methylphenol and 2-methoxyphenol showed only a slight deviation (Fig. 2(a)).

Due to the catalytic activity the yields of furan ring containing compounds considerably increased, as it is shown in Fig. 3. Furan was not present and benzofuran appeared only in small amounts in the pyrolysate of the uncatalysed reaction, whereas high yields of furan and larger amounts of furfural and benzofuran were obtained from each catalysed conversion. Another important furan type compound is 2-(5H)-furanone (Fig. 1, peak 7). Its amount slightly decreased when the K1 and K2 catalysts were applied. 5-Hydroxymethyl-furfural (Fig. 4) is formed

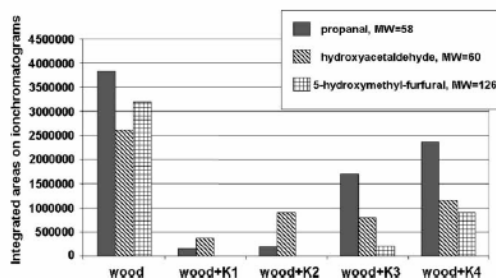


Fig. 4. Comparison of the yields of aldehydes formed in Py-GC/MS experiments.

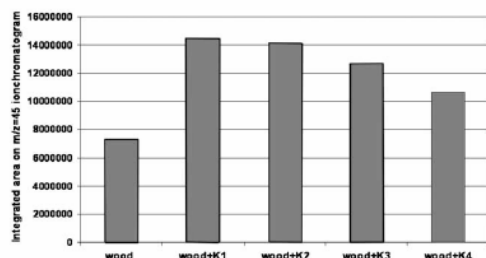


Fig. 5. Comparison of the yields of acetic acid formed in Py-GC/MS experiments.

in negligible amounts in the presence of K1, K2 catalysts compared to the uncatalysed experiment. A somewhat higher amount of this compound is formed when the pyrolysis vapours were catalysed with the K3 and K4 catalysts; however, this yield is still considerably lower compared to the amount formed in the pyrolysis of wood without catalyst.

Aldehydes in bio-oil are responsible for a range of reactions that cause instability. That is why a great emphasis has been put on monitoring the formation of these compounds. The influence of catalysis on aldehyde

formation is very significant. As it can be seen, the amount of furfural increased (Fig. 3), while the yields of other evaluated aldehydes (Fig. 4) decreased significantly. Note, the same trend can be observed for propenalphenol in Fig. 2(b). These results indicate that catalysis decreases the aldehyde yield but promotes furan-ring formation, which could be a reason why furfural increases.

Besides the aldehydes, the organic acids also play an important role in the determination of the quality of bio-oils. The larger the amount of acids, the more problems may occur in the engines during combustion owing to corrosion. The variation of acetic acid yield in the presence of different types of catalysts is shown in Fig. 5. The highest amount of acetic acid was produced using K1 catalyst, whereas the lowest amount was formed applying K4 as catalyst. The acetic acid yield is very high when using K2 catalyst as well. As the results imply the acetic acid yield increased with the catalyst use and it can be concluded that acid production is a disadvantage of applying these catalysts.

3.2. TG/MS

The formation of volatile products has also been monitored during thermal decomposition of wood with the help of thermogravimetry/mass spectrometry. In this

Table 3

Proposed identity of selected ions and integrated areas of molecular and fragment ion curves monitored in TG/MS runs

| m/z | Ion | Temperature interval (°C) | Integrated area (counts) from sample | | | | |
|-----|--|---------------------------|--------------------------------------|---------|---------|---------|---------|
| | | | Wood | Wood+K1 | Wood+K2 | Wood+K3 | Wood+K4 |
| 15 | CH ₃ ⁺ | 250–800 | 13,200 | 22,900 | 22,000 | 21,300 | 19,400 |
| 16 | CH ₂ ⁺ | 350–500 | 7600 | 8000 | 9200 | 9100 | 8900 |
| 16 | CH ₂ ⁺ | 500–780 | 5700 | 14,800 | 12,800 | 12,200 | 10,500 |
| 18 | H ₂ O ⁺ | 220–730 | 129,700 | 214,300 | 221,600 | 222,300 | 222,800 |
| 26 | C ₂ H ₂ ⁺ | 250–430 | 1800 | 2100 | 1800 | 1800 | 1700 |
| 26 | C ₂ H ₂ ⁺ | 430–720 | 1000 | 1700 | 1400 | 1800 | 1400 |
| 27 | C ₂ H ₃ ⁺ | 270–430 | 2800 | 3200 | 3100 | 2800 | 2700 |
| 27 | C ₂ H ₃ ⁺ | 430–720 | 1400 | 2000 | 2200 | 2100 | 2100 |
| 28 | CO ⁺ | 250–420 | 19,800 | 38,700 | 27,800 | 24,900 | 24,100 |
| 29 | CHO ⁺ | 200–540 | 17,600 | 15,500 | 16,500 | 16,300 | 15,200 |
| 30 | CH ₂ O ⁺ | 180–550 | 8800 | 7400 | 8800 | 8700 | 8100 |
| 31 | CH ₃ O ⁺ | 220–500 | 9000 | 5200 | 5400 | 5500 | 4500 |
| 32 | CH ₃ OH ⁺ | 220–500 | 5300 | 2700 | 4100 | 1700 | 2000 |
| 42 | CH ₂ CO ⁺ /C ₃ H ₂ ⁺ | 230–700 | 3000 | 3100 | 2900 | 3400 | 3000 |
| 43 | CH ₃ CO ⁺ | 270–540 | 7200 | 6600 | 6600 | 6700 | 5800 |
| 44 | CO ₂ | 200–700 | 22,900 | 26,000 | 36,800 | 42,000 | 54,100 |
| 45 | COOH ⁺ /C ₂ H ₅ O ⁺ | 230–410 | 800 | 600 | 500 | 0500 | 400 |
| 46 | HCOOH ⁺ | 280–420 | 300 | 100 | 50 | 50 | 50 |
| 55 | C ₂ H ₇ ⁺ /C ₃ H ₅ O ⁺ | 270–700 | 700 | 4100 | 3800 | 3900 | 3400 |
| 57 | C ₂ H ₉ ⁺ /C ₃ H ₅ O ⁺ | 280–430 | 900 | 600 | 800 | 700 | 700 |
| 58 | CH ₂ CH ₂ CHO ⁺ | 240–420 | 600 | 600 | 0500 | 600 | 600 |
| 60 | HOCH ₂ CHO ⁺ /CH ₃ COOH | 220–500 | 700 | 400 | 0400 | 400 | 300 |
| 68 | C ₂ H ₄ O ⁺ | 200–420 | 300 | 1400 | 1000 | 700 | 500 |
| 82 | C ₃ H ₆ O ⁺ | 270–430 | 200 | 600 | 500 | 400 | 300 |
| 95 | C ₃ H ₅ O ₂ ⁺ | 240–420 | 200 | 300 | 300 | 200 | 200 |
| 96 | C ₃ H ₄ O ₂ ⁺ | 200–420 | 200 | 300 | 300 | 300 | 200 |
| 98 | C ₃ H ₆ O ₂ ⁺ | 200–420 | 300 | 300 | 300 | 200 | 200 |

The integrated areas are normalized for the mass of wood.

method a low heating rate is applied and the product evolution is monitored as a function of the decomposition time/temperature. These results show how spruce wood behaves and how the catalysts influence the product yields under slow pyrolysis conditions.

The TG and the DTG curves of both the wood and wood+catalyst samples are rather similar (not shown). In the presence of catalysts, the char yield slightly increases and the thermal decomposition takes place more slowly than in the decomposition of wood without catalyst.

More information can be gained about the effect of catalysis if one compares the evolution profiles of the various volatile products formed during thermal decomposition. The integrated areas of several molecular and fragment ion curves monitored in the TG/MS experiments are listed in Table 3. It must be noted that the mass spectrometry has different selectivity for the different compounds, thus limited quantitative possibilities; however, the rows are quantitatively comparable. Some selected characteristic ions of the products and their relative abundances are shown in Figs. 6–9. It should be noted that this method is suitable for measuring the products of lower molecular mass.

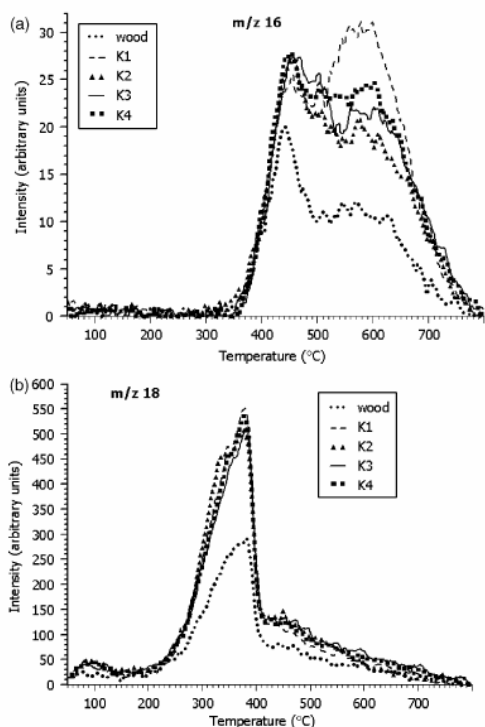


Fig. 6. Formation of (a) methane, represented by m/z 16 molecular ion and (b) water, represented by m/z 18 molecular ion during TG/MS experiments.

The methane yield can be monitored by following the molecular ion intensity at m/z 16 (Fig. 6(a)). An ion at the same mass can also be the fragment of other molecules: that is why the computer program subtracts the m/z 16 fragment ion of water, carbon-monoxide, and carbon-dioxide. The m/z 16 ion has two peaks, one in the range of 350–500 °C, which can be attributed mainly to methane evolution from lignin [23]. The other peak is located in the temperature range of 500–780 °C, which indicates a char formation process. The peaks are higher when catalysts are applied, and the second peak is the highest in the case of K1 catalyst usage. Thus, it is in agreement with the TG results that in the presence of catalysts, higher amounts of char are formed.

The formation of water is monitored by its molecular ion, m/z 18 (Fig. 6(b)). Below 150 °C, small peaks can be observed, which are due to the removal of adsorbed water from wood and catalyst. As it is shown in Fig. 6(b), during pyrolysis in the presence of catalysts, more water is formed in the 220–730 °C temperature range than in the uncatalysed pyrolysis. The water formed in this region can be attributed to the degradation of higher molecular weight molecules. The catalyst seemingly promotes the elimination of water

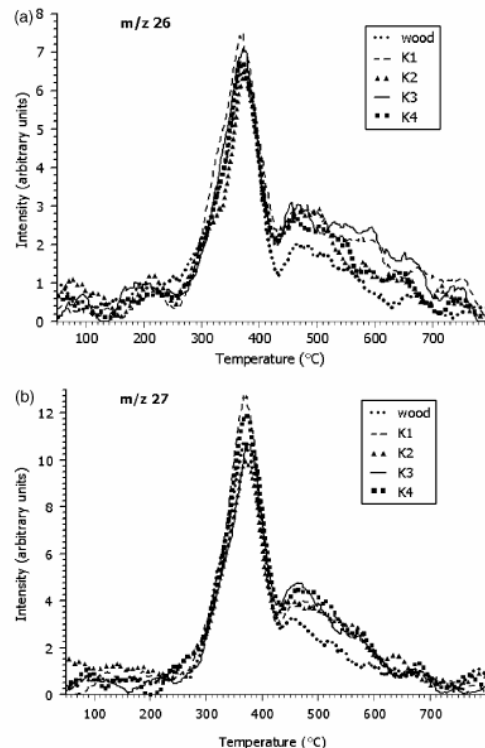


Fig. 7. Formation of (a) m/z 26 and (b) m/z 27 fragment ions (from hydrocarbons) during TG/MS experiments.

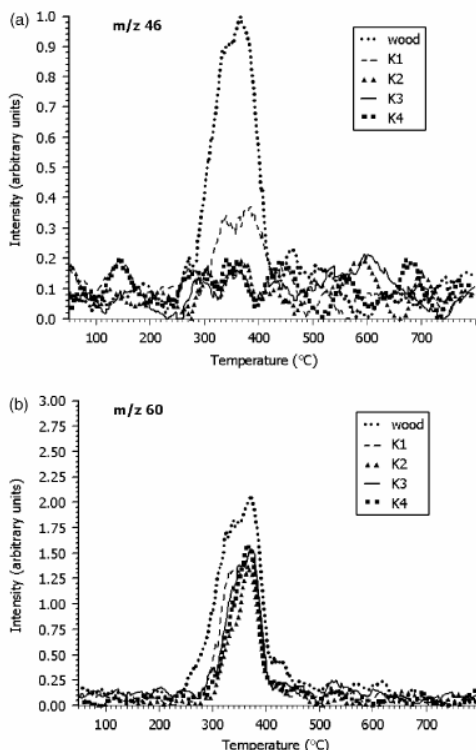


Fig. 8. Formation of (a) formic acid, represented by m/z 46 ion and (b) acetic acid and hydroxyacetaldehyde, represented by m/z 60 ion in TG/MS experiments.

from hydroxyl group containing molecules. There are no significant differences between different studied catalysts with respect to water formation.

The fragment ions of m/z 26 ($C_2H_2^+$) and m/z 27 ($C_2H_3^+$) are representatives for hydrocarbons (Fig. 7); however, they can be formed from several other compounds in the mass spectrometer (e.g. aldehydes). Thus, the main peak at around 360 °C may represent various products. However, the oxygen-containing organic products do not have significant intensities at around 500 °C, as will be shown later. Therefore the m/z 26 and m/z 27 ions can be attributed mainly to the evolution of hydrocarbons in the temperature region of 430–700 °C. The amount of hydrocarbons formed above 430 °C increased in the presence of catalysts, similarly to the yield of methane as demonstrated in Fig. 6.

Changes in organic acid formation can be followed by monitoring the m/z 45, m/z 46 and m/z 60 ions. The yields of organic acids decrease when catalysts are applied. This effect is more pronounced with the modified catalysts.

The evolution of formic acid is shown in Fig. 8(a). As it is shown, the yield of formic acid decreased drastically as a result of catalysis. As acidity is an undesired bio-oil property, reduction in yields of organic acids is an advantage of the catalyst usage.

The m/z 60 ion (Fig. 8(b)) represents the molecular ions of acetic acid and hydroxyacetaldehyde. Both compounds are released during wood pyrolysis from polysaccharides in significant amounts. The total yield of acetic acid and hydroxyacetaldehyde decreased to some extent due to catalyst activity. This observation is in contrast to the Py-GC/MS results, as shown in Fig. 5, where the acetic acid yield increased. The reason for this is that the two methods have different heating rates, and the Py-GC/MS method is more relevant to fast pyrolysis.

Aldehyde formation can be followed by monitoring m/z 29 (CHO^+), m/z 30 ($HCHO$) and m/z 31 (CH_3O^+) ions. There are only slight differences in m/z 29 ion formation between the different samples. The evolution profile is similar for all samples, the amount of this product

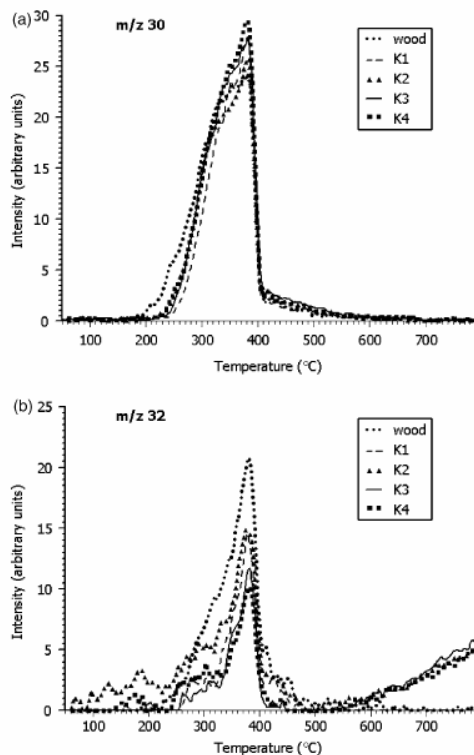


Fig. 9. Formation (a) formaldehyde, represented by m/z 30 ion and (b) methanol, represented by m/z 32 fragment ion in TG/MS experiments.

decreases very slightly owing to the effect of catalysis (Table 3). The m/z 30 ion originates mainly from formaldehyde. Fig. 9(a) shows that there are only slight differences in formation of the m/z 30 ion, the formaldehyde yield shows no difference between the catalysed samples. The m/z 31 fragment ion can originate from both hydroxyacetaldehyde and methanol and the catalyst activity reduces the formation of the m/z 31 fragment ion (Table 3). Hydroxyacetaldehyde is formed in degradation of cellulose and methanol is formed in lignin and polysaccharide degradation. The reduced yield is an advantage in case of aldehyde, as aldehydes are responsible for ageing and a disadvantage in the case of methanol, which is a fuel. Fig. 9(b) shows the evolution profile of methanol (m/z 32), which indicates also a considerable reduction in methanol yield upon the effect of catalysts.

The yield of furan derivatives changed similarly in the TG/MS experiments (Table 3) as during fast pyrolysis (Fig. 3). The yields of furan (m/z 68) and furfural (m/z 96) are increased, while the intensity of hydroxymethyl furan (m/z 98) is reduced in the catalytic experiments.

4. Conclusions

Due to the catalytic activity, there are several changes in the pyrolysis product composition. The most important catalytic effect on the products of pyrolysis of wood is the lack of levoglucosan. This is typical for each catalyst studied in this work. Catalysis increases the yield of acetic acid (especially under pyrolysis at a high heating rate) and that of furanes, but lowers the yields of higher molecular mass phenols. The catalyst usage increases the yield of phenol and slightly the hydrocarbons yields—which is an advantage.

The effect of MCM-41 type catalyst on the pyrolysis products of spruce wood seem to be related to the size of the pores of the catalyst. Pore size enlargement and transition metal incorporation reduces the yield of acetic acid and water among pyrolysis products.

The pores in K3 are larger than in the K2 catalyst. Pyrolysis vapours of spruce wood catalysed by K2 catalyst results in similar volatile product distributions compared to that obtained with the unmodified one (K1), probably because the pore sizes of K1 and K2 catalyst are similar. Higher molecular mass products are obtained when the Al-MCM-41 catalyst prepared with a larger template (K3) or when the Cu containing catalyst (K4) are used.

Acknowledgements

J. Adam is indebted to the Norwegian Research Council for her PhD grant and M.H. Nilsen thanks the Norwegian University of Science and Technology for the Post-doc grant. M. Stöcker and A. Bouzga acknowledge the financial support of the European Union (ENK 6-CT2001-00049). The work of E. Mészáros and M. Blazsó was supported by the Hungarian National Research Fund (OTKA T037704-05).

References

- [1] Bridgwater AV, Meier D, Radlein D. *Org Geochem* 1999;30:1479.
- [2] Dobele G, Meier D, Faix O, Radtke S, Rossinskaja G, Telysheva G. *J Anal Appl Pyrolysis* 2001;58–59:453.
- [3] Huffman DR, Vogiatzis AJ, Bridgwater AV. The characterization of fast pyrolysis bio-oils. In: Bridgwater AV, editor. *Advances in thermochemical biomass conversion*, vol. 2. London: Blackie; 1994. p. 1095.
- [4] Maggi R, Delmon B. Characterization of bio-oils produced by pyrolysis. In: Bridgwater AV, editor. *Advances in thermochemical biomass conversion*, vol. 2. London: Blackie; 1994. p. 1086.
- [5] Milne T, Agblevor F, Davis M, Deutch S, Johnson D. A review of the chemical composition of fast-pyrolysis oils from biomass. In: Bridgwater AV, Boocock DGB, editors. *Developments in thermochemical biomass conversion*, vol. 1. London: Blackie; 1997. p. 409.
- [6] Sipilä K, Kuoppala E, Fagermäs L, Oasmaa A. *Biomass Bioenergy* 1998;14:103.
- [7] Faix O, Fortmann I, Meier D. *Holz Roh Werkst* 1990;48:281.
- [8] Faix O, Fortmann I, Meier D. *Holz Roh Werkst* 1990;48:351.
- [9] Faix O, Fortmann I, Bremer J, Meier D. *Holz Roh Werkst* 1991;49:213.
- [10] Faix O, Fortmann I, Bremer J, Meier D. *Holz Roh Werkst* 1991;49:299.
- [11] Boucher ME, Chaala A, Roy C. *Biomass Bioenergy* 2000;19:337.
- [12] James P, Diebold PE. A review of the chemical and physical mechanisms of the storage stability of fast pyrolysis bio-oils. In: Bridgwater AV, editor. *Fast pyrolysis of biomass—a handbook*, vol. 2. Newbury, UK: CPL Press; 2002. p. 243.
- [13] Czernik S, Maggi R, Peacocke GVC. Review of methods for upgrading biomass-derived fast pyrolysis oils. In: Bridgwater AV, editor. *Fast pyrolysis of biomass—a handbook*, vol. 2. Newbury, UK: CPL Press; 2002. p. 141.
- [14] Boucher ME, Chaala A, Roy C. *Biomass Bioenergy* 2000;19:337.
- [15] Adjaye JD, Bakshi NN. *Fuel Process Technol* 1995;45:161.
- [16] Adjaye JD, Bakshi NN. *Fuel Process Technol* 1995;45:185.
- [17] Garcia L, French R, Czernik S, Chornet E. *Appl Catal, A-Gen* 2000;201:225.
- [18] Dobele G, Meier D, Faix O, Radtke S, Rossinskaja G, Telysheva G. *J Anal Appl Pyrolysis* 2001;58–59:453.
- [19] Trong On D, Desplandier-Giscard D, Danumah C, Kaliaguine S. *Appl Catal, A-Gen* 2003;253:545.
- [20] Catani R, Mandreoli M, Rossini S, Vaccari A. *Catal Today* 2002;75:125.
- [21] Noreña-Franco L, Hernandez-Perez I, Aguilar-Pliego J, Maubert-Franco A. *Catal Today* 2002;75:189.
- [22] Sheldon RA, Downing RS. *Appl Catal, A-Gen* 1999;189:163.
- [23] Jakab E, Faix O, Till F. *J Anal Appl Pyrolysis* 1997;40–41:171.

Paper III.

Submitted to "Microporous and Mesoporous Materials".

In-situ catalytic upgrading of biomass derived fast pyrolysis vapours in a fixed bed reactor using mesoporous materials

Judit Adam^{a,*}, Eleni Antonakou^b, Angelos Lappas^b, Michael Stöcker^c, Merete H. Nilsen^c, Aud Bouzga^c, Johan E. Hustad^a, Gisle Øye^d

^a*Department of Energy and Process Engineering, Norwegian University of Science and Technology, K. Hejesvei 1A, N-7491 Trondheim, Norway*

^b*CPERI Chemical Process Engineering Research Institute (CPERI), Center for Research and Technology Hellas (CERTH), Thessaloniki, P.O. Box 361 GR-570 01, Greece*

^c*SINTEF Materials and Chemistry, P.O. Box 124 Blindern, N-0314 Oslo, Norway*

^d*Ugelstad Laboratory, Department of Chemical Engineering, Norwegian University of Science and Technology, Sem Sælandsvei 4, N-7491 Trondheim, Norway*

**Corresponding author, E-mail address: judit.adam@ntnu.no*

Abstract

Seven mesoporous catalysts were compared in how they can convert the pyrolysis vapours of spruce wood in order to obtain improved bio-oil properties. Four Al-MCM-41 type catalysts with a Si/Al ratio of 20, a commercial FCC catalyst, a pure siliceous SBA-15 and an aluminium incorporated SBA-15 materials were tested. The catalytic properties of Al-MCM-41 catalyst were modified by pore enlargement that allows the processing of larger molecules and by introduction of Cu cations into the structure.

Spruce wood pyrolysis at 500 °C was performed in a lab-scale fixed bed reactor, the solid, gaseous and liquid products were separated and the gases and the organic part of the liquids were analysed with the help of gas chromatography and mass spectrometry.

The gas yield increased in each catalytic case, the coke yield remained the same or slightly decreased compared to the non-catalytic experiments. The aqueous part in the liquid phase increased in the catalytic runs.

The obtained products in the organic phase were grouped into eight groups and further into desirable and undesirable product groups, and the yields were evaluated. In the catalytic experiments the hydrocarbon and acid yields increased, while the carbonyl and the acid yields decreased. All catalysts tested reduced the undesirable product yield, while the desirable product yield remained the same or increased.

To study the feedstock effect on the catalytic upgrading of the pyrolysis vapours, some tests were performed with Miscanthus biomass. With spruce the FCC, with Miscanthus the unmodified Al-MCM-41 are the best performing catalysts. Concerning the feedstocks, with Miscanthus a better quality bio-oil has been obtained.

Keywords: Mesoporous materials; MCM-41; SBA-15; Biomass; Bio-oil

1. Introduction

Biomass and alternative energy sources in general are widely recognized as a potential future solution to the energy problems worldwide. The energy from biomass can be obtained by various techniques, such as combustion or upgrading into a more valuable fuel, gas or oil. It can also be transformed into a source of higher value products for the chemical industry [1] by using a thermochemical method, such as pyrolysis.

The liquid product of biomass pyrolysis, known as bio-oil or pyrolysis oil, is a complex mixture of several hundreds of organic compounds that exhibit a wide range of chemical functionality. Bio-oil consists of two phases, an aqueous phase containing oxygenated organic compounds of lower molecular weight and a non-aqueous phase, which contains organic compounds (mainly aromatics) [2]. Characteristic examples of oxygenated compounds in the oils are phenols, cresols, benzenedioles and their alkylated products [3,4]. The major aromatic hydrocarbon compounds present in the oil are single ring aromatic compounds and polycyclic aromatic hydrocarbons (PAH). Single ring aromatic compounds consist of benzene, toluene, indene and alkylated products [3,4].

Pyrolysis oil in order to be used either as a fuel or as a source of valuable chemicals exhibits two main problems: the high amount of water produced and its instability because of the presence of certain 'undesirable' organic compounds. Stabilisation of bio-oils can be achieved by upgrading them, mainly with the help of catalysts. Nevertheless, catalytic reactions usually lead to an additional water and coke production and they also decrease the yield in organic product. The search for a suitable catalyst for the pyrolysis process and the upgrading of the oil is the aim of many research activities. Catalysts have been tested under pyrolysis conditions in order to favour desirable reactions and to inhibit undesirable reactions.

The upgrading possibilities are reviewed by Czernik et al. [5]. Vitolo et al. [6] studied different types of zeolites to upgrade bio-oil to fuel. They studied the influence of residence time and temperature in a fixed bed microreactor, too. Simionescu et al. [7] investigated the catalytic pyrolysis of various hydrocarbon products. They concluded that the catalysts cause an increase in the amount of gas, and 5-10% coke deposits on the catalyst.

The mesoporous molecular sieve of M41S family was discovered in 1992 and, with the main representative of MCM-41, opened a new area in the catalytic application of these materials. MCM-41, one of the latest members of the mesoporous family possesses a hexagonal array of uniform mesopores whose dimensions can vary from 1.4 nm to greater than 10 nm in size [8] and also exhibit high surface areas ($>1000 \text{ m}^2 \text{ g}^{-1}$).

A combination of the large pore dimensions of mesoporous materials with the strong acid sites present in zeolite-like structures would be highly advantageous leading to a novel and probably useful catalytic material. The properties of these materials were expected to affect the cracking of the high molecular weight lignocellulosic molecules of bio-oil. Hydrocarbon reactions for example, involving large organic molecules that cannot enter the small pores of a zeolite catalyst may be catalyzed by the new material having a mesoporous framework structure with accessible acid sites on the surface of these large pores.

Corma et al. [9] have compared Al-MCM-41, amorphous silica-alumina and USY zeolite (Zeolite Y) in the catalytic cracking of *n*-heptane. For this reaction, the activity of the USY zeolite was approximately 140 times that of Al-MCM-41. This was ascribed to more and stronger Bronsted acid sites in the zeolite. The Al-MCM-41 activity was higher than for the amorphous silica-alumina and approached that for the USY zeolite in the processing of large oil molecules. The selectivity of Al-MCM-41 in the gas oil cracking resulted in more liquid fuels and less gases and coke compared to the amorphous silica-alumina. Compared with the USY zeolite, the diesel formation was higher and gave less gasoline and more coke.

Vartuli et al. [10] compared the benzene sorption capacity of the MCM-41 and MCM-48 catalysts. They found that the hydrocarbon sorption increases with pore diameter for the calcined versions. The sorption of hydrocarbons by M41S materials is a unique feature not observed with microporous molecular sieves.

As a drawback of the MCM-41 catalyst, the hydrothermal stability depends on the preparation method, the aluminium content and the thickness of pore walls. Up to now the results are still not satisfactory [11-13].

Stucky and co-workers [14-15] introduced a new synthesis route involving amphiphilic di- and tri-block copolymers as organic structure directing agents. These materials, exemplified by hexagonal (p6 mm) SBA-15, have long range order, large monodispersed mesopores (up to 50 nm) and thicker walls (typically between 3 and 9 nm) which make them more thermally and hydrothermally stable than MCM-41 type materials. Yue et al. [16] obtained aluminium incorporated SBA-15 mesoporous materials by direct synthesis. The resulting materials retained the hexagonal order and physical properties of purely siliceous SBA-15 and presented higher catalytic activities in the cumene cracking reaction than Al-MCM-41 materials.

Several types of mesoporous materials have been studied in the current paper, in order to investigate how far they can modify the pyrolysis vapour composition and thus the bio-oil quality. Fast pyrolysis of spruce wood was performed in a fixed bed reactor at 500°C, and the pyrolysis vapours were led through a catalyst layer, which was present in the reactor and separated from the wood. The present set was chosen to avoid condensation, and secondary reactions in the pyrolysis vapours before catalysis. The catalyst performance on the vapours has been evaluated compared to non-catalytic experiments (in the presence of inert material) as well as a commercial FCC catalyst. Some experiments with another biomass feedstock (energy crop) were also performed to verify the action of specific catalysts.

2. Experimental

2.1. Materials

Barkless spruce wood was milled and sieved and a fraction of particle diameter 0.5-1.4 mm was used in the experiments. The water content of the sample was approximately 6 %.

Some experiments were performed with Miscanthus biomass, which was milled and sieved. The sample had a particle size of 1-1.5 mm and its moisture content was 6 %.

Seven different catalysts have been tested; four mesoporous Al-MCM-41 catalysts (K1-K4), a commercial FCC catalyst (K5) and two SBA-15 catalysts (K6-K7). The Al-MCM-41 catalyst group had a Si/Al ratio of 20 and consisted of an unmodified Al-MCM-41 (K1 sample), two catalysts with enlarged pores (K2 and K3 samples) and a transition metal (Cu) modified catalyst (K4 sample). The pore enlargement in sample K2 was carried out with a spacer (mesitylene, C₉H₁₂), and in sample K3 by altering the template chain length from C₁₄ to C₁₈. The SBA-15 catalyst group consisted of a siliceous SBA-15 (K6) and an SBA-15 with aluminium incorporation (K7).

The Cu containing catalyst was calcined following a specific protocol, since, from previous calcinations we experienced some problems in retaining the structure because of hot spots: 6 g of the mesoporous material was weighed and the sample was initially heated in a fixed bed reactor in the presence of N₂ (100ml/min), the temperature was

gradually increased every 20°C until the temperature of 200°C. Afterwards the temperature was gradually increased every 50°C until the temperature of 300°C. The sample was left for 30 min in the temperature of 300°C. After that, the gas was changed from N₂ to air and left at 300°C for 1h. The temperature was then gradually increased up to 540°C. The sample was left for 6 hours in the presence of air (flow rate 100ml/min). After the 6h period the oven was shut down and the sample was cooled in the presence of nitrogen (flow rate 30 ml/min) overnight. The other catalysts were calcined in air at 600 °C for 6 hours (the heating rate was 200°C/h). After calcination the catalysts were pelletised into 20 mm diameter and 0.5-1 mm height cylinder pellets. The pellets were crashed and sieved to remove the particles which were smaller than 45 µm.

2.2. Catalyst preparation

K1: Al-MCM-41

Molar composition: 1 Si : 0.06 Al : 0.4 C₁₄ : 68 H₂O.

The surfactant, C₁₄H₂₉(Me)₃NBr (tetradecyltrimethylammonium bromide, 15.15 g), was dissolved in water (95 g). Sodium-aluminate (0.43 g) was added and the solution was stirred overnight. Silica source, sodium-meta-silicate-5-hydrate (8.9% Na₂O + 28% SiO₂, 19.4 g), H₂SO₄ (10%, 5.6 g) and water (15 g) was added, and the solution was stirred for 30 minutes. The pH was adjusted to ~10.

The solution was filled in a teflon-flask, heated at 100°C for 6 days, washed with distilled water or centrifuged until pH 5 was obtained. The white product was dried at 100°C overnight.

K2: MCM-41 with a spacer

Molar composition: 1 Si : 0.06 Al : 0.6 C₁₄ : 1.3 C₉H₁₂ : 64 H₂O.

The surfactant, C₁₄H₂₉(Me)₃NBr (tetradecyltrimethylammonium bromide, 15.5 g) was dissolved in water (50 g) and stirred for 30 minutes. Sodium-aluminate (54% Al₂O₃, 41% Na₂O, 0.43 g) was dissolved in water (40 g) and H₂SO₄ (95%, 1.4 g) was added to the solution, then it was stirred for 30 minutes. The solution of aluminium was then added dropwise to the solution of surfactant and the mixture was stirred for one hour. Sodium-meta-silicate-5-hydrate (8.9% Na₂O + 28% SiO₂, 19.7 g) was dissolved in water (15 g) and stirred for 30 minutes before it was added dropwise to the solution described above and stirred for 1 hour. The spacer, mesitylene, (C₉H₁₂, 14.4 g) was added dropwise, and stirred for 24 hours. The final solution was treated as described above.

K3: MCM-41 with C₁₈ as surfactant

Molar composition: 1 Si : 0.06 Al : 0.4 C₁₈ : 87 H₂O.

The synthesis was carried out at 50°C. The surfactant, C₁₈H₃₇(Me)₃NBr (octadecyltrimethylammonium bromide, C₁₈, 15.7 g) was added to water (100 g) and stirred for 1 hour. Sodium-aluminate (54% Al₂O₃, 41% Na₂O, 0.44 g) was added to the solution and stirred for 4 hours, then H₂SO₄ (10%, 5.7 g) was added to it. Sodium-meta-silicate-5-hydrate (8.9% Na₂O + 28% SiO₂, 18.7 g) was added to water (40 g), and stirred for a few minutes. The mixture was added dropwise to the acidic solution of C₁₈ and aluminium. A yellow-coloured product was formed. After stirring for 30 minutes, a homogenous, light pink solution was obtained. The final solution was treated as described above.

K4: Cu-Al-MCM-41

Molar composition: 1 Si : 0.06 Al : 0.1 Cu : 0.2 C₁₄ : 64 H₂O.

The surfactant C₁₄H₂₉(Me)₃NBr (tetradecyltrimethylammonium bromide, 7.1 g) was dissolved in water (50 g) and stirred for 1 hour. Sodium-aluminate (54% Al₂O₃, 41% Na₂O, 0.45 g) was dissolved in water (40 g) and H₂SO₄ (95%, 1.5 g) and was added to the solution, which was stirred for 45 minutes. Copper acetate (2.0 g) was added to the solution of aluminium, and stirred for 1 hour. The solution obtained was then added dropwise to the solution of template. The light blue solution was stirred for one hour. Sodium-meta-silicate-5-hydrate (8.9% Na₂O + 28% SiO₂, 18,7 g) was dissolved in water (15 g) and stirred for 50 minutes before it was added dropwise to the solution described above and stirred for 2 hours. The pH in the final solution was 10. The final solution was treated as described above. The product is light-blue.

K5: FCC

FCC catalyst is a commercial catalyst provided by GRACE GmbH und Co.KG.

K6: SBA-15

Molar composition: 1 Si : 0.02 EO₂₀PO₇₀EO₂₀ : 5 HCl + water.

The synthesis was carried out at 40 °C.

The surfactant (poly(ethylene glycol)-block-poly(propylene glycol)-block-poly(ethylene glycol): EO₂₀PO₇₀EO₂₀) was heated to 50 °C overnight.

Hydrochloric acid (120.6 g, 2M) was heated to 40 °C. Water (30 g) was added and the solution was heated until the temperature was stabilised at 40 °C. The surfactant (4.6 g) was added and this mixture was stirred for 5 hours. TEOS (tetraethoxysilan, 9 g) was added dropwise, and the clear solution was stirred overnight.

The homogenous, white solution was transferred to a Teflon flask, which was sealed with Teflon tape and heated at 100 °C for 48 hours.

The white solid was washed with warm distilled water or centrifuged until pH 5 was obtained. The white product was dried at 100°C overnight.

K7: Al-SBA-15

Molar composition: 1 Si : 0.05 Al : 0.02 EO₂₀PO₇₀EO₂₀ : 0.5 HCl + water.

The surfactant (poly(ethylene glycol)-block-poly(propylene glycol)-block-poly(ethylene glycol): EO₂₀PO₇₀EO₂₀, 20g) was heated 50°C and solved in 400 g 0.1M hydrochloric acid, and stirred over night at 25-30°C. TEOS (tetraethoxysilan, 40 g) was added under stirring. The solution was stirred for 1 hour before sodium-aluminate (54% Al₂O₃, 41% Na₂O, 0.92 g) was added and stirred over night at 25°C. pH in the solution was measured.

Next morning the temperature was changed to 40°C, after about 30 min a gel was formed and after 2-3 hours white precipitate was observed. The white precipitate solution was then stirred for 4 hours before the pH of the solution was changed to pH 2.5 with 4M NaOH and was stirred for 1 hour at 40°C.

The solution was transferred to Teflon flasks and was allowed to react at 100°C for 72 hours. The white products formed were washed with distilled water and centrifuged until pH 5 was obtained.

The samples were dried at 90°C for 3 days followed by drying at 100°C overnight before formulation.

2.3 Experimental Procedure

All experiments took place in the Laboratory of Environmental Fuels and Hydrocarbons, situated in CPERI, Thessaloniki, Greece. The reactor (Fig. 1) was filled with 0.7 g catalyst, or glassbeads for the non-catalytic tests and the piston was filled with biomass (1.5 g). Glasswool was placed in the bottom of the reactor, the top of the piston and inside the bed in order to separate the catalyst and the biomass bed.

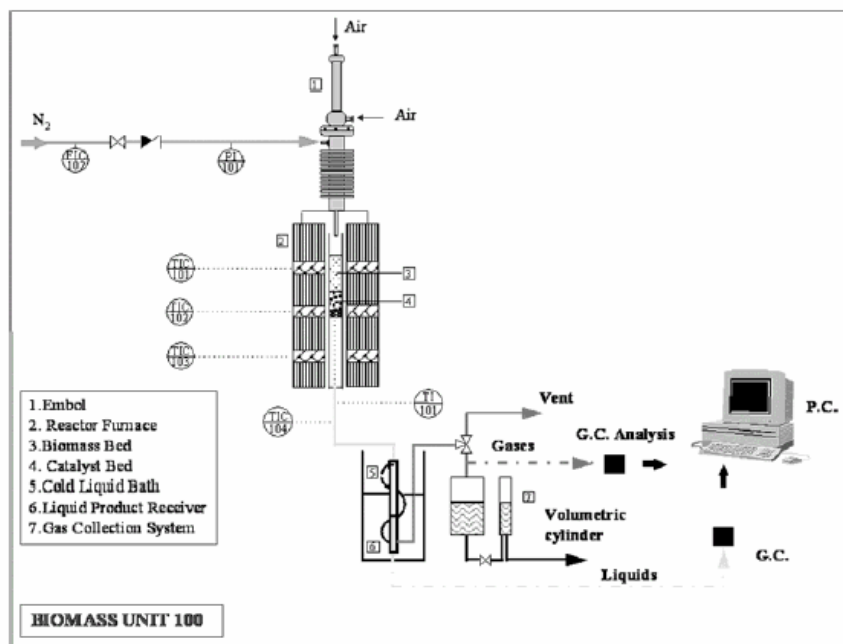


Fig. 1. The fixed bed reactor system

The reactor and the piston were connected and placed into the oven. The leaks of the system were controlled, in case of no leaking, the oven was switched on. The system was always heated in the presence of N_2 (30 cc/min) and, by using a temperature controller, the temperature of each zone of the furnace was controlled. As soon as the reaction temperatures were achieved, biomass entered the reactor and the experiment started. During the time of the experiment (15 min) the piston did not return to its original position in order to be checked after the end of the experiment. At the end of the experiment purging (30 min) was performed. Both the experiment (100cc/min) and purging (30cc/min) were performed in the presence of N_2 . During purging, temperatures of the first and the second zone were switched off and 20 min later every heating resource was shut down. The pressure was controlled, before and after the entrance of the piston into the reactor to identify potential blockage.

The liquid products were collected in a liquid bath ($-17\text{ }^\circ\text{C}$) and quantitatively measured in a pre-weighted glass receiver. The two phases of the liquid – organic and aqueous were separated with an organic solvent (dichloromethane). The gaseous products were collected and measured by water displacement. The amount of coke formed was measured by direct weighting. The reaction temperature was kept at $500\text{ }^\circ\text{C}$, reported to be the optimum temperature for biomass pyrolysis [17-18].

The liquid samples were analysed by GC/MS analysis in a HP 5989 MS ENGINE (Electron energy 70eV; Emission 300V; Helium flow rate: 0.7cc/min; Column:HP-5MS(30m x 0.25mmID x 0.25 μ m)) for the identification of compounds in the organic phase. The GC-MS technique cannot give the quantitative analysis of bio-oil. However, based on literature [19] we can make an estimate of the organics composition based on the peak area of the GC/MS chromatogram (the % area of the GC/MS chromatogram is considered linear with the compound concentrations). It must be noted that this estimate is only useful for the relative comparison of the compounds produced from the different catalysts.

Using the GC/MS technique the qualitative analysis of the organic fraction was performed. GC/MS chromatogram reveals several hundreds of different organic compounds in the organic part of bio-oil. Some of these compounds can be ranked as hydrocarbons, phenols, carboxylic and carbonyl.

The gaseous products were analysed in a HP 6890 GC, equipped with four columns (Precolumn:OV-101; Columns: Porapak N, Molecular Sieve 5A and Rt-Qplot (30m x 0.53mm ID) and two detectors (TCD and FID). The chromatograph was standardized with gases at known concentrations as standard mixtures (std A: methane, ethane, ethylene, propane, propylene, n-butane, iso-pentane, n-pentane, n-hexane, carbon monoxide, carbon dioxide, hydrogen and helium, std B: methane, propane, propylene, carbon monoxide, carbon dioxide, hydrogen, nitrogen and helium).

3. Results and discussion

3.1 Catalyst properties

The characterisation results of the Al-MCM-41 catalysts (K1-K4) can be found in Table 1. The results show high surface areas for all the Al-MCM-41 catalysts. The K1 and K4 catalysts have the same mesopore size, and the pore size increase is clearly shown in Table 1. The K3 catalyst has the largest mesopore size, but the K2 catalyst pore size is still larger than that of the K1 and K4 catalysts. The micropore size remained unmodified.

Table 1
Al-MCM-41 catalysts characterisation results

| CATALYST NAME | K1 | K2 | K3 | K4 |
|----------------------------------|------|------|------|------|
| Surface area (m ² /g) | 917 | 947 | 928 | 816 |
| Total pore volume (ml/g) | 1.23 | 1.43 | 1.26 | 1.46 |
| Micropore volume (ml/g) | 0.48 | 0.56 | 0.28 | 0.3 |
| Micropore diameter (Å) | 8 | 7.9 | 8.1 | 8 |
| Mesopore diameter (Å) | 24 | 28 | 30 | 24 |

Table 2 shows the properties of the FCC catalyst (K5) used in the experiments. The FCC catalyst has lower surface area than the other catalysts and was used for comparison purposes.

Table 2
FCC catalyst properties

| CATALYST NAME | FCC-1 |
|---|--------------|
| Total surface area (m²/g) | 178.4 |
| Zeolite area (m²/g) | 58.5 |
| Matrix area (m²/g) | 119.9 |
| Z/M | 0.49 |
| UCS (Å) | 24.26 |
| Ni (ppm) | 150 |
| V (ppm) | 367 |

The characterisation results of the SBA-15 catalysts (K6-K7) are shown in Table 3. The catalysts have high surface areas, however, the aluminium incorporation at K7 sample seems to reduce the surface area. The SBA-15 catalysts (K6 and K7) have clearly larger mesopore diameter and less micropore volume, than the MCM-41 type(K1-K4) catalysts.

Table 3
SBA-15 type catalysts characterisation results

| CATALYST NAME | K6 | K7 |
|---------------------------------------|-----------|-----------|
| Surface area (m²/g) | 817 | 536 |
| Total pore volume (ml/g) | 1.53 | 1.23 |
| Micropore volume (ml/g) | 0.015 | 0.0 |
| Micropore diameter (Å) | 6.5-7.5 | 6-7.5 |
| Mesopore diameter (Å) | 68; 78-95 | 63; 78 |

The total surface areas, pore volumes and pore sizes of the calcined mesoporous MCM-41 and SBA-15 materials were calculated from the nitrogen adsorption-desorption isotherms, from measurements on Quantachrome - Autosorb -1 apparatus and the results are summarised in Tables 1, and 3.

3.2 Comparison of catalysts

The liquid, the gas and the coke yields of the experiments are shown in Fig. 2.

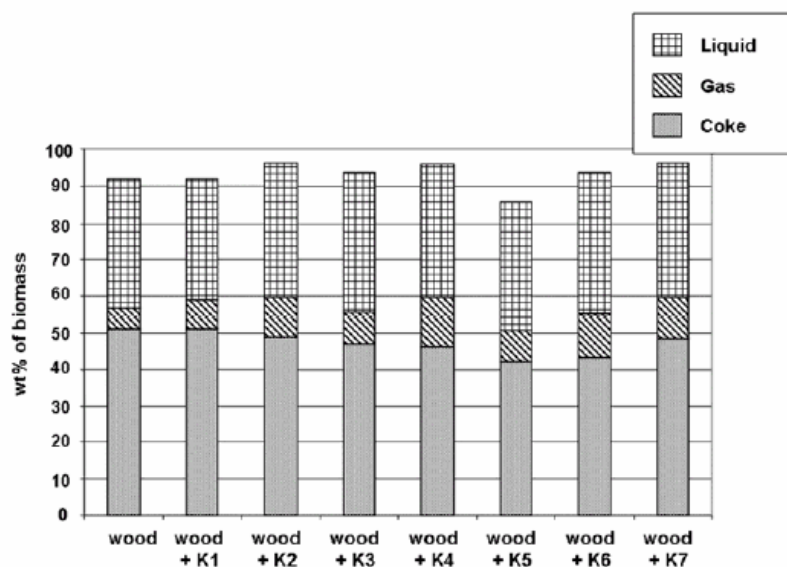


Fig. 2. Pyrolysis product distributions in the fixed bed experiments

As Fig. 2 shows, the liquid yield was reduced, where the vapours contacted the K1 and K5 catalysts, otherwise increased compared to the non-catalysed sample. The gas yield increased in each catalytic case, mostly with the transition metal modified catalysis (K4). The coke yield remained the same with K1, K2, and K7 catalysts, and slightly decreased with the other catalysts. Sample K5 produced the least amount of coke however, it should be mentioned that we had probably more coke loss during the experiments because of the very fine coke powder we experienced with this sample. Experiments with the K5 catalyst were the only where the mass balance recovery did not reach 90%.

Due to the presence of the catalyst the composition of the liquid phase varied (Fig. 3).

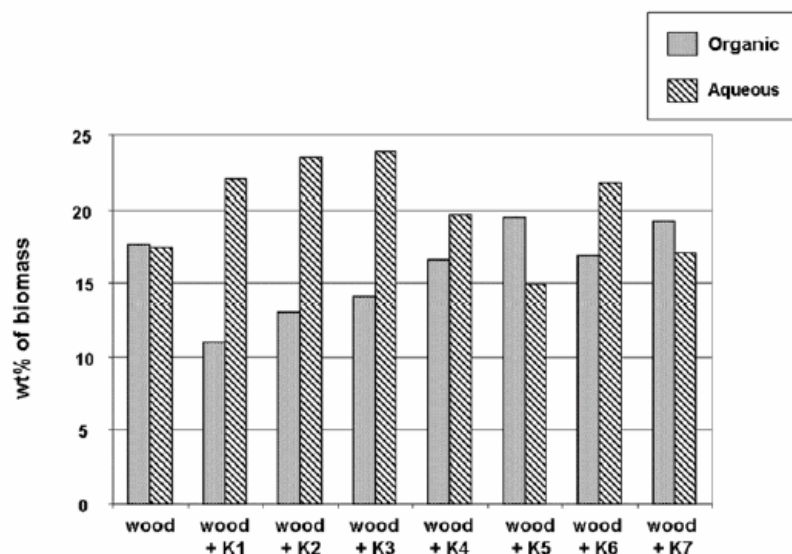


Fig. 3. Liquid phase composition

The MCM-41 type catalysts produced less organic phase, which indicates a strong catalytic activity, since the water is the product of many catalytic reactions, and the yield of organic phase increased with increasing pore size (order of pore size: $K1 < K2 < K3$, where $K1$ and $K2$ catalysts have nearly the same pore sizes), but remained under the non-catalytic yield. Introduction of copper in MCM-41 catalyst ($K4$) increases also the organic phase to a yield close to the non-catalytic level. Pure siliceous SBA-15 ($K6$) and FCC ($K5$) catalysts did not change the organic phase yield compared to non-catalytic experiments, but with Al-SBA-15 ($K7$) catalyst the organic phase yield increased slightly.

The MCM-41 type catalysis produced most aqueous phase, which increased with increasing pore size. The Cu modified sample ($K4$) produced less aqueous phase compared to other MCM-41 catalysts, but it was still higher than the non-catalytic aqueous phase yield. The FCC catalyst ($K5$) produced the least amount of aqueous phase. SBA-15 catalyst ($K6$) produced also a high amount of aqueous phase during the experiments, but this yield decreased when aluminium was incorporated into the catalyst ($K7$).

The identified compounds of organic phase were grouped into eight groups: hydrocarbons, phenols, furans, acids, alcohols, carbonyls, polycyclic aromatic hydrocarbons (PAHs), and heavy compounds. The amount of the group of compounds together with unidentified ones is shown in Table 4.

The quality of oil is characterised by the carbonyls and heavy compounds yield, since they are responsible for many reactions in the aging procedure, by the acid yield, since low pH values make introduction in engines difficult due to corrosion and PAH is considered as hazardous for the environment. The phenol yield is also interesting because of its commercial value: high phenol yield makes the process more

economically attractive. The amounts of different compounds have been altered due to the catalytic process.

Table 4
Composition of the organic phase (wt% of the organic fraction)

| | wood | wood + K1 | wood + K2 | wood + K3 | wood + K4 | wood + K5 | wood + K6 | wood + K7 |
|------------------------|------|--------------|--------------|--------------|--------------|--------------|--------------|--------------|
| Hydrocarbons | 0.7 | 11.7 | 12.2 | 6.9 | 3.8 | 16.3 | 6.7 | 9.5 |
| Phenols | 18.9 | 26.3 | 22.5 | 29.1 | 31.4 | 32.0 | 29.0 | 28.9 |
| Furans | 3.9 | 15.2 | 15.5 | 10.6 | 15.7 | 16.3 | 19.3 | 11.4 |
| Acids | 4.6 | 0.0 | 0.0 | 1.0 | 0.5 | 1.3 | 2.3 | 1.5 |
| Alcohols | 4.9 | 0.7 | 2.4 | 1.2 | 2.6 | 1.8 | 5.0 | 4.7 |
| Carbonyls | 29.9 | 14.5 | 17.7 | 24.8 | 16.4 | 16.0 | 19.2 | 16.2 |
| PAH | 0.4 | 17.1 | 8.2 | 11.4 | 5.4 | 2.2 | 0.5 | 10.6 |
| Heavy compounds | 9.9 | 2.7 | 7.8 | 5.7 | 7.2 | 4.6 | 3.4 | 10.0 |
| Unidentified | 27.0 | 11.9 | 13.8 | 9.3 | 17.0 | 9.5 | 14.8 | 7.1 |

The amount of hydrocarbons increased in each catalytic experiment, mostly with FCC (K5), but the increase was significant with K1 and K2 catalysts too. Concerning the phenolic fraction, this increased significantly also, due to the catalyst. FCC catalyst (K5) and transition metal modified catalyst (K4) improve mostly the phenols yield. Aluminium incorporation into SBA-15 framework does not seem to have an influence on the phenols yield. The furan yields have been increased using the catalytic samples as well, mostly with pure siliceous SBA-15 (K6) catalyst. Due to aluminium incorporation into this catalyst (K7), the furan yield decreased significantly. The acid yield decreased in each catalytic sample. However, it needs to be mentioned that the acid yields (and also the alcohols) are considered only in the organic fraction. The pH in the aqueous fraction was found below 2 in each sample (based on pH paper measurements only), which means that some parts of the acids/acidic compounds are water-soluble. The alcohol yields compared to the non-catalysed sample remained nearly the same with SBA-15 catalysts (K6 and K7) and decreased with the other catalysts. The yields of carbonyls decreased also in catalytic experiments. However, they seem to increase with the pore size of the MCM-41 catalyst. PAH formed at elevated amounts at each catalytic sample, least of all with the siliceous SBA-15 (K6), and most with the Al-MCM-41 catalyst (K1). The heavy compounds yield decreased mostly in the catalysed samples, the only catalyst, which had about the same yield of heavy compounds, was Al-SBA-15 (K7). In the catalysed samples identification of the compounds was easier. The amount of the unidentified compounds in the non-catalysed sample was almost 27% and this amount decreased to about 10-15% in all catalytic runs. Unidentified compounds are usually a mixture of several compounds which correspond to a single peak in the chromatogram, mainly in the heavy regions. They are compounds with heteroatoms, small monomers, parts of lignin, or compounds which are very unlikely to be identified correctly.

The obtained products were further grouped in order to simplify the treatment of the results (Fig. 4.). Hydrocarbons and alcohols are considered as fuels, thus desirable compounds in the bio-oil, together with phenols, which will increase the commercial

value of the bio-oil, while acids, carbonyls and PAH were considered as undesirable compounds among the pyrolysis products.

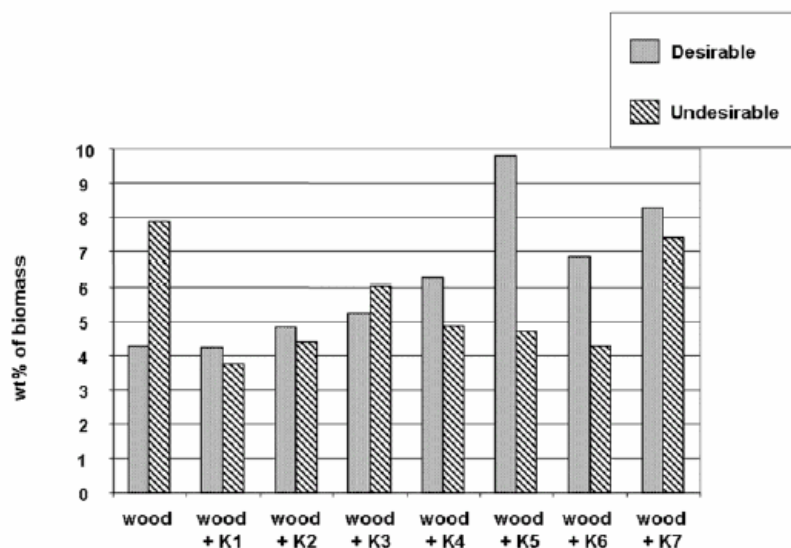


Fig. 4. Desirable and undesirable product compounds in the organic phase

As it can be seen on Fig. 4, the wood pyrolysis, where the vapours remain unmodified produced far more undesirable than desirable products. This improved when the vapours were contacted with catalysts. Catalytic samples produced generally more desirable products than undesirable, the only exception is the K3 sample. All catalysed samples produced less undesirable products and more desirable than the non-catalytic sample. The unmodified Al-MCM-41 catalysis (K1) produced approximately the same amount of desirable products, but the amount of the undesirable products decreased with nearly 50% compared to the non-catalytic experiment. Pore size enlargement seems to increase both the desirable and undesirable product yields, undesirable products increased at elevated rates. Transition metal modified Al-MCM-41 catalyst (K4) produces the best organic phase of the Al-MCM-41 type catalysts. With FCC catalyst (K5) the best pyrolysis product was obtained. More than 8 % of the biomass weight was converted to desirable products, while the undesirable product yield remained low. The obtained organic phase is favourable also with SBA-15 catalyst (K6), and Al-incorporation into the SBA-15 (K7) increases both the desirable and the undesirable product yields.

The pyrolysis gases composition is shown in Table 5.

Table 5
Composition of pyrolysis gases (wt % of the biomass)

| | wood | wood + K1 | wood + K2 | wood + K3 | wood + K4 | wood + K5 | wood + K6 | wood + K7 |
|-------------|------|--------------|--------------|--------------|--------------|--------------|--------------|--------------|
| CxHy | 0.31 | 0.97 | 1.16 | 0.91 | 1.56 | 1.24 | 1.18 | 1.35 |
| CH4 | 0.16 | 0.30 | 0.40 | 0.34 | 0.54 | 0.39 | 0.49 | 0.45 |
| CO | 1.95 | 3.41 | 4.73 | 4.00 | 6.53 | 5.09 | 5.80 | 4.99 |
| CO2 | 2.50 | 2.98 | 4.74 | 3.83 | 4.38 | 2.99 | 3.97 | 4.62 |

The main products in the gas phase were carbon-monoxide and carbon-dioxide. In addition, methane arose also in significant amounts. Hydrogen was found in samples catalysed by K1 and K4 catalysts. The gas compound yields varied slightly due to catalysis, generally more methane and carbon-monoxide produced, while the carbon-dioxide yield decreased. This is due to lower oxygen content of the catalytic upgraded bio-oil.

3.3 Comparison of feedstocks

Additional experiments were performed with Miscanthus biomass as an attempt to study the effect of the biomass feedstock to the pyrolysis products. As it is shown in Fig. 5, the biomass type has an important role on the in-situ catalytic upgrading of pyrolysis vapours.

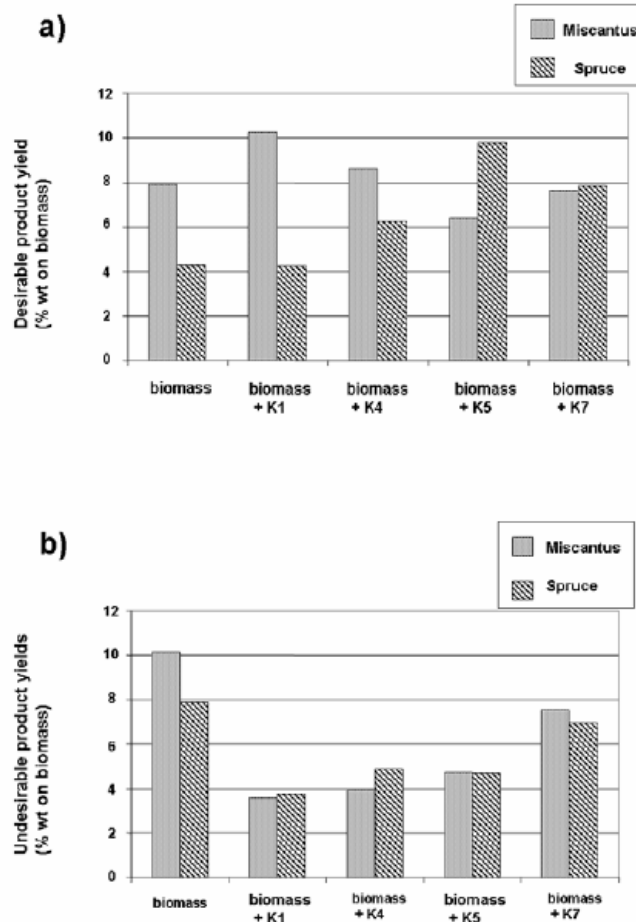


Fig. 5. Desirable (a) and undesirable (b) products from different biomass: comparison of Miscanthus and spruce

As it was mentioned above with spruce biomass the FCC catalyst (K5) produces the more promising product. However, with Miscanthus, the Al-MCM-41 (K1) produces the highest desirable product yield and the Cu-modified catalyst (K4) produces also more desirable compounds than the uncatalysed sample, but with FCC catalyst (K5), the desirable product yield remains below the uncatalysed product yield. Concerning the undesirable products yield, K1, K4 and K5 catalysts perform the same with Miscanthus biomass: the yield is approximately half of the uncatalysed yield. Using Al-SBA-15 catalyst (K7) the biomass influence is not significant. This catalyst converts approximately 8 % of the biomass to desirable compounds both in case of spruce wood and Miscanthus pyrolysis, which makes it an interesting catalyst in case of mixed biomass feed. However, the undesirable product yield is high with both biomass feeds, which is a drawback of this catalyst. The difference between softwood and agricultural

plants is in the hemicellulose and lignin composition and their percentage in the plant, which is expected to affect the rate of degradation of the polymeric molecules and thus the distribution of compounds in the final pyrolysis product.

4. Conclusions

Due to the catalytic activity there are several changes in the final bio-oil composition. The hydrocarbon and phenol yields increased in the organic phase, while the carbonyl and acid yield decreased. This confirms that catalyst usage can be advantageous. One of the catalyst's drawback is the PAH formation. All catalysts studied reduce the amounts of the undesirable compounds in the bio-oil, while more desirable compounds are obtained. The pore size enhancement of Al-MCM-41 catalysts seems to worsen the situation: with increasing pore size, the yield of undesirable products increases at higher rates than the desirable products yield. Transition metal incorporation into the MCM-41 structure, on the other hand, increases the amount of desirable products more than undesirable products. Aluminium incorporation into SBA-15 framework results in very high content of desirable products in the bio-oil, however, the undesirable product yield increased in this case as well.

Concerning the comparison of the two different feedstocks it seems that in the presence of spruce, the commercial FCC catalyst performs best, while when the feedstock is Miscanthus, the unmodified Al-MCM-41 is the most advantageous catalyst.

Between all the catalysts tested, the Al-SBA-15 catalyst performs more balanced; the biomass type does not seem to have a significant influence on the desirable and undesirable product yields.

Acknowledgements

J. Adam is indebted to the Norwegian Research Council for her Ph. D. grant and M. H. Nilsen thanks the Norwegian University of Science and Technology for the Post-doc grant. E. Antonakou, A. Lappas, M. Stöcker and A. Bouzga acknowledge the financial support of the European Union (ENK 6-CT2001-00049).

References

- [1] A. Bridgewater, *Appl. Catal. A* 116 (1994) 5.
- [2] A. Demirbas, *Energy Convers. Manage.* 42 (2001) 1375.
- [3] P. Williams and N. Nugranad, *Energy* 25 (2000) 493.
- [4] A. Lappas, M. Nilsen, A. Bouzga, M. Stöcker, E. Antonakou and I. Vasalos, in: *Proceedings 8th Symposium of the Hellenic Catalysis Society, Cyprus, 30 October 2004*, p.73.
- [5] S. Czernik, R. Maggi, G. V. C. Peacocke *Fast Pyrolysis of Biomass: A Handbook Vol. 2.* (Ed A. V. Bridgewater) CPL Press, Newbury, UK; 2002. p. 141.
- [6] S. Vitolo, M. Seggiani, P. Frediani, G. Ambrosini, L. Politi, *Fuel* 78 (1999) 1147.

- [7] Cr. I. Simonescu, C. Vasile, P. Onu, M. Sabliovschi, G. Moroi, V. Barboiu, D. Ganju, M. Florea, *Thermochim. Acta* 134 (1988) 301.
- [8] J. Beck, J. Vartuli, W. Roth, M. Leonowicz, C. Kresge, K. Schmitt, C. Chu, D. Olson, E. Sheppard, S. McCullen, J. Higgims and J. Schlenker, *J. Am. Chem. Soc.* 114 (1992) 10834.
- [9] Corma, M. S. Grande, V. Gonzalez-Alfaro, A. V. Orchilles, *J. Catal.* 159 (1996) 375.
- [10] J.C. Vartuli, A. Malek, W. J. Roth, C. T. Kresge, S. B. McCullen, *Microporous Mesoporous Mater.* 44-45 (2001) 691.
- [11] R. Mokaya, *Chem. Commun.* (2001) 633.
- [12] T. R. Pauly, V. Petkov, Y. Liu, S. J. L. Billinge, T. J. Pinnavaia, *J. Am. Chem. Soc.* 124 (2002) 97.
- [13] A. Corma, M. T. Navarro *Studies in surface science and catalysis* (Ed. R. Aiello, G. Giordano, and F. Testa) Elsevier Science B.V.; 2002. p. 487.
- [14] G. D. Stucky, D. Zhao, P. Yang, W. Lukens, N. Melosh, B. F. Chmelka, *Stud. Surf. Sci. Catal.* 117 (1998) 1.
- [15] D. Zhao, J. Feng, Q. Huo, N. Melosh, G. H. Fredrickson, B. F. Chmelka, G. D. Stucky, *Science* 279 (1998) 548.
- [16] Y. Yue, A. Gédéon, J. L. Bonardet, N. Melosh, J. B. D'Espinose, J. Fraissard, *Chem. Commun.* (1999) 1967.
- [17] A. V. Bridgwater, D. Meier, D. Radlein, *Org. Geochem.* 30 (1999) 1479.
- [18] T. Milne, F. Agblevor, M. Davis, S. Deutch, D. Johnson, *Developments in Thermochemical Biomass Conversion* (Ed. A. V. Bridgwater and D. G. B. Boocock), Blackie Academic and Professional, Volume 1, London; 1997. p. 409.
- [19] Samolada, M., Papafotica A., Vasalos, I., *Energy Fuels*, 14 (2000) 1161.

Paper IV.

Submitted to and accepted as a poster presentation in the "14th European Biomass Conference and Exhibition", Paris, France, October 2005.

VAPOUR PHASE UPGRADING OF BIOMASS PYROLYSIS PRODUCTS WITH SBA-15 AND COMMERCIAL FCC CATALYSTS

Judit Adam^{a*}, Marianne Blazsó^b, Erika Mészáros^b, Michael Stöcker^c, Merete H. Nilsen^c, Aud M. Bouzga^c, Johan E. Hustad^a

^a*Department of Energy and Process Engineering, Norwegian University of Science and Technology, K. Hejesvei 1A, N-7491 Trondheim, Norway*

^b*Institute of Materials and Environmental Chemistry, Chemical Research Centre, Hungarian Academy of Sciences, P.O. Box 17 H-1525 Budapest, Hungary*

^c*SINTEF Materials and Chemistry, P.O. Box 124 Blindern, N-0314 Oslo, Norway*

**Corresponding author, E-mail: judit.adam@ntnu.no, Telephone: +4773590623, Fax: +4773598390*

Abstract

Bio-oil derived from wooden biomass has the opportunity to become a renewable and environmental friendly fuel and a source for the production of valuable chemicals. However, bio-oil has a tendency to lose its desirable properties during storage. One of the possibilities to improve the storage properties is the application of a catalyst during the production or upgrading of the produced liquid. Changing the pyrolysis oil composition by using catalytic materials during the pyrolysis process can improve the oil properties during storage.

Spruce wood was subjected to analytical pyrolysis at 500 °C for 20 sec using on-line pyrolysis-gas chromatography/mass spectrometry (Py-GC/MS). The volatile decomposition products were separated by gas chromatography and the components were analysed by mass spectrometry. In addition, thermogravimetry/mass spectrometry (TG/MS) experiments were applied for monitoring the weight loss and the product evolution under slow heating conditions (20 °C/min) from 50 to 800 °C.

New mesoporous materials (SBA-15) and a commercial FCC catalyst were tested in this work. During the pyrolysis experiments, the biomass and the catalyst were placed in two layers, with the catalyst on top in order to ensure that the pyrolysis vapours pass through the catalyst.

Due to the catalytic activity, the product distribution of pyrolysis vapours changed significantly. As expected, higher coke and water formation was observed during the reaction, and the yields of several compounds were altered. The amount of the evolved organic acids and aldehydes decreased, while the amount of hydrocarbons increased. The studied catalysts showed different influences on the product distribution and the largest effect was achieved by using the commercial FCC catalyst. The results show that catalyst usage can be advantageous in the production of better quality bio-oils.

1. Introduction

Biomass and the alternative energy sources in general are widely recognized as a potential future solution to the energy problems worldwide. The energy from biomass can be obtained by various techniques, such as combustion or upgrading into a more valuable fuel, gas or oil. It can also be transformed into a source of higher value products for the chemical industry [1] by using a thermochemical method, such as pyrolysis.

The liquid product of biomass pyrolysis, known as bio-oil or pyrolysis oil, is a complex mixture of several hundreds of organic compounds that exhibit a wide range of chemical functionality. Bio-oil consists of two phases, an aqueous phase containing oxygenated organic compounds of lower molecular weight and a non-aqueous phase, which contains organic compounds (mainly aromatics) [2]. Characteristic examples of oxygenated compounds in the oils are phenols, cresols, benzenedioles and their alkylated derivatives [3,4]. The major aromatic hydrocarbon compounds present in the oil are single ring aromatic compounds, like benzene, toluene, indene, alkylated products and polycyclic aromatic hydrocarbons (PAH) [3,4].

The use of pyrolysis oil either as a fuel or as a source of valuable chemicals exhibits two main problems: the high amount of water produced during pyrolysis and the oil's instability because of the presence of certain 'undesirable' organic compounds. Stabilisation of bio-oils can be achieved by upgrading them, mainly with the help of catalysts.

The upgrading possibilities are reviewed by Czernik et al. [5]. Vitolo et al. [6] studied different types of zeolites to upgrade bio-oil to fuel. They studied the influence of residence time and temperature in a fixed bed microreactor, too. Simionescu et al. [7] investigated the catalytic pyrolysis of various hydrocarbon products. They concluded that the catalysts cause an increase in the amount of gas, and 5-10% coke deposits on the catalyst's surface.

Catalytic cracking of hydrocarbons combined with fluid bed processes (FCC) is one of the most important and most profitable processes in the petroleum refining industry. FCC units are used to upgrade heavy gas oils to gasoline, diesel fuel and light gases. The catalytic cracking is catalysed by materials having acidic properties (FCC catalysts).

Stucky and co-workers [8-9] introduced a new synthesis route involving amphiphilic di- and tri-block copolymers as organic structure directing agents. These materials, exemplified by hexagonal (p6 mm) SBA-15, have long range order, large monodispersed mesopores (up to 50 nm) and thicker walls (typically between 3 and 9 nm), which make them thermally and hydrothermally more stable than MCM-41 type materials. Yue et al. [10] obtained aluminium incorporated SBA-15 mesoporous materials by direct synthesis. The resulting materials retained the hexagonal order and physical properties of purely siliceous SBA-15 and presented higher catalytic activities in the cumene cracking reaction than Al-MCM-41 materials.

In a previous work [11], four mesoporous Al-MCM-41 catalysts were tested. In this work we aimed at studying different types of catalysts. Experiments were carried out with a commercial FCC catalyst in order to compare the new catalysts with a commercially available one, and two SBA-15 catalyst (a pure siliceous and an aluminium incorporated) because of their better hydrothermal stability.

2. Experimental

2.1. Materials

Barkless spruce wood (*Picea abies*) was milled and sieved and a fraction of particle diameter 0.5-1.4 mm was used in the experiments. The water content of the sample was approximately 6%.

2.2. The catalyst preparation

FCC

FCC catalyst is a commercial catalyst provided by GRACE GmbH und Co. KG.

SBA-15

Molar composition: 1 Si : 0.02 EO₂₀PO₇₀EO₂₀: 5 HCl + water.

The synthesis was carried out at 40 °C.

The surfactant (poly(ethylene glycol)-block-poly(propylene glycol)-block-poly(ethylene glycol): EO₂₀PO₇₀EO₂₀) was heated to 50 °C overnight.

Hydrochloric acid (120.6 g, 2M) was heated to 40 °C. Water (30 g) was added and the solution was heated until the temperature was stabilised at 40 °C. The surfactant (4.6 g) was added and this mixture was stirred for 5 hours. TEOS (tetraethoxysilan, 9 g) was added dropwise, and the clear solution was stirred overnight.

The homogenous, white solution was transferred to a Teflon flask, which was sealed with Teflon tape and heated at 100 °C for 48 hours.

The white solid was washed with warm distilled water or centrifuged until pH 5 was obtained. The white product was dried at 100°C overnight.

Al-SBA-15

Molar composition: 1 Si : 0.05 Al : 0.02 EO₂₀PO₇₀EO₂₀: 0.5 HCl + water.

The surfactant (poly(ethylene glycol)-block-poly(propylene glycol)-block-poly(ethylene glycol): EO₂₀PO₇₀EO₂₀, 20g) was heated to 50°C and dissolved in 400 g 0.1M hydrochloric acid, and stirred overnight at 25-30°C. TEOS (tetraethoxysilan, 40 g) was added under stirring. The solution was stirred for 1 hour before sodium-aluminate (54% Al₂O₃, 41% Na₂O, 0.92 g) was added and stirred overnight at 25°C.

Next morning the temperature was increased to 40°C, after about 30 min a gel was formed and after 2-3 hours white precipitate was observed. The white precipitate solution was then stirred for 4 hours before the pH of the solution was changed to pH 2.5 with 4M NaOH and was stirred for 1 hour at 40°C.

The solution was transferred to Teflon flasks and was allowed to react at 100°C for 72 hours. The formed white products were washed with distilled water and centrifuged until pH 5 was obtained.

The samples were dried at 90°C for 3 days followed by drying at 100°C overnight before formulation.

The total surface areas, pore volumes and pore sizes of the calcined mesoporous SBA-15 materials were calculated from the nitrogen adsorption-desorption isotherms, from measurements on Quantachrome - Autosorb -1 apparatus, and the results are summarised in Table 1.

Table 1. Main characteristics of SBA-15 type catalysts.

| CATALYST NAME | K6 | K7 |
|---------------------------------------|-----------|-----------|
| Surface area (m²/g) | 817 | 536 |
| Total pore volume (ml/g) | 1.53 | 1.23 |
| Micropore volume (ml/g) | 0.015 | 0.0 |
| Micropore diameter (Å) | 6.5-7.5 | 6-7.5 |
| Mesopore diameter (Å) | 68; 78-95 | 63; 78 |

2.3 Experimental Procedure

2.3. Py-GC/MS

Py-GC/MS (pyrolysis-gas chromatography/mass spectrometry) experiments were performed in a Pyroprobe 2000 pyrolyser (Chemical Data System) interfaced to a gas chromatograph (Agilent 6890) coupled to a mass selective detector (Agilent 5973) operating in electron impact mode (EI) at 70 eV. The pyrolysis was carried out at 500°C, for 20 sec using a platinum coil probe and quartz sample tubes.

The same amounts (1.5-2.0 mg) of wood and catalyst were weighed into the pyrolysis tube. The wood to catalyst ratio was 1:1 by weight % in most experiments. However, the FCC catalyst was heavier than expected and the catalyst amount equivalent to 50% wt (FCC/1 sample) did not cover the wood completely. In order to have a complete coverage and the same catalyst thickness as in case of the other experiments, we used more catalyst in the FCC/2 sample. Here, the catalyst amount was 3 times more than in the FCC/1 sample. The wood was placed in the middle of the pyrolysis tube and the catalyst next to the wood at both ends of the tube. This arrangement was chosen to ensure good control of the wood to catalyst ratio, and the arrangement of sample between two catalyst layers guarantees that all vapours produced from wood during pyrolysis travel through the catalyst and cannot pass by.

A helium carrier gas of 20 mL/min flow rate purged the pyrolysis chamber which was held at 250°C. A split of the carrier gas (1:20) was applied. The temperature of the GC/MS injector was held at 280 °C. The GC separation was carried out on a fused silica capillary column (Hewlett-Packard 5MS), 30m x 0.25mm. A temperature program from 50 to 300 °C at 10 °C/min heating rate was applied with an isotherm period of 1 min at 50°C and of 4 min at 300°C.

2.4. TG/MS

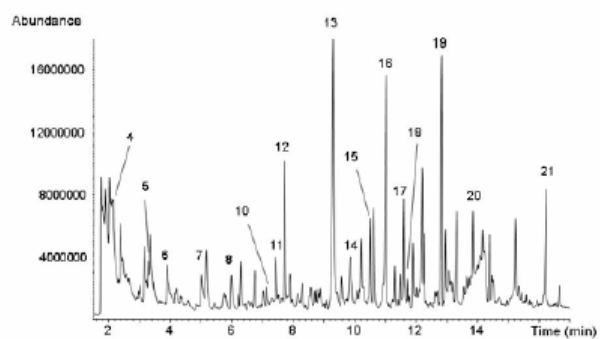
TG/MS experiments were carried out on a Perkin-Elmer TGS-2 thermobalance coupled to a HIDEN HAL 2/301 PIC quadrupole mass spectrometer through a glass-lined metal capillary heated to 300°C. Wood samples of 3 mg were placed into a platinum pan and the catalyst (3 mg) was layered on it, to ensure that vapours pass through the catalyst. In case of FCC/2, the catalyst amount was approximately 3 times more than in the FCC/1 sample. The samples were heated at a rate of 20 °C/min in argon atmosphere. The flow rate of the argon purge gas was 140 mL/min. A portion of the evolved products was introduced into the mass spectrometer operating in electron impact ionization mode at 70 eV electron energy. The mass spectrometric intensities of the products were normalized to the sample mass and the intensity of the ³⁸Ar isotope in order to avoid errors caused by the shift in sensitivity of the mass spectrometer.

3. Results and discussion

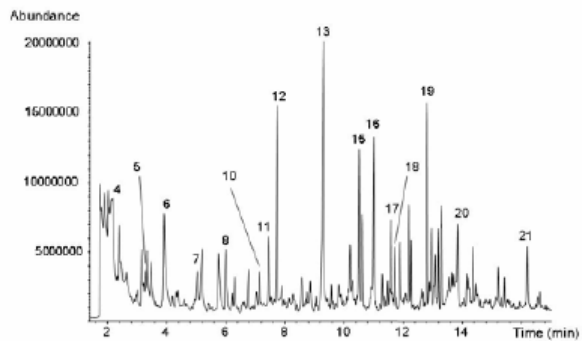
3.1 Py-GC-MS

Fig. 1. a-e display the pyrograms of wood and wood + catalyst samples. The identities of the peaks shown in these figures are listed in Table 2. It can be seen that as the result of catalysis levoglucosan (peak 20) disappeared from the wood + FCC/2 (Fig. 1.c) and wood + Al-SBA-15 (Fig. 1.e) samples, and partly degraded in wood + FCC/1 (Fig. 1.b) and wood + SBA-15 (Fig. 1.d) samples. These results imply that the catalytic upgrading of pyrolysis vapours was not successfully catalysed with FCC/1 and SBA-15 catalysts. The FCC catalyst is much heavier than the other catalysts, and 50 wt% catalyst did not cover the wood completely. As a result, a part of the vapours formed in pyrolysis could avoid the interaction with the catalyst. In case of the SBA-15 catalyst, the wood sample was completely covered with the catalyst, however, as the results indicate, the SBA-15 catalyst is less effective without aluminium incorporation. The yields of heavy compounds and the overall vapour yields also showed the same trends as the levoglucosan formation: less heavy and vapour yields are achieved with the FCC/2 and Al-SBA-15 catalysts, than with the FCC/1 and SBA-15 catalysts. (Note, the corresponding peak areas in the different chromatograms in Fig 1. are comparable, because the mass of the pyrolysed wood sample was the same within 10 wt% in the different experiments.).

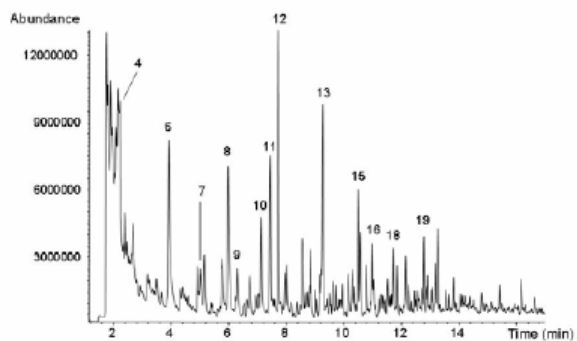
a) wood



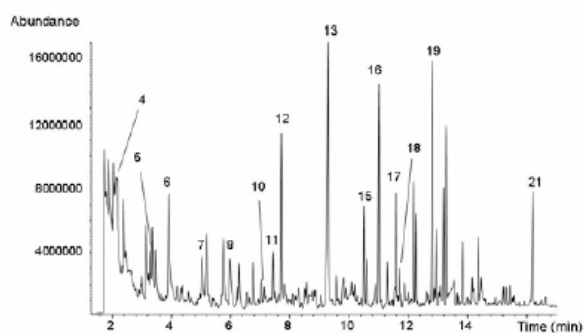
b) wood + FCC/1



c) wood + FCC/2



d) wood + SBA-15



e) wood + Al-SBA-15

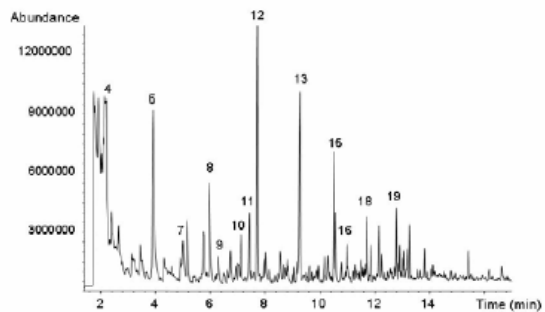


Figure 1. Total ion chromatograms of spruce wood pyrolysis: (a) wood, (b) wood + FCC/1, (c) wood + FCC/2, (d) wood + SBA-15 and (e) wood + Al-SBA-15 samples.

Table 2. Identification of the peaks of total ion chromatograms displayed in Fig. 1.

| Peak N° | Retention time (min) | Compound name |
|---------|----------------------|---------------------------------|
| 1 | 1.9 | water* |
| 2 | 2.0 | furan* |
| 3 | 2.2 | hydroxyacetaldehyde* |
| 4 | 2.3 | acetic acid |
| 5 | 3.4 | propanal |
| 6 | 4.0 | furfural |
| 7 | 5.2 | 2(5H)-furanone |
| 8 | 6.1 | phenol |
| 9 | 6.4 | benzofuran |
| 10 | 7.3 | 2-methylphenol |
| 11 | 7.6 | 4-methylphenol |
| 12 | 7.8 | 2-methoxyphenol |
| 13 | 9.5 | 2-methoxy-4-methylphenol |
| 14 | 10.0 | 5-hydroxymethylfurfural |
| 15 | 10.6 | 4-ethyl-2-methoxyphenol |
| 16 | 11.1 | 4-ethenyl-2-methoxyphenol |
| 17 | 11.7 | 6-methoxy-3-(2-propenyl)-phenol |
| 18 | 11.8 | 2-methoxy-4-propylphenol |
| 19 | 12.4 | 2-methoxy-4-(1-propenyl)-phenol |
| 20 | 14.2 | levoglucosan |
| 21 | 16.4 | 2-methoxy-4-propenalphenol |

* unresolved peak in TIC

It is also interesting to compare the yields of some selected products besides the chromatograms to get a deeper insight into the effect of catalysis on the upgrading of pyrolysis vapours. Monitoring the phenol yield is interesting because of its commercial value since high phenol yield makes the process economically more attractive. Figure 2 shows the amounts of (a) phenol and the light phenol substitutes ($MW \leq 124$) and (b) the heavy phenol substitutes ($MW \geq 138$) evolved during the fast pyrolysis of wood in the presence of different catalysts.

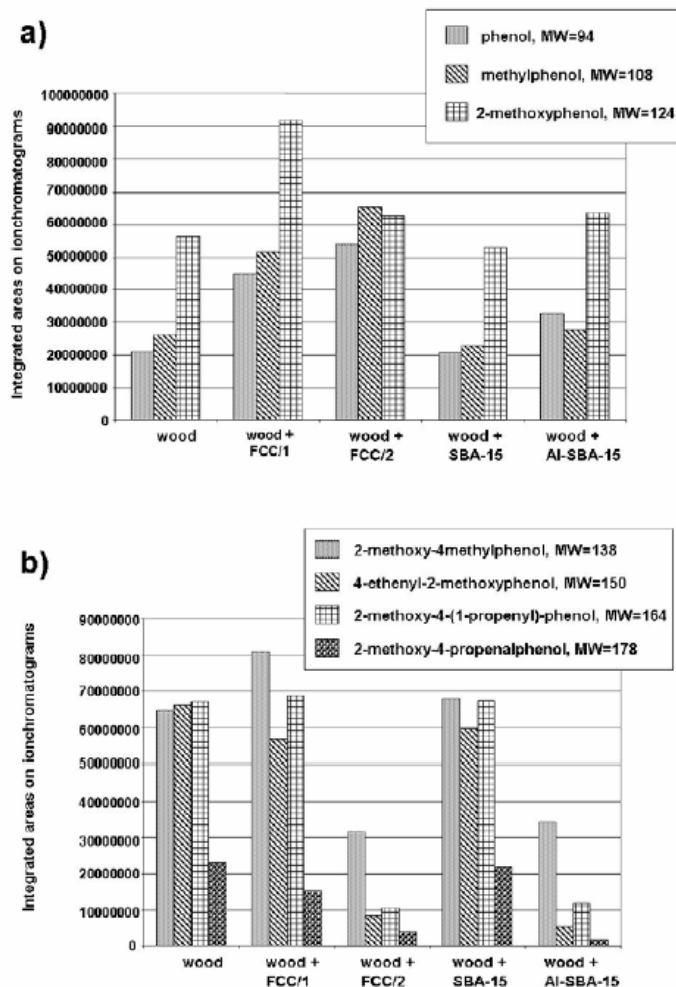


Figure 2. The evolution of (a) phenol and the light phenol substitutes ($MW \leq 124$) and (b) the heavy phenol substitutes ($MW \geq 138$).

The presence of FCC catalyst (FCC/2) increases the yield of phenol (see also Fig 1. peak 8) and light phenol substitutes (see also Fig. 1. peak 10-12) and decreases that of the heavy phenol substitutes (see also Fig. 1. peak 13, 15-19 and 21), while the SBA-15 does not change them considerably compared to the uncatalysed run. The Al-SBA-15 catalyst seems to break down the heavy phenols, but the yield of light phenolics is not influenced significantly.

Previous experiments [11] showed that due to mesoporous catalysis with MCM-41 type catalysts the yields of furan ring containing compounds considerably increased. The

catalysts studied in this work have a similar effect on the yields of furan ring containing compounds (Fig. 3.).

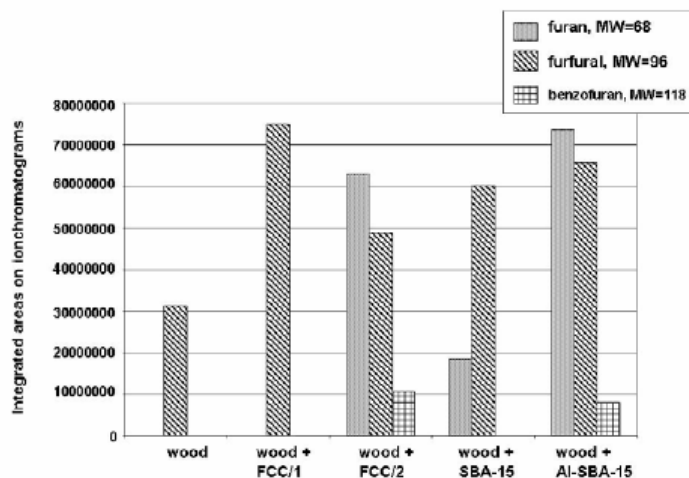


Figure 3. The yields of furan-ring containing compounds.

Furan (see also Fig. 1. peak 2) and benzofuran (see also Fig. 1. peak 9) were present in larger amounts in the wood + FCC/2 and wood + Al-SBA-15 samples i.e. the samples with most effective catalysis. Some furan was also produced from the wood + SBA-15 sample, but the yield was much lower here. The furfural yield (see also Fig. 1. peak 6) increased in each catalytic case, the highest amount of furfural was obtained from the wood + FCC/1 sample, which is not fully catalysed. It decreased if the catalysis was more effective (wood + FCC/2). With SBA-15 catalysis the furfural yield is also high. The aluminium incorporation into SBA-15 framework did not change the furfural yield significantly, compared to the yield obtained with the original SBA-15 catalyst.

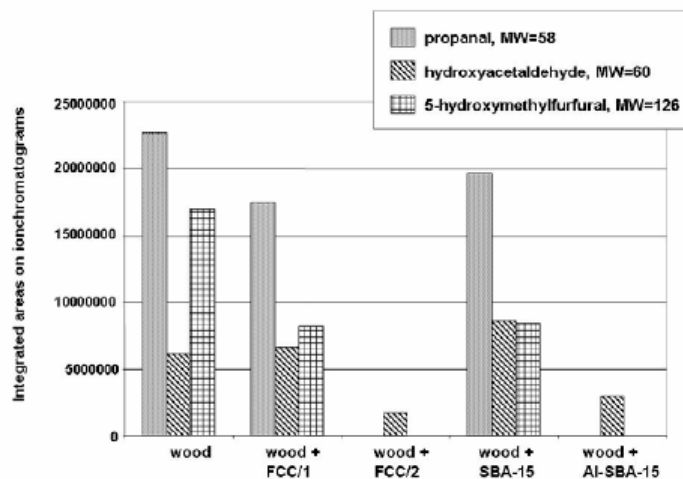


Figure 4. Aldehyde yields.

Aldehydes in bio-oil are responsible for a range of reactions that cause instability. That is why a great emphasis has been put on monitoring these compounds. The influence of catalysis on aldehyde formation is very significant (Fig. 4.) According to the experimental results, the amount of most of the aldehydes decreased with FCC/2 and Al-SBA-15 catalysts, apart from furfural (Fig. 3.). The effect of the other catalysts on aldehyde yield is less pronounced, although a smaller decrease in the amounts of some aldehydes can be observed.

It is also important to monitor the organic acid yields because organic acids are responsible for the low pH value of bio-oils, which causes corrosion problems in the combustion engines. The formation of acetic acid is shown as an example of the effect of catalysis on acid evolution.

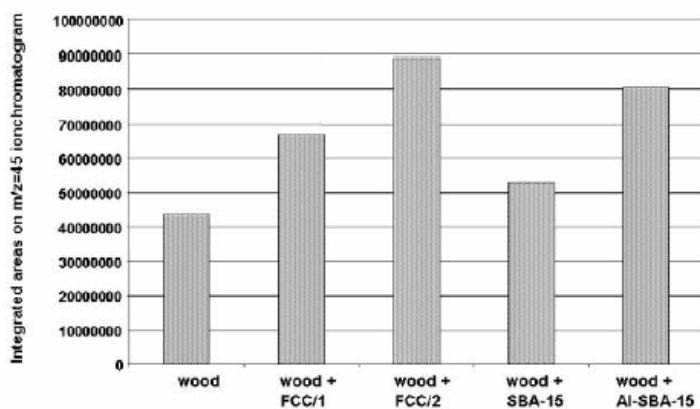


Figure 5. Acetic acid formation during Py-GC/MS.

The yield of acetic acid (Fig. 5, see also Fig. 1, peak 4.) increased in the presence of catalysts, compared to the uncatalysed sample. The most acetic acid is produced with the FCC/2 and the Al-SBA-15 catalysts. Unfortunately the studied catalysts seem to increase the acid yield.

3.2 TG-MS

The formation of volatile products has also been monitored during thermal decomposition of wood with the help of thermogravimetry/mass spectrometry. In this method a low heating rate is applied and the product evolution is monitored as a function of time/temperature.

The integrated mass spectrometric intensities of some selected products are shown in Table 3.

Table 3. The integrated intensities of selected products formed in the TG/MS experiments.

| <i>m/z</i> | ion | Temperature interval (°C) | Integrated area (counts) from sample | | | | |
|------------|---|---------------------------|--------------------------------------|--------------|--------------|---------------|------------------|
| | | | wood | wood + FCC/1 | wood + FCC/2 | wood + SBA-15 | wood + Al-SBA-15 |
| 15 | CH ₃ ⁺ | 250-800 | 18500 | 21000 | 25400 | 26600 | 29000 |
| 16 | CH ₄ ⁺ | 350-500 | 5800 | 7200 | 8000 | 9300 | 9000 |
| 16 | CH ₄ ⁺ | 500-780 | 5900 | 9000 | 12100 | 12600 | 14300 |
| 18 | H ₂ O ⁺ | 220-730 | 131500 | 175400 | 256400 | 201400 | 217600 |
| 26 | C ₂ H ₂ ⁺ | 250-430 | 2500 | 3600 | 3300 | 3000 | 3600 |
| 26 | C ₂ H ₂ ⁺ | 430-720 | 1300 | 1100 | 1900 | 2400 | 1700 |
| 27 | C ₂ H ₃ ⁺ | 270-430 | 4800 | 5900 | 5000 | 5200 | 5300 |
| 27 | C ₂ H ₃ ⁺ | 430-720 | 2700 | 2200 | 3700 | 4500 | 3100 |
| 28 | CO ⁺ | 250-420 | 29800 | 34700 | 52100 | 31200 | 43000 |
| 29 | CHO ⁺ | 200-540 | 25200 | 26500 | 20400 | 27000 | 23500 |
| 30 | CH ₂ O ⁺ | 180-550 | 10000 | 10000 | 7800 | 10500 | 9400 |
| 31 | CH ₃ O ⁺ | 220-500 | 12000 | 11700 | 6400 | 11600 | 9700 |
| 32 | CH ₃ OH ⁺ | 220-500 | 6800 | 9000 | 4500 | 5900 | 5500 |
| 42 | CH ₂ CO ⁺ | 230-700 | 3800 | 4600 | 3900 | 5400 | 5300 |
| | /C ₃ H ₄ ⁺ | | | | | | |
| 43 | CH ₃ CO ⁺ | 270-540 | 8750 | 10700 | 8600 | 10200 | 9500 |
| 44 | CO ₂ | 200-700 | 25800 | 30500 | 35100 | 31500 | 31600 |
| 45 | COOH ⁺ | 230-410 | 1100 | 1000 | 800 | 1000 | 900 |
| | /C ₂ H ₅ O ⁺ | | | | | | |
| 46 | HCOOH ⁺ | 280-420 | 400 | 300 | 100 | 300 | 200 |
| 55 | C ₄ H ₇ ⁺ | 270-700 | 3500 | 4200 | 4000 | 4300 | 3700 |
| | /C ₃ H ₅ O ⁺ | | | | | | |
| 57 | C ₄ H ₉ ⁺ | 280-430 | 900 | 1300 | 700 | 900 | 900 |
| | /C ₃ H ₅ O ⁺ | | | | | | |
| 58 | CH ₃ CH ₂ CHO ⁺ | 240-420 | 700 | 800 | 500 | 600 | 700 |
| 60 | HOCH ₂ CHO ⁺ | 220-500 | 800 | 800 | 500 | 800 | 700 |
| | /CH ₃ COOH | | | | | | |
| 68 | C ₄ H ₄ O ⁺ | 200-420 | 400 | 1000 | 1300 | 600 | 1100 |
| 82 | C ₅ H ₆ O ⁺ | 270-430 | 100 | 300 | 400 | 200 | 500 |
| 95 | C ₅ H ₃ O ₂ ⁺ | 240-420 | 100 | 200 | 200 | 200 | 300 |
| 96 | C ₅ H ₄ O ₂ ⁺ | 200-420 | 200 | 300 | 200 | 200 | 200 |
| 98 | C ₅ H ₆ O ₂ ⁺ | 200-420 | 200 | 200 | 200 | 200 | 200 |

As Table 3 shows, the methane yield, represented by m/z 16, increased in the catalytic experiments both in the temperature range between 350-500 °C (which can be attributed mainly to methane evolution from lignin [12]) and 500-780 °C (which indicates a char formation process). An ion at the same mass can also be the fragment of other molecules: that is why the computer program subtracts the m/z 16 fragment ion of water, carbon-monoxide and carbon-dioxide. The use of the SBA-15 catalyst group (SBA-15 and Al-SBA-15) resulted in the production of the highest amount of methane.

The formation of water is monitored by its molecular ion, m/z 18. Compared to the uncatalysed run, the water yield increased with all catalysts. The highest water yield was obtained with the FCC/2 catalyst. The water formed can be attributed to the degradation of higher molecular weight molecules.

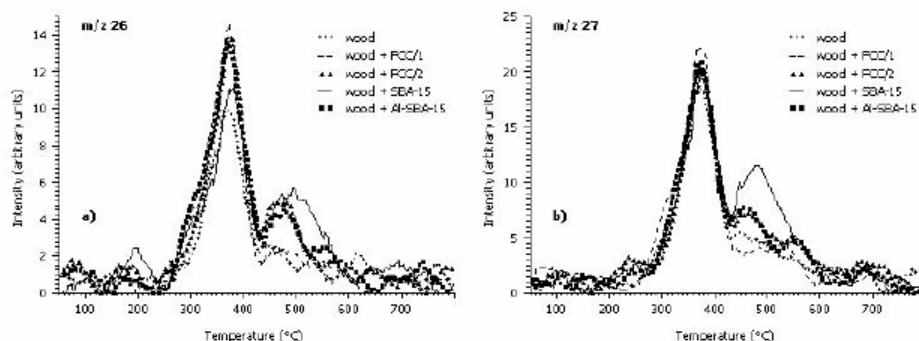


Figure 6. Evolution of (a) m/z 26 and (b) m/z 27 fragment ions during TG/MS experiments

The fragment ions of m/z 26 ($C_2H_2^+$) and m/z 27 ($C_2H_3^+$) are representatives for hydrocarbons (Fig. 6.), however, they can be formed from several other compounds through fragmentation in the mass spectrometer (e.g. aldehydes). Thus, the main peak at around 360°C may represent various products. However, the oxygen-containing organic products do not have significant intensities at around 500°C [11]. Therefore the m/z 26 and m/z 27 ions can be attributed mainly to the evolution of hydrocarbons in the temperature region of 430-700°C. When a smaller amount of FCC was used (FCC/1), the hydrocarbon yield showed a slight decrease, in the other cases, the intensities of m/z 26 and m/z 27 in the 430-700°C temperature range increased. The largest effect can be observed with the SBA-15 catalyst.

Aldehyde formation can be followed by monitoring the m/z 29, m/z 30 and m/z 31 ions. The m/z 29 and m/z 30 yield did not change significantly in the presence of catalysts. A small decrease with FCC catalyst (wood + FCC/2) can be observed. The changes in m/z 31 yield were more significant here, we can see a decrease of nearly 50% in case of FCC catalysis (wood + FCC/2).

The organic acid yields are represented by m/z 45, m/z 46 and m/z 60 ions. The m/z 46 ion represents formic acid ($HCOOH^+$). It can be seen that the amount of this product decreases with all catalysts. The FCC/2 catalyst proved to be the most effective in decreasing the formic acid yield. A smaller decrease in the amount of other acids (m/z 45 and m/z 60) can also be observed. Note, that m/z 45 and m/z 60 ions can represent other

products besides the organic acids. m/z 45 can be either COOH^+ or a fragment of ethanol ($\text{C}_2\text{H}_5\text{O}^+$). The m/z 60 ion can be attributed to acetic acid produced from hemicellulose and hydroxyacetaldehyde produced from cellulose.

Conclusions

In this paper the upgrading possibilities of bio-oil have been studied in the presence of different catalysts (FCC, SBA-15 and AL-SBA-15). Slow and fast pyrolysis experiments have been performed with TG/MS and Py-GC/MS techniques, respectively. FCC has been found to be the most effective catalyst, and it has also been proven that aluminium incorporation to an SBA type catalyst increases the effectiveness of the compound in the upgrading of pyrolysis vapours.

The presence of catalysts significantly changes the bio-oil composition. It increases the amount of light phenol substitutes, and decreases that of the heavy phenolic compounds. The amounts of furan and furan derivatives increases as well, whereas the yield of aldehydes decreases. Char and water formation is enhanced in the presence of catalysts. The yield of organic acids also changes, however, this change, however, depends on the experimental conditions: a high heating rate favours the increase of the amount of acidic compounds, a slow heating rate results in a decrease of organic acid yield.

Most of the experiments were carried out with a wood to catalyst ratio: 1:1. Additional experiments have been carried out with the FCC catalyst to get information about the role of layer thickness. It was found that if the catalyst layer is thin, some of the vapours formed during pyrolysis may escape without reaction with the catalyst. With a larger layer thickness appropriate upgrading of the pyrolysis oil is possible.

Acknowledgements

J. Adam is indebted to the Norwegian Research Council for her Ph. D. grant and M. H. Nilsen thanks the Norwegian University of Science and Technology for the Post-doc grant. M. Stöcker and A. Bouzga acknowledge the financial support of the European Union(ENK 6-CT2001-00049). The work of E. Mészáros and M. Blazsó was supported by the Hungarian National Research Fund (OTKA T037704-05).

References

- [1] A. V. Bridgwater, *Appl. Catal. A* 116 (1994) 5.
- [2] A. Demirbas, *Energy Convers. Manage.* 42 (2001) 1375.
- [3] P. Williams and N. Nugranad, *Energy* 25 (2000) 493.
- [4] A. Lappas, M. Nilsen, A. Bouzga, M. Stöcker, E. Antonakou and I. Vasalos, in: *Proceedings 8th Symposium of the Hellenic Catalysis Society, Cyprus, 30 October 2004*, p.73.
- [5] S. Czernik, R. Maggi, G. V. C. Peacocke *Fast Pyrolysis of Biomass: A Handbook Vol. 2.* (Ed A. V. Bridgwater) CPL Press, Newbury, UK; 2002. p. 141.
- [6] S. Vitolo, M. Seggiani, P. Frediani, G. Ambrosini, L. Politi, *Fuel* 78 (1999) 1147.

- [7] Cr. I. Simionescu, C. Vasile, P. Onu, M. Sabliovschi, G. Moroi, V. Barboiu, D. Ganju, M. Florea, *Thermochim. Acta* 134 (1988) 301.
- [8] G. D. Stucky, D. Zhao, P. Yang, W. Lukens, N. Melosh, B. F. Chmelka, *Stud. Surf. Sci. Catal.* 117 (1998) 1.
- [9] D. Zhao, J. Feng, Q. Huo, N. Melosh, G. H. Fredrickson, B. F. Chmelka, G. D. Stucky, *Science* 279 (1998) 548.
- [10] Y. Yue, A. Gédéon, J. L. Bonardet, N. Melosh, J. B. D'Espinose, J. Fraissard, *Chem. Commun.* 19 (1999) 1967.
- [11] J. Adam, M. Blazsó, E. Mészáros, M. Stöcker, M. H. Nilsen, A. Bouzga, J. E. Hustad, M. Grønli, G. Øye, *Fuel* 84 (2005) 1494.
- [12] E. Jakab, O. Faix, F. Till, *J. Anal. Appl. Pyrolysis* 40-41 (1997) 171.